



Universiteit
Leiden

The Netherlands

Assessing global regionalized impacts of eutrophication on freshwater fish biodiversity

Zhou, J.

Citation

Zhou, J. (2024, January 30). *Assessing global regionalized impacts of eutrophication on freshwater fish biodiversity*. Retrieved from <https://hdl.handle.net/1887/3715136>

Version: Publisher's Version

License: [Licence agreement concerning inclusion of doctoral thesis in the Institutional Repository of the University of Leiden](#)

Downloaded from: <https://hdl.handle.net/1887/3715136>

Note: To cite this publication please use the final published version (if applicable).

**Assessing global regionalized impacts
of eutrophication on freshwater fish
biodiversity**

Jinhui Zhou

© Jinhui Zhou (2024)

Assessing global regionalized impacts of eutrophication on freshwater fish
biodiversity

PhD Thesis at Leiden University, The Netherlands

The research described in this thesis was conducted at the Institute of Environmental
Sciences (CML), Leiden University, the Netherlands. All rights reserved. No parts of
this publication may be reproduced in any form without the written consent of the
copyright owner.

ISBN: 9789051916669

Cover: Images were created and drawn by Jinhui Zhou. The use of icons and fonts
obeys the license policies of Adobe Photoshop and Canva.

Layout: Jinhui Zhou

Printing: Print & Bind

**Assessing global regionalized impacts of eutrophication on freshwater fish
biodiversity**

Proefschrift

ter verkrijging van

de graad van doctor aan de Universiteit Leiden,
op gezag van rector magnificus prof.dr.ir. H. Bijl,
volgens besluit van het college voor promoties
te verdedigen op dinsdag 30 januari 2024

klokke 10.00 uur

door

Jinhui Zhou

geboren te Changsha, China

in 1992

Promotor:

Prof.dr.ir. P.M. van Bodegom

Co-promotores:

Dr. J.M. Mogollón

Dr. L.A. Scherer

Promotiecommissie:

Prof.dr.ing. M.G. Vijver

Prof.dr.ing. J.W. Erisman

Prof. dr. W. de Vries (Wageningen University & Research)

Dr. R. van Zelm (Radboud Universiteit)

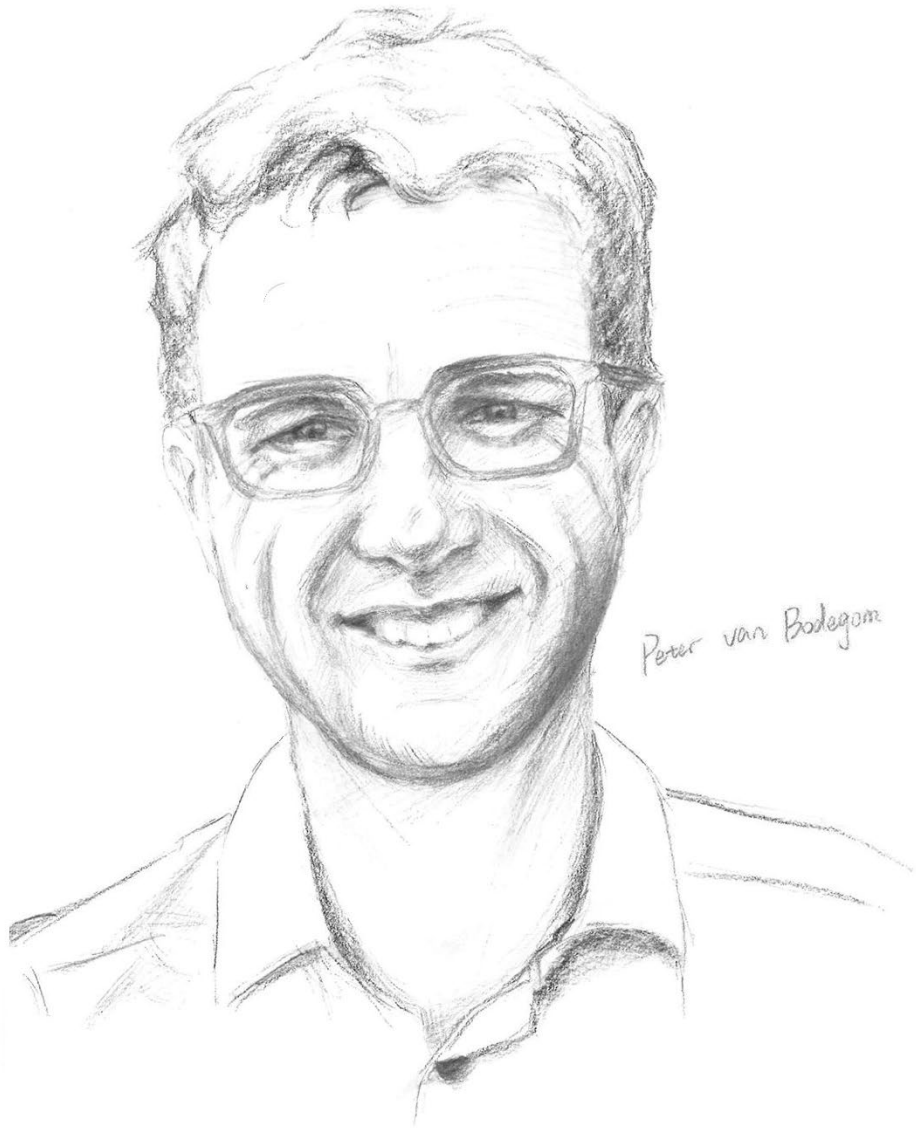
Dr. V. Barbarossa

Table of contents

Chapter 1.....	1
General introduction	
Chapter 2.....	15
Regionalized nitrogen fate in freshwater systems on a global scale	
Chapter 3.....	57
A comparison between global nutrient retention models for freshwater systems	
Chapter 4.....	101
Effects of nitrogen emissions on fish species richness across the world's freshwater ecoregions	
Chapter 5.....	121
Global regionalized characterization factors for phosphorus and nitrogen impacts on freshwater fish biodiversity	
Chapter 6.....	153
General discussion	
References.....	167
Summary.....	183
Samenvatting	187
Acknowledgments	192
Curriculum vitae	195
List of publications	196
Presentations	197
Propositions	198

Chapter 1

General introduction



1.1 Challenges in biodiversity worldwide

Biodiversity refers to the variety of life forms on Earth, including ecosystems, species, and genetic diversity (Wilson, 1999). It is essential for the functioning of ecosystems and provides numerous benefits to human well-being (Kumar, 2005; Verma, 2016). For instance, biodiversity plays a crucial role in maintaining the stability and resilience of ecosystems because each species has a unique role within its ecosystem and their interactions contribute to the balance of the ecosystem (Feng et al., 2017; Mori et al., 2017, 2013; Swift et al., 2004). Biodiversity also supports human life through providing ecosystem services, which comprise, among others, the provision of food and fibers, water purification, pollination, nutrient cycling, and the regulation of diseases (Haines-Young and Potschin, 2010; Mori et al., 2017). Furthermore, the diversity of nature is beneficial for the mental well-being of people (Haines-Young and Potschin, 2010).

The Earth is currently facing a biodiversity crisis, marked by ecosystem degradation and unprecedented rates of species loss (Arya, 2021; Díaz et al., 2019; Savage, 1995). This loss of biodiversity can lead to a decline in ecosystem services and the stability of ecosystems, eventually harming human livelihoods and well-being (Corvalan et al., 2005). Specifically, the biodiversity crisis is associated with some practices of human interference (Savage, 1995). One of the human interferences is the conversion of natural lands for agriculture, urbanization, and resource extraction. It leads to habitat loss and fragmentation of ecosystems (Prakash and Verma, 2022). Humans have emitted excessive greenhouse gases and thus causing the rapidly changing climate, which has been found to disrupt ecosystem performance and affect the distribution and behavior of species (IPCC, 2018). Moreover, overexploitation by mankind, such as unsustainable hunting, fishing, logging, and harvesting of wildlife for trade, coupled with illegal activities, even pushes some species to extinction (Prakash and Verma, 2022). Last but not least, pollution from anthropogenic activities, such as industrial production, agricultural practices, and improper waste disposal, can contaminate air, water, and soil (Akhtar et al., 2021; Havugimana et al., 2017; Ogidi and Akpan, 2022). These consequences of human interferences have jeopardized species' survival and

reproductive success and thus pose a significant threat to biodiversity (Prakash and Verma, 2022).

Across different ecosystem types, freshwater species are of utmost concern since they are the most endangered overall and decline the fastest compared with terrestrial and marine species (Dudgeon et al., 2006; Harrison et al., 2018). Freshwater species have lost on average 83% of the population since 1970 (Grooten and Almond, 2018). Within freshwater ecosystems, fish biodiversity holds particular significance, serving as an indicator of ecosystem health and contributing to the overall integrity of these fragile habitats (Villéger et al., 2017). Researching fish biodiversity across global freshwater ecoregions is crucial in addressing the challenges posed by environmental threats that further exacerbate the ongoing biodiversity crisis (Whitfield and Elliott, 2002).

Among the anthropogenic drivers, pollution from agriculture is the most prominent driver of freshwater biodiversity loss (Díaz et al., 2019). Pollution overall threatens 49.4% of the threatened fish species and 63% of freshwater fish species (Miranda et al., 2022). It goes without saying that biodiversity conservation from agricultural pollution, particularly fertilizer use is important. Yet to what extent this pollution has contributed to the deterioration of biodiversity is still insufficiently understood, especially for different locations all over the world.

1.2 Global nexus of eutrophication and freshwater fish biodiversity

Agricultural activities, especially fertilizer use, have caused an abundance of contaminants in soil and aquatic systems (Beusen et al., 2016; Bouwman et al., 2009). One of the primary pollutants is nutrients. Excessive nutrient enrichment in aquatic environments characterizes eutrophication, resulting in detrimental effects on the overall biodiversity of ecosystems (Chislock et al., 2013; Müller et al., 2012; Jenny et al., 2016; Vonlanthen et al., 2012; Schindler and Vallentyne, 2008).

Within the context of freshwater biodiversity, eutrophication presents the critical challenge of algal blooms (Wurtsbaugh et al., 2019). Increased nutrient levels fuel the

growth of algae, forming dense layers that block sunlight from reaching lower layers of water and leading to the depletion of oxygen (Chislock et al., 2013; Müller et al., 2012). The shading of light prevents predators such as fish from hunting prey and reduces the chances of survival of predators (Lehtiniemi et al., 2005). Oxygen depletion, creating hypoxic or anoxic conditions in the water, can have severe impacts on fish and other aquatic organisms that rely on adequate oxygen availability for survival (Jenny et al., 2016). Therefore, eutrophication can cause not only the local loss of species and populations but also shifts in species composition, favoring certain algal species over others and altering the intricate balance of the ecosystem (Wang et al., 2021). These consequences can adversely disrupt vital ecological processes within freshwater ecosystems and further cause extinction of species in the long term (Dodds and Smith, 2016). Eventually, it becomes a major threat to fish species richness (Dorgham, 2014).

Understanding the role of eutrophication across global freshwater ecoregions is essential for addressing the threats to freshwater biodiversity. Research efforts aimed at assessing the influence of eutrophication on fish species provide valuable insights into the general impacts of eutrophication on freshwater biodiversity. By studying fish as indicators of ecosystem health, researchers can inform conservation strategies, ecosystem management plans, and policy decisions to mitigate the detrimental effects of eutrophication and preserve the integrity of freshwater ecosystems worldwide.

1.3 Environmental complexity hinders eutrophication assessments

Human activities have nearly doubled the global delivery of nitrogen (N) and phosphorus (P) to freshwater systems and led to a rise in eutrophication worldwide (Beusen et al., 2016). Looking ahead, the trend of nutrient accumulation in freshwater systems is expected to continue due to increased fertilizer use and global population growth (Mogollón et al., 2018b). Additionally, climate change impacts on the hydrological cycle, including increased evaporation and freshwater advection, are likely to exacerbate changes in global nutrient cycles (Bouraoui et al., 2004; Statham, 2012). Consequently, the complex interactions between environmental factors and

nutrient cycles make accurate eutrophication predictions challenging (van Vliet et al., 2019).

To effectively address the rising eutrophication trend in global aquatic systems, it is crucial to assess the fate of N and P through global nutrient models. However, current global estimates of nutrient exports vary significantly, highlighting the difficulties in modeling and predicting eutrophication (van Vliet et al., 2019). The discrepancies arise from differences in hydrological data, spatial resolution, and process modeling methods such as retention (van Vliet et al., 2019). Nutrient retention, influenced by various hydrological processes and drivers, plays a crucial role in eutrophication dynamics. Identifying the most effective models for globally predicting nutrient retention can improve our understanding of eutrophication impacts.

In addition, eutrophication impact is reliant on algal blooms (Ansari et al., 2011; Wurtsbaugh et al., 2019). To address the issue of algal blooms, it is crucial to have access to information on the algal distribution and the drivers of their growth. The drivers have been found as nutrient concentrations and bioavailability (Francoeur et al., 1999). The primary focus is usually on managing the concentrations and bioavailability of N and P (McDowell et al., 2020). Therefore, considering the spatial distribution of limiting nutrients can help to disentangle eutrophication impacts.

Given the complex interactions between environmental factors, nutrient cycles, eutrophication processes, and algal growth, the accuracy of the representativeness of nutrient dynamics and nutrient limitation becomes inherently important. The choice of nutrient models and the consideration of nutrient limitations that account for the intricate relationships and feedback mechanisms within aquatic ecosystems are crucial for advancing our understanding of eutrophication and effectively managing its impacts.

1.4 Life cycle impact assessment of freshwater eutrophication

Several methods for assessing the environmental impacts of eutrophication have been developed to quantify the preservation of ecosystem quality. An extensively used

approach to evaluate the environmental impacts is life cycle assessment (LCA) (Muralikrishna and Manickam, 2017). Within contemporary economic activities, global environmental impacts are evidently generated in international value chains, encompassing the production, use, and disposal of goods or services. LCA allows for monitoring and evaluating these impacts comprehensively, adopting a system's perspective. LCA aims to pinpoint strategies for enhancement without resorting to the transfer of burdens and can be distinguished into phases (Figure 1.1) (Hellweg and Canals, 2014). The first phase involves outlining the goal and scope, encompassing the definition of research objectives and establishing the system boundaries. In the second phase, inventory analysis gathers inputs and outputs for each life cycle process, consolidating them system-wide. This typically involves quantifying hundreds of emissions and resources. The third phase, known as life-cycle impact assessment (LCIA), assesses the impact of emissions and resources based on their impact categories, which are converted into common impact units to facilitate comparability (Hellweg and Canals, 2014). The final phase is the interpretation of the inventory and impact assessment results to address the aim of the LCA study. The focus of concern in the LCIA method is characterization factors (CFs), as CFs quantitatively represent the relative importance of a specific influence from emissions and resources (Payen et al., 2019). CFs establish a connection between emissions and an environmental impact, such as the loss of biodiversity, through midpoint-level and endpoint-level indicators (Rosenbaum et al., 2007). In the context of eutrophication, midpoint-level indicators represent the fate of nutrients and their exposure to the environment, whilst endpoint-level indicators describe the ultimate effect of eutrophication on species occurrences (Payen et al., 2019).

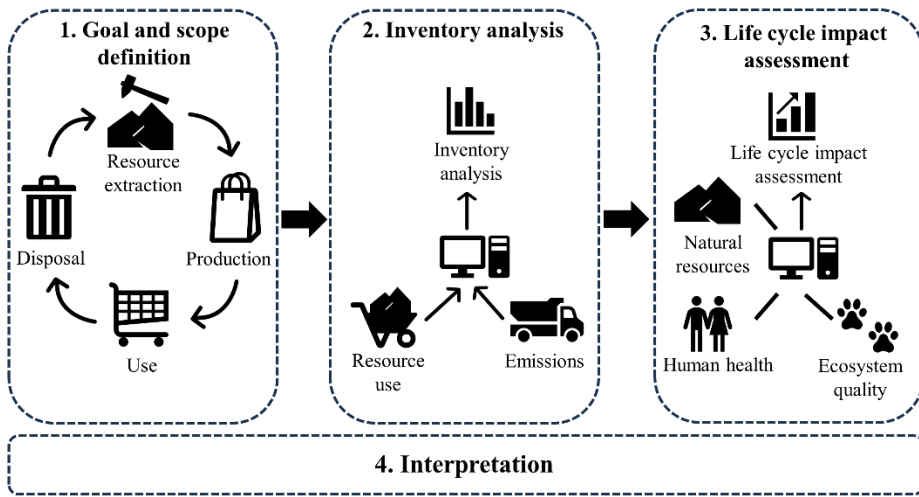


Figure 1.1 Four phases of life cycle assessment (LCA), modified from Hellweg and Canals (2014)

In freshwater ecosystems, impacts on fish biodiversity have been widely explored by LCA studies given its importance to ecosystem health (Villéger et al., 2017; Whitfield and Elliott, 2002). Various environmental stressors to freshwater fish biodiversity loss have been quantified and converted to CFs, including climate change (de Visser et al., 2023; Hanafiah et al., 2011), water consumption (Hanafiah et al., 2011; Pierrat et al., 2022), and hydropower (Turgeon et al., 2021). All these studies focus on the global scale. These global studies use different degrees of regionalization from biomes to the grid level to capture variation in environmental impacts. Also in the case of freshwater eutrophication, regionalization is essential to account for the influence of diverse environmental conditions on the relationship between eutrophication and biodiversity loss. This influence encompasses spatial variations in phosphorus (P) and nitrogen (N) impacts due to varying nutrient limitations and species compositions. Current studies on CFs solely focus on either P-related freshwater eutrophication (e.g., LC-IMPACT (Azevedo et al., 2020), ReCiPe2016 (Huijbregts et al., 2017), and Jwaideh et al. (2022)) or N-related marine eutrophication in CFs (e.g., (Cosme and Hauschild, 2017)). Yet as we mentioned, it is crucial to consider both P and N to decide which nutrient restricts

algal growth, as it characterizes the regionalized impact of eutrophication on freshwater ecosystems. Additionally, the spatial representation of these studies is insufficient as these studies only specify the species loss relating to P and N for four or five geographical zones globally, which is too few for characterizing the global variation in impacts.

There are standardizations and guidelines that can be used for the evaluation of the impact. In 2020, the United Nations Environment Programme (UNEP) initiated the third phase of the Global Life Cycle Impact Assessment Method (GLAM) project as part of the broader "Life Cycle Initiative", whose primary objective is to establish global standardization and harmonization of LCIA methods (Verones et al., 2019). GLAM advocates for the adoption of spatially explicit models with global coverage for the midpoint and endpoint levels (Payen et al., 2019). For the midpoint-level indicators, GLAM recommends to use global nutrient models with a fine resolution to develop the fate of environmental drivers and emphasizes capturing physical and biogeochemical processes in assessment models. When it comes to the endpoint level, GLAM recommends summarizing the assessment of impacts on species richness of fish as has previously been employed in LCIA studies. However, historical studies hamper the characterization of the fine spatial variability in both the nutrient fate and its effect on species. As a result, developing spatially explicit fate factors (FFs), effect factors (EFs), and CFs at a finer resolution is essential for accurate impact assessment.

Considering global species loss can offer a broader insight into the interactions of nutrient inputs and the impacts on freshwater ecosystems than when restricting the analysis solely to local or regional species loss. As a consequence, global extinction probabilities (GEPs) have recently been developed within the framework of GLAM (Verones et al., 2022). GEPs can translate the regional species loss to global species loss by a simple multiplication with CFs.

In summary, the objective of achieving a more comprehensive assessment of eutrophication impacts on global freshwater biodiversity requires improvements in the

spatial representation of nutrient fate, understanding the relationship between nutrients and their effects on species richness, and quantitatively evaluating CFs for the current state. Drawing upon previous research, these enhancements can be achieved by prioritizing the regionalization of fate and effect, encompassing both P and N impacts, integrating GEPs, and acknowledging nutrient limitations.

1.5 Aims and research questions

The overall aim of this thesis is to disentangle the impact of eutrophication from other anthropogenic impacts on global freshwater fish biodiversity. I therefore developed region-specific and inclusive indicators for nutrient fate and effects, followed by improving nutrient retention predictions, and subsequently quantified the impacts on freshwater fish species richness. These indicators can be integrated into LCIA methods, thereby enhancing their predictive power and ecoregional precision. To achieve this aim, this research can be subdivided into several questions (Q):

Q1: What is the pattern of regionalized nutrient fate, and how do drivers affect the nutrient fate over the global freshwater?

As mentioned above, fate factors are the midpoint-level components of CFs. Historically, studies on fate factors for freshwater systems focus on P but lack a view on N. To better represent nutrient fate in LCIA methods, the fate factors not only need to be regionalized to reproduce the transport of N, but also should characterize N fate from the direct emissions, diffuse emissions, and erosions. It is also important to explore the role of drivers in nutrient fate to know the contributors to freshwater eutrophication. The same method can be used for assessing P fate.

Q2: How can retention equations improve model performance?

fate factors are based on the simulation of P and N dynamics, which is achieved by using a global nutrient model. In the process of nutrient modeling, retention is of utmost importance. Assessing the performance of retention models in the global nutrient model helps to optimize the simulation of nutrient fate.

Q3: What is the pattern of the regionalized effect on fish species loss across the global freshwater ecosystem?

Current LCIA indicators only characterize the effect of P on species in four geographical zones for freshwater and the effect of N in five geographical zones for marine globally. However, due to a large variation in hydro-climatic conditions and human stressors over the world, the response of fish species differs across the freshwater ecoregions. Nutrients are such drivers that are affected by hydrological conditions and human emissions. Thus, the effects of nutrients on fish species richness need to be assessed more site-specifically.

Q4: What is the impact of eutrophication on global fish species loss in freshwater ecosystems?

Characterization factors can reflect the hotspots of impact from P and N emissions per unit of inventory on species. However, so far, characterization-factor-related studies lack the regionalization of both P and N and the knowledge of which nutrient influences fish biodiversity where. As discussed in the above sections, such innovative work is necessary to be done for evaluating the eutrophication impact on global ecosystems, such as freshwater systems.

1.6 Thesis outline

This thesis is composed of six chapters (Figure 1.2). The first chapter, the general introduction, gives an overview of the background, motivation, and the outline of the thesis. To realize the objectives, the thesis focuses on deriving spatially explicit fate factors (FFs), effect factors (EFs), and resulting characterization factors (CFs) for N and P to use in life cycle impact assessments by employing IMAGE-GNM. This thesis reproduces the major processes of nutrient inputs, eutrophication, and the impacts (Figure 1.3). This is done in Chapter 2 for fate factors of N, in Chapter 3 by assessing the importance of alternative descriptions of nutrient retention on fate factors, in Chapter 4 for effect factors of N (linking N concentrations to fish species loss) and

finally for CFs in Chapter 5 by linking fate and effect factors. Finally, the last chapter of the general discussion encompasses the limitations and implementation of the thesis. The narrative of Chapters 2 – 6 is further expanded upon below.

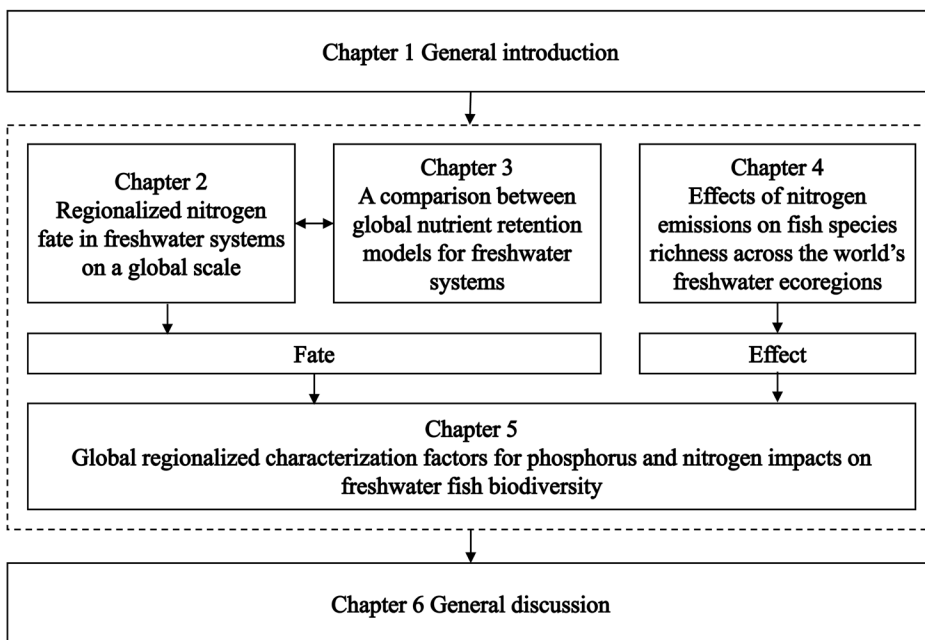


Figure 1.2 Outline of the thesis

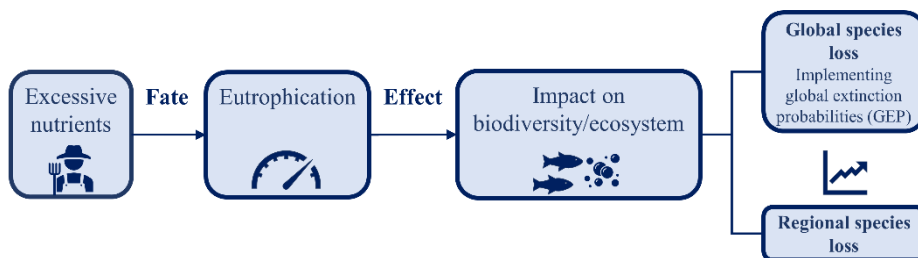


Figure 1.3 A schematic diagram of the major processes and interactions of nutrient inputs, eutrophication, and the impacts

Chapter 2 addresses the first research question. It provides regionalized FFs for N in global freshwater at half-degree resolution and at the country level. These FFs specify N fate from the direct and diffuse emissions, as well as erosion. This chapter

complements current analyses of freshwater eutrophication about P. It presents a quantitative analysis of N fate against hydrological parameters and illustrates their spatial heterogeneity, highlighting the importance of regionalization in LCIA indicators.

Chapter 3 answers the second research question. It assesses the performance of the global nutrient model that was used in the calculation of FFs in Chapter 2. This research quantifies the improvement of model performance in the best-fit retention equation compared to the currently used one. The results present the importance of retention in the prediction of nutrient fate.

Chapter 4 answers the third research question. This chapter regionalizes the effect of eutrophication on species richness by establishing the relationship between nutrient concentration (the stressor) and the potentially disappeared fraction (PDF) of species richness. This research regresses the curve of how PDF changes due to N concentration across hundreds of freshwater ecoregions based on observed data and calculates the EFs at half-degree resolution. The method can also be applied to P and used for calculating CFs.

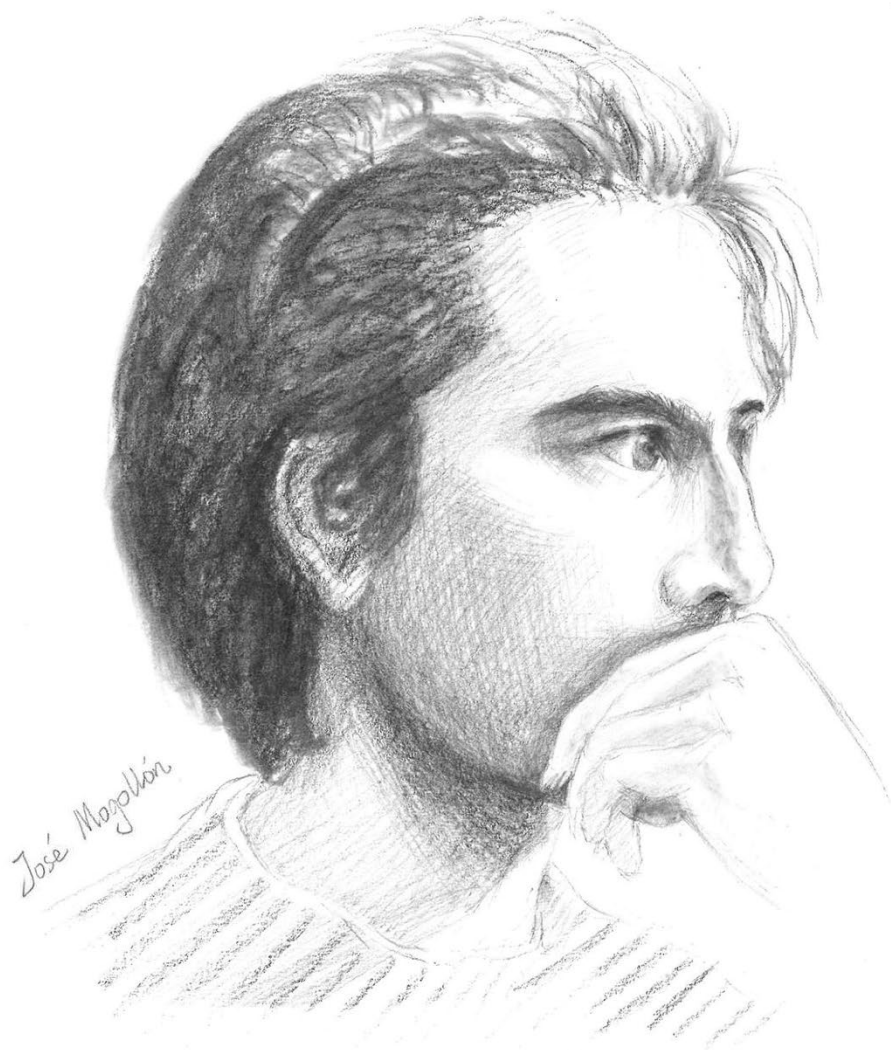
Chapter 5 addresses the fourth research question. This chapter calculates regionalized CFs at half-degree resolution and at the country level based on the fate and effect research in this thesis. It provides both views of eutrophication CFs on regional species loss and global species loss (by integrating regional species loss with GEP, Figure 1.3). This research also gives nutrient limitation at the same resolution, which can guide the users of life cycle assessment to determine whether P or N should be considered in the use of CFs.

Chapter 6 provides a general discussion on Chapters 2-5. This chapter summarizes the answers to the questions, the limitations of the research, and the implications of this thesis.

Chapter 2

Regionalized nitrogen fate in freshwater systems on a global scale

This chapter has been published as Zhou, J., Scherer, L., van Bodegom, P.M., Beusen, A., Mogollón, J.M., 2022. Regionalized nitrogen fate in freshwater systems on a global scale. *J Ind Ecol* 26, 907–922.



Abstract

Excessive nitrogen (N) use in agriculture, industry, and household waste leads to widespread N release throughout the environment, causing eutrophication in both freshwater and coastal areas. To better understand N-induced eutrophication and other N-use-related environmental impacts at the local scale, improvements in the spatial resolution of LCIA measures are required. Here, we present a method to estimate gridded fate factors (FFs) at a half-degree resolution based on the IMAGE-Global Nutrient Model (GNM) to provide eutrophication indicators for global N-related manufacture, trade, and consumption in LCA. Across global freshwater systems, our cumulative FFs have a 5th percentile of 0.9 days and a 95th percentile of 184.0 days. Aggregated FFs for administrative units range from 0.3 days to 211.9 days. The hotspots of cumulative FFs are mainly distributed upstream of large reservoirs or lakes. On a global level, advection is the dominant process controlling the FF (69.7% of areas), followed by retention (29.0%), and water consumption (1.3%). N retention dominates in advection-favoring, high-discharge regions due to the high residence times, while water consumption tends to dominate water-scarce zones. The results demonstrate the importance of gridded information to assess eutrophication impacts, as it characterizes N emissions from anthropogenic sources at high spatial resolution in comparison to basin- or country-level assessments. Introducing soil-freshwater N fate complements existing P-related fates to improve global assessments of eutrophication.

2.1 Introduction

Human activities, including food production, detergent and fertilizer use, and waste such as sewage from households and industry, have exacerbated nutrient emissions to the environment, posing a pervasive threat to aquatic ecosystems. Nitrogen (N) is an important nutrient for life, but in excess can lead to eutrophication, hypoxia, and the deterioration of ecosystems (Jenny et al., 2016; Muller et al., 2012; Vonlanthen et al., 2012). Global N input to freshwater systems has grown from 34 to 64 Tg year⁻¹ from

1900 to 2000 (Beusen et al., 2016), leading to an increase in eutrophic (and hypoxic) areas in freshwater and coastal systems (Jenny et al., 2016). Eutrophication can induce excessive reproduction of pernicious algae blooms (Chislock et al., 2013), whose decomposition consumes oxygen and can lead to hypoxia/anoxia in the water column. These conditions may be unable to sustain many aquatic organisms and thus jeopardize biodiversity (Schindler and Vallentyne, 2008), and may lead to a collapse of the aquatic ecosystem. This deterioration of aquatic ecosystems may last months or even years (e.g. algae blooms in Taihu Lake, (Duan et al., 2015)) and is highly likely to intensify because of increasing demand for food, fertilizer use, and industrial production with population growth (Jenny et al., 2016; Mogollón et al., 2018a; Tilman et al., 2001).

Life cycle assessment (LCA) provides a widely recognized framework to quantify environmental impacts, such as eutrophication, throughout the whole life cycle of a specific product (Hellweg and Milà i Canals, 2014; Payen et al., 2019). In the Life Cycle Impact Assessment (LCIA) phase of LCA, characterization factors (CF) relate the emissions or resource use from various life cycle stages to associated environmental impacts. For eutrophication, the fate factor (FF) describes the nutrient fate originating from various anthropogenic emissions and serves as the first step toward assessing the environmental impact of the nutrients from an LCIA standpoint.

Historically, LCA research has evaluated eutrophication indicators ignoring geospatial variation, a limitation that has been pointed out in previous research (Hauschild, 2006; Hauschild and Potting, 2005; Morelli et al., 2018). For instance, the Tool for the Reduction and Assessment of Chemical and other environmental Impacts (TRACI) (Bare, 2011, 2002; Bare et al., 2012) provides a midpoint eutrophication indicator by multiplying a nutrient factor and a transport factor. Nonetheless, TRACI does not model explicit N processes; instead, it derives the nutrient factor from the Redfield ratio to describe the relative influence of P versus N (Norris, 2002). Further, the transport factor, which is the same for N and P, ranges from 0 to 1 to represent the probability of the release arriving in an aquatic environment. TRACI assumes that all emitted nitrogen contributes to eutrophication, and ignores biogeochemical transformations of N before

reaching water bodies and during transport through water bodies (Payen and Ledgard, 2017). More recently, however, coupling LCA with geographic information systems (GIS) has allowed for the ability to identify locations undergoing (or that are susceptible to) N-induced impacts. Helmes et al. (2012) made the first big step towards regionalizing eutrophication impacts by developing a gridded FF model for phosphorus (P). They simulated P fate from its emissions and their model was later integrated into ReCiPe 2016 (Huijbregts et al., 2017), IMPACT World+ (Bulle et al., 2019), and LC-IMPACT (Verones et al., 2020). LCA models focusing specifically on N have mainly been developed for marine ecosystems (Payen et al., 2019), even though N has also been regarded as a nutrient sometimes contributing to freshwater eutrophication (Dodds and Smith, 2016; Lewis et al., 2011; Payen et al., 2019; Schindler, 2006; Vollenweider, 1968). The study of Cosme and Hauschild (2017) estimated CFs for N in 66 large marine ecosystems (LMEs) and their corresponding watershed based on the global Nutrient Export from WaterSheds (NEWS) 2 model (Mayorga et al., 2010). However, a grid-scale FF model for freshwater N is not available globally. Large watersheds are often quite heterogeneous. Thus, gridded models, consisting of much smaller spatial units, can better help evaluate local hotspots where nutrients may accumulate within watersheds. Furthermore, grid cells can be aggregated more accurately than watersheds to any scale, such as the country scale, which is the typical spatial unit of life cycle inventory data. Based on a review of existing spatially explicit fate models, NEWS 2, SWAT (Soil and Water Assessment Tool, (Kalcic et al., 2015)), and IMAGE-GNM (the Integrated Model to Assess the Global Environment–Global Nutrient Model, (Beusen et al., 2015)) have been the recommended options for the quantification of N fate factors for use in LCIA on a watershed scale (Morelli et al., 2018). Among them, NEWS 2 can simulate the nutrient fate for rivers and watersheds, but the resolution is limited to the watershed scale. SWAT can simulate organic nitrogen, organic phosphorus, nitrate, and dissolved inorganic phosphorus at the scale of user-defined hydrologic response units within a basin, but it is seldom applied to wide geographic coverage, let alone globally. Since it provides global nutrient loads and emissions at a half-degree resolution, Cosme

et al. (2018) and Morelli et al. (2018) suggested IMAGE-GNM as the most comprehensive option for developing a grid-scale FF model.

In this study, we present a grided, spatially explicit FF model for N emissions to freshwater systems over the globe. We extract information about inland N fate from IMAGE-GNM at $0.5^\circ \times 0.5^\circ$ grid cells on a global scale for the year 2000, and also run the model for 1998 and 1999 to display the dynamics of N fate in subsequent years. IMAGE-GNM is a dynamic, distributed model with a yearly time step. It depicts nutrient reaction and delivery processes in soils and freshwater systems. The N retention, the N withdrawn via water consumption, and the N advection towards downstream cells – henceforth collectively termed “N removal processes” following Cosme et al. (2018) and Helmes et al. (2012) – as well as the drivers and accompanying uncertainties, are analyzed to better contextualize the meaning of the obtained FFs. By highlighting the importance of the link between the hydraulic drivers and FFs, this analysis allows identifying the possible impact of N in distinctive regions to improve the management of emission sources from production activities.

2.2 Methods

2.2.1 Model structure

N fate in soil and freshwater depends on its input, transport, and removal processes (Helmes et al., 2012; Mayorga et al., 2010; Seitzinger et al., 2005). At any location on land, N is imported from applications, depositions, erosion, and fixation, and further transported to the freshwater. For each grid cell, the N sources compose so-called soil N budgets (the difference between those inputs and N eliminations due to harvesting, grass cutting, and grazing) in IMAGE-GNM. Surplus N is transported via leaching into groundwater or surface runoff. During the soil to freshwater transport, N concentration declines due to absorption, uptake by plants, and denitrification. N is transported to open freshwater bodies via surface runoff, shallow groundwater transport, and deep groundwater transport.

Denitrification occurs in surface water and shallow groundwater that feeds into rivers along various flow paths, while N percolating from shallow to deep groundwater is assumed to not undergo denitrification (Beusen et al., 2015). Finally, the N contained in surface runoff and groundwater arrives at rivers and large water bodies (e.g. lakes and reservoirs). Note that in IMAGE-GNM all N processes (e.g. reaction and transport) taking place within multi-grid water bodies are assumed homogeneous and modeled at the single-cell outlet. IMAGE-GNM also models the treated sewage as a point source emitted directly to freshwater system. The spatial data used in IMAGE-GNM includes land cover, soil, lithology, and climate obtained from open-access databases.

IMAGE-GNM simulates the overall fate of N inputs. While IMAGE-GNM splits emissions into natural sources (e.g. biological fixation) and anthropogenic sources (e.g. synthetic fertilizers and manure), once these sources enter the compartment, they constitute total nitrogen (TN). The ratio of N decay from soil emissions to freshwater does not change within a cell, as it is determined by climate, soil texture, aeration, and soil organic carbon (C) content as opposed to the N soil content. The same applies to N emitted to freshwater, as the retention and residence time depend on the hydrological conditions of the water bodies. Therefore, the separation of natural and anthropogenic does not affect the calculation of cumulative FFs, but it could influence the emission-weighted FFs (i.e., regional average FFs) for diffuse emissions.

Here we estimated FFs for the year 2000, as it represents the most recent year available in IMAGE-GNM (Beusen et al., 2016). To show the temporal variation of FFs, we also examined the years 1998 and 1999, and displayed the relative standard deviation (RSD) of FFs for direct emissions to freshwater in the Supporting Information Figure S2.9. Our method can be replicated for other (more recent) years, once the data become available.

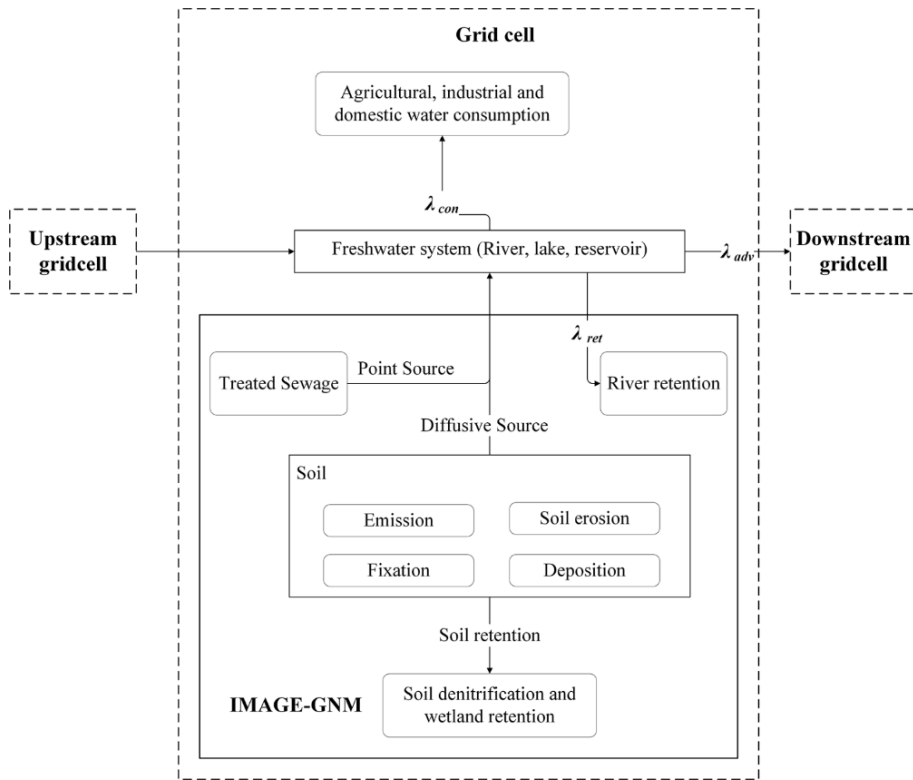


Figure 2.1 Model structure and spatial relation between the model grid cells. λ_{adv} , λ_{ret} , and λ_{con} indicate N removal rate constants for advection, retention, and water consumption, respectively.

N fate in this study is determined by retention and water consumption, as well as advection transporting N to downstream grid cells. We ran IMAGE-GNM and used the model inputs (e.g. emission data), intermediate variables (e.g. retention), and outputs (e.g. nutrient loading) to calculate rate constants (λ_{adv} , λ_{ret} , and λ_{con} , respectively), which we implemented as the advection, retention, and consumption removal processes (Figure 2.1) in the fate factor model. These rate constants, which were calculated for each grid cell, are explained further in sections 2.2.1.1 to 2.2.1.3.

The cumulative fate factors ($FF_{e \rightarrow i}$, days, Eq. 2.1) follow the approach of Helmes et al. (2012) and LC-IMPACT (Azevedo et al., 2020). $FF_{e \rightarrow i}$ denotes the sum of individual

fate factors from emission source e in cell i and all the downstream cells. The individual fate factors ($FF_{e \rightarrow i \rightarrow j}$, days) indicate FFs of the N emitted from source e in cell i to a specific receiving cell j . They are the product of the fraction of N transported from the emission to freshwater ($fr_{e \rightarrow i}$, dimensionless), the fraction of N delivered from the source cell i to receptor cell j by the freshwater system ($f_{i,j}$, dimensionless), and the persistence of N in the receiving compartment j (τ_j , year⁻¹):

$$FF_{e \rightarrow i} = \sum_j FF_{e \rightarrow i \rightarrow j} = 365 \cdot fr_{e \rightarrow i} \cdot \sum_j f_{i,j} \cdot \tau_j \quad (2.1)$$

The resulting $FF_{e \rightarrow i}$ is spatially differentiated and it provides a basis for the environmental impact analysis caused by N emissions. A larger cumulative FF suggests that emissions in the source cell result in a higher possibility and duration of N remaining in the receiving water bodies.

Point sources are regarded as direct loads to the water bodies, and thus $fr_{e \rightarrow i, freshwater}$ equals 1. In contrast, nutrients in the soil are transformed/removed/retained during the transport from the soil to freshwater. For example, during the process of fertilizer application, N may be partially left in the soil compartment and absorbed by plants, and only the remainder of N can be delivered to the freshwater system. IMAGE-GNM distinguishes two emission routes from the soil to freshwater: losses from recent nutrient applications in the form of fertilizer, manure, or organic matter transported by runoff and subsurface delivery (Hart et al., 2004), as well as losses from long-term accumulation in soil compartments, which may be subject to erosion (McDowell and Sharpley, 2001; Tarkalson and Mikkelsen, 2004).

In IMAGE-GNM, the diffuse emissions excluding erosion only include agricultural applications (i.e. it excludes sludge). The transfer fraction of N losses from recent nutrient applications (i.e. nutrient budget which contains fertilizer, animal manure application, and biological N fixation subtracting crop harvesting, grass cutting, and ammonia volatilization) is considered as an export fraction of diffuse loads from the

soil through runoff, drainage, and leaching into groundwater ($fr_{e \rightarrow i, diffuse}$, kg N_{water} / kg N_{emission}).

$$fr_{e \rightarrow i, diffuse} = \frac{L_{e \rightarrow i, diffuse}}{E_{e \rightarrow i, diffuse}} \quad (2.2)$$

where $E_{e \rightarrow i, diffuse}$ is the diffuse emission of source e from recent nutrient applications to the soil within grid cell i (kg year⁻¹), and $L_{e \rightarrow i, diffuse}$ is the load produced by source e in grid cell i (kg year⁻¹).

The transfer fraction of soil erosion ($fr_{i, erosion}$, kg N_{water} / (km²·year)) depends on the land use type.

$$fr_{i, erosion, landuse} = \frac{L_{i, erosion, landuse}}{A_{i, landuse}} \quad (2.3)$$

where $L_{i, erosion, landuse}$ is the soil N eroded to freshwater systems within grid cell i (kg year⁻¹), A_i is the area of a given land use type in grid cell i (km²). IMAGE-GNM distinguishes arable land, grassland, and natural land. Note that in each grid cell, $f_{i, j}$ and τ_j is the same for all land types, but erosion FFs of different land-use types are distinguished via the enhanced transfer fraction of soil erosion ($fr_{i, erosion, landuse}^*$). This latter parameter reflects anthropogenic pressures due to a relative change from natural land to grassland and arable land ($c_{landuse}$).

$$\begin{aligned} fr_{i, erosion, landuse}^* &= fr_{i, erosion, landuse} - fr_{i, erosion, natural} \\ &= \frac{fr_{erosion, landuse} - fr_{erosion, natural}}{fr_{erosion, natural}} \cdot fr_{i, erosion, natural} \\ &= c_{landuse} \cdot fr_{i, erosion, natural} \end{aligned} \quad (2.4)$$

Calculating $fr_{i, erosion, landuse}$ for arable land and grassland as well as $fr_{i, erosion, natural}$ by using Eq. 2.3, we found that $c_{landuse}$ is a constant with values of 2.41 and 45.30 for grassland and arable land, respectively. Given the constant conversion between different land uses and thus equal spatial patterns, FFs of natural land erosion were shown as the baseline in section 2.3.1.

The persistence of N in the receiving water τ_j is defined as the reciprocal of the removal rates. It is related to advection rate ($\lambda_{adv,j}$, year⁻¹), the retention rates ($\lambda_{ret,j}$, year⁻¹) and the removal rates by consumptive water use ($\lambda_{con,j}$, year⁻¹) in estuaries, river reaches, and lakes.

$$\tau_j = \frac{1}{\lambda_{adv,j} + \lambda_{ret,j} + \lambda_{con,j}} \quad (2.5)$$

The transport fraction of freshwater $f_{i,j}$ can be expressed as a ratio between advection rate and the combined removal rates (Eq. 2.6). In contrast to the persistence τ_j , the transport fraction of N in the source cell i delivered to receptor cell j ($f_{i,j}$) is dimensionless, and is calculated as the ratio of N that reaches the receptor cell j to the N export from the source cell i (where n denotes the grid cell along the flow path between the source cell i to the upstream cell adjacent to the receptor cell j). Since the index cell j starts in source cell i , when $j = i$, $f_{i,i} = 1$. Due to the removal by retention and water consumption along the flow path, the further away from source cell i , the less impact is caused in the receptor cell j .

$$f_{i,j} = \prod_{n=i}^{j-1} \frac{\lambda_{adv,n}}{\lambda_{adv,n} + \lambda_{ret,n} + \lambda_{con,n}} \quad (2.6)$$

We elaborate on the components of Eq. 2.5 and Eq. 2.6 in sections 2.2.1.1 – 2.2.1.3.

In our global analysis, we excluded FFs from arid and low-discharge cells. In many of these systems, surface water is highly likely to be unavailable or insufficient to meet the local water demand and could bias the resulting FFs. Here, arid cells were defined to be cells with an aridity index (AI, obtained from Trabucco and Zomer, (2019)) of less than 0.2 (Middleton and Thomas, 1997). However, we still included the dominant rivers (e.g. the Nile River) flowing within arid zones. For arid zones, cells, where the discharge is higher than the median of discharge in non-arid zones (325 mm year⁻¹), were kept, whereas, in non-arid zones, the cells where the discharge is lower than the median of discharge in arid zones (6 mm year⁻¹) were excluded.

2.2.1.1 Advection

The advection rate constant (λ_{adv} in Figure 2.1) was calculated following Helmes et al. (2012), following the principle that each grid cell undergoes advection from the local cell to a downstream cell.

IMAGE-GNM uses the hydrological model PCRaster Global Water Balance (PCR-GLOBWB (Wood et al., 2011)), where the river channel network is based on the DDM30 flow direction map of Döll and Lehner (2002), which links the upstream and downstream cells. The advection rate constant, $\lambda_{adv,i}$, is related to the water travel rate in river channels. This parameter equals the reciprocal of water residence time $t_{r,j}$ for water bodies, which is determined by the discharge Q_i ($\text{m}^3 \text{ year}^{-1}$) and volume V_i (m^3) of the water body.

$$\lambda_{adv,i} = \frac{1}{t_{r,j}} = \frac{Q_i}{V_i} \quad (2.7)$$

Water from the ground surface, soil, or aquifer is transported to the river network. Besides exchange between surface and subsurface water through infiltration and percolation, PCR-GLOBWB also simulates direct runoff, interflow, and base flow which are converted into discharge (Beusen et al., 2015). Reservoir regulation is also introduced in discharge modeling. However, the discharge does not reflect consumptive water use in IMAGE-GNM. Therefore, lakes and reservoirs are only included if the volume outstrips the water storage capacity within a cell (Beusen et al., 2015). Lake volumes and areas were taken from the Global Lakes and Wetlands Database version 1 (GLWD1) (Lehner and Döll, 2004), while reservoir data are from the Global Reservoir and Dam (GRanD) database (Lehner et al., 2011). In PCR-GLOBWB, the reservoirs were included in the model dynamically, according to their reported construction time.

2.2.1.2 Retention

N retention (λ_{ret} in Figure 2.1) consists of denitrification in water, sedimentation, and uptake by aquatic plants. As opposed to P, N undergoes little absorption in sediments. Thus, the advection rate of N better approximates the reciprocal of the water residence time. The analysis of hundreds of rivers and lakes by present studies (Behrendt and Opitz, 1999; Seitzinger et al., 2005; Venohr et al., 2005) that also indicated the link between N retention and hydrology. IMAGE-GNM employs the empirical retention equation of Wollheim et al. (2008), where the retention R_i (dimensionless) in cell i is a first-order degradation process, shown in Eq. 2.8.

$$R_i = 1 - \exp\left(-\frac{v_{f,i}}{H_{L,i}}\right) \quad (2.8)$$

where H_L (m year^{-1} , Eq. 2.9) is the hydraulic load, and v_f (m year^{-1} , Eq. 2.10) is the net uptake velocity. The hydraulic load represents the hydrological characteristics of water bodies. It is determined by the depth (D_i , m) and residence time ($t_{r,i}$, year) of the water body within a cell.

$$H_{L,i} = \frac{D_i}{t_{r,i}} \quad (2.9)$$

The net uptake velocity v_f is affected by the biological and chemical features of the nutrient. In IMAGE-GNM, v_f for N takes a base value of 35 m year^{-1} from Wollheim et al. (2008, 2006) and is modified by the annual temperature T ($^{\circ}\text{C}$) and N concentration C_N :

$$v_f = 35 \cdot f(T) \cdot f(C_N) \quad (2.10)$$

$f(C_N)$ represents the effect of concentration on denitrification resulting from electron donor limitation if excessive N is transported into the water (Mulholland et al., 2008).

Alexander et al. (2004) proposed that the retention rate $\lambda_{ret,i}$ (year^{-1} , Eq. 2.11) in cell i is related to the net uptake velocity v_f and the depth (D_i , m) of water bodies. Based

on the in-stream retention R_i given by IMAGE-GNM, $\lambda_{ret,i}$ can be derived from a function of a natural logarithm of $(1 - R_i)$ and advection rate $\lambda_{adv,i}$:

$$\lambda_{ret,i} = \frac{v_{f,i}}{D} = -\ln(1 - R_i) \cdot \lambda_{adv,i} \quad (2.11)$$

2.2.1.3 Water consumption

Humans withdraw water from rivers, lakes, and reservoirs for irrigation, industrial production, and households. Some of the water withdrawal returns to the freshwater system, while the rest of the water is consumed, along with a net removal of N from freshwater (λ_{con}), which is not considered as an N output by IMAGE-GNM. Therefore, we introduce N removal from consumption of both surface water and groundwater into the removal rates. The removal rate due to water consumption ($\lambda_{con,i}$, year⁻¹, Eq. 2.12) corresponds to a product of all fractions of water consumption ($f_{con,i}$, dimensionless, Eq.2.13) and the advection removal rate ($\lambda_{adv,i}$, year⁻¹).

$$\lambda_{con,i} = \sum f_{con,i} \cdot \lambda_{adv,i} = (f_{agr,i} + f_{dom,i} + f_{elc,i} + f_{man,i} + f_{lvs,i}) \cdot \lambda_{adv,i} \quad (2.12)$$

where $f_{agr,i}$, $f_{dom,i}$, $f_{elc,i}$, $f_{man,i}$, and $f_{lvs,i}$ (dimensionless) are the fractions of water consumption for agriculture, domestic, thermoelectric, manufacturing, and livestock use, respectively. The fraction of water consumption $f_{con,i}$ is the ratio between the volumetric extraction rate of water consumption $U_{con,i}$ (m³ year⁻¹) and the available water in the form of river discharge Q_i within a cell.

$$f_{con,i} = \frac{U_{con,i}}{Q_i} \quad (2.13)$$

Global agricultural water consumption data were obtained from Pfister and Bayer (2014). The domestic, industrial, and livestock water consumption data are from Flörke and Eisner (2011).

2.2.2 Aggregation of FFs

With the emissions of N applications (i.e. diffuse and point sources) and land use (through soil erosion) in any location quantified, the cumulative FFs can be used to predict the N fate at a half-degree resolution. Unlike Helmes et al. (2012) who weighted FFs based on population, we aggregated FFs by weighting according to the respective inventories for each emission route. We use the emission-weighting data of direct emissions to freshwater and diffuse emissions to the soil, while we weight erosion FFs using the areas of three land use types (Supporting Information Figures S2.1 to S2.5). These weighting data were given at the same spatial resolution and for the same representative year as the cumulative FFs. The impact of direct N emissions to freshwater and diffuse emissions to the soil over a region was assessed via emission-weighted FFs (Eq. 2.14):

$$FF_{region,e}^{average} = \frac{1}{\sum_i E_{e \rightarrow i \in r}} \cdot \sum_i FF_{e \rightarrow i \in r} \cdot E_{e \rightarrow i \in r} \quad (2.14)$$

The regional (e.g. country) average fate factor ($FF_{region}^{average}$, days) is used to represent the aggregation of FFs over a region r . $E_{e \rightarrow i \in r}$ is the emission from diffuse or point source e in grid cell i (kg year^{-1}), provided by IMAGE-GNM.

Regional FFs of erosion $FF_{region,erosion}^{average}$ ($\text{days} \cdot \text{kg N}_{\text{water}} / (\text{km}^2 \cdot \text{year})$) aggregate nonzero FFs of erosion over a region and all land-use types through area-weighting:

$$FF_{region,erosion}^{average} = \frac{1}{\sum_i A_{i \in r}} \sum_{i,landuse} FF_{i \in r,erosion,landuse} \cdot A_{i \in r,landuse} \quad (2.15)$$

where $A_{i \in r}$ (km^2) is the total land area of grid cell i ; $A_{i \in r,landuse}$ (km^2) is the area of this land-use type; $FF_{i \in r,erosion,landuse}$ ($\text{days} \cdot \text{kg N}_{\text{water}} / (\text{km}^2 \cdot \text{year})$) is the individual FF of soil erosion of the site-specific land use in grid cell i .

2.2.3 Net removal rate

Helmes et al. (2012) developed a method to calculate the net removal rate to assess dominant processes for phosphorous persistence in freshwater, and we apply this

method to N. For the advection process, the net removal rate (k_{adv} , dimensionless) can be calculated directly by excluding retention and water consumption processes in the reciprocal of the FF of freshwater (Eq. 2.16). However, during the calculation of the FF, advection cannot be omitted and thus the net removal rates for retention and water use were estimated indirectly as the difference between the overall net removal rate (k_{all} , dimensionless) and the net removal rate excluding the corresponding process (Eq. 2.17 and Eq. 2.18). Finally, the dominant process is determined by the largest net removal rate occupied in each cell.

$$k_{adv} = \frac{1}{FF_{adv}} \quad (2.16)$$

$$k_{ret} = k_{all} - k_{nocon} = \frac{1}{FF_{all}} - \frac{1}{FF_{nocon}} \quad (2.17)$$

$$k_{con} = k_{all} - k_{nocon} = \frac{1}{FF_{all}} - \frac{1}{FF_{nocon}} \quad (2.18)$$

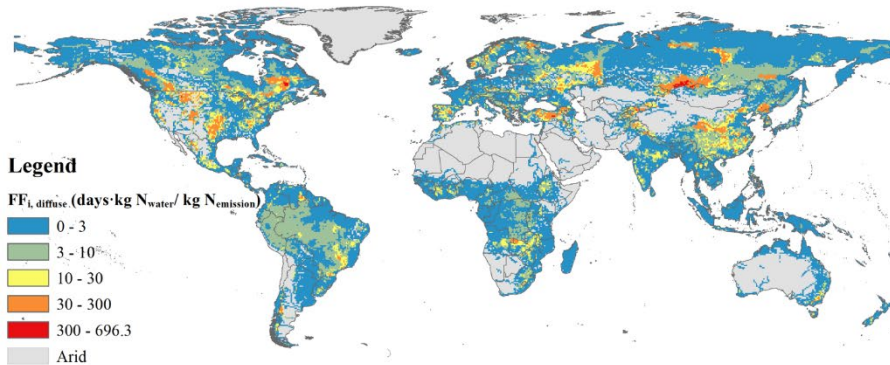
2.3 Results

2.3.1 Global spatially explicit fate factors

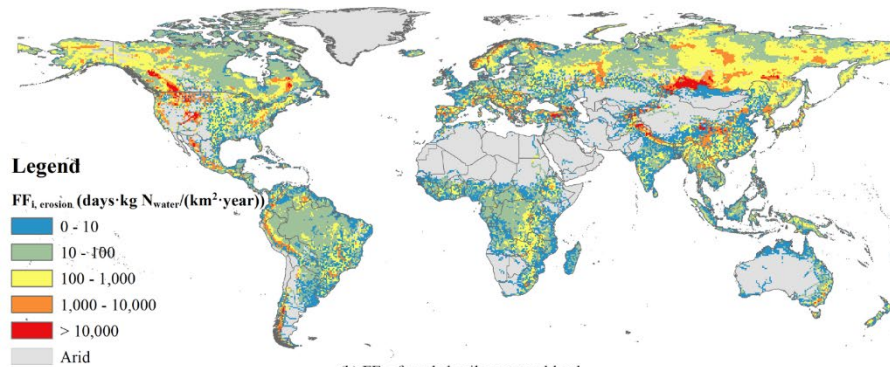
The cumulative FFs (Figure 2.2) show a distinctive spatial differentiation pattern over the globe. For instance, the fate factor of freshwater ($FF_{i,freshwater}$) has hotspots mainly located in North America, Central Asia, Russia, and Turkey; with high values also occurring in the east of South America, South Africa, East Asia, and East Europe. Furthermore, $FF_{i,freshwater}$ has a considerable variability, as its 5th and 95th percentiles are 0.9 and 184.0 days, respectively. The hotspots and high values of the $FF_{i,freshwater}$ are distributed in large reservoirs and lakes and their upstream sources. For instance, in North America, the hotspots of the $FF_{i,freshwater}$ are distributed in the upper reach of Colorado River, at the upstream of Lake Powell and Lake Mead, together with Missouri River, at the upstream of Lake Sakakawea, Manicouagan reservoir, and Lake Oahe. In Asia, the hotspots are situated Lake Qinghai, Lake Baikal,

and the Keban Baraji reservoir. In Europe, the hotspots of FFs appear in North Europe, Spain, and Turkey. Low values of $FF_{i,freshwater}$ are commonly situated near the coast.

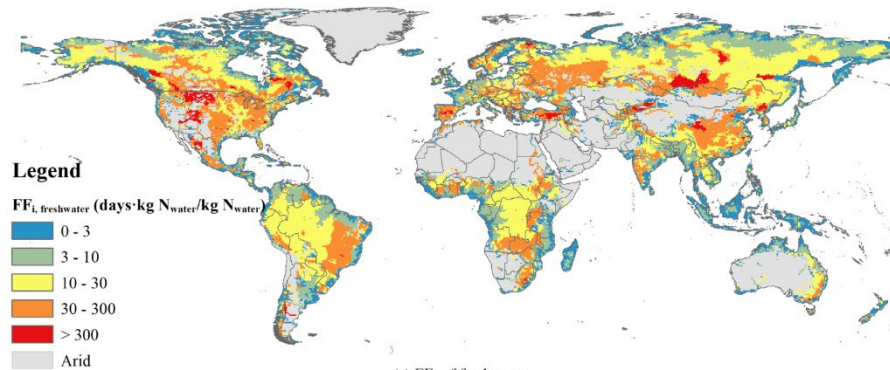
The cumulative FFs of direct emission to freshwater, diffuse emission, and erosion show similar patterns. The 5th and 95th percentiles are 0.04 and 27.3 days·kg N_{water} / kg $N_{emission}$ for $FF_{i,diffuse}$, and 5.2 and 2496.6 days·kg N_{water} / (km²·year) for $FF_{i,erosion,natural}$.



(a) FF_i of diffusive source on the soil



(b) FF_i of eroded soil on natural land



(c) FF_i of freshwater

Figure 2.2 Cumulative FFs (fate factors) for N emission to freshwater for $0.5^\circ \times 0.5^\circ$ grid cells. (a) diffuse sources excluding erosion, (b) baseline erosion on natural land, and (c) direct emissions to freshwater, including point sources. For erosion, the

difference of FFs between anthropogenic and natural erosion can be derived by multiplying with $c_{landuse}$. $c_{landuse}$ for arable land and grassland are 45.30 and 2.41, respectively.

2.3.2 Regional averages of fate factors

Since life cycle inventories are usually reported at the national level (e.g. ecoinvent, (Wernet et al., 2016)), we also analyze the regional average FFs to match that spatial scale (Figure 2.3, data can be found in Supporting Information Table S2.1). Generally, geographic regions that contain no large lakes or reservoirs tend to have lower cumulative FFs, and thus emissions from those regions typically have less impact on the regional FFs. Conversely, regions that have a large portion of lakes and reservoirs, tend to exhibit higher regional FFs. For instance, there are 5 geographic regions with a regional average FF of direct emission to freshwater larger than 100 days, while 39 geographic regions have an average FF lower than 3 days (Figure 2.3). As for continents, the regional average FFs of direct emission to freshwater varies from 20.0 days in Africa to 41.2 days in North America as calculated from aggregated values in Figure 2.3. The emission-weighted global average FFs for direct emission to freshwater is 29.3 days.

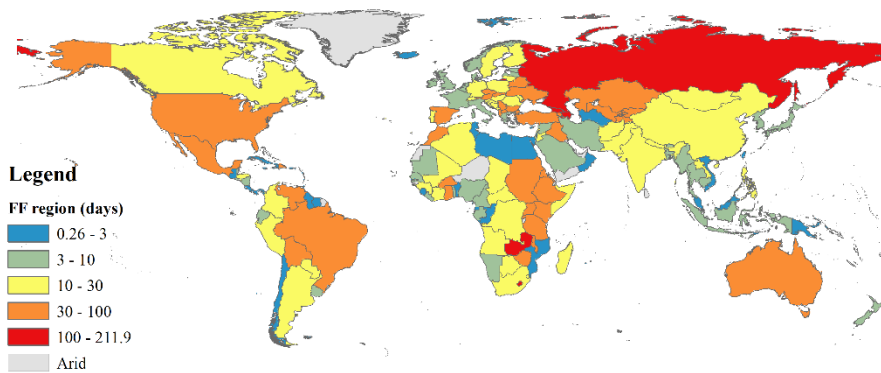


Figure 2.3 FF_{region} . This figure presents cumulative FFs (fate factors) of direct

emission of N to freshwater over geographic regions (e.g. country scale). Other regional FFs are given in the Supporting Information Table S2.1.

2.3.3 Dominant removal process for N fate

The dominant removal process for N transported to freshwaters differs across the globe (Figure 2.4). In the northern hemisphere, retention dominates the cumulative FFs in most areas of North America, Eastern Europe, and Central Asia, while in the southern hemisphere, retention dominates in the eastern side of the continents. In contrast, advection is the main contributor in coastal areas as well as South America, northern and eastern Asia. Water consumption dominates in some water-deficient areas, e.g. Northern India and the Beijing-Tianjin Metropolitan Region in Northern China. Globally, advection is the largest net removal process, dominating 69.7% of the global area; while retention is the main removal process for 29.0% of the global area; and water consumption is the prevailing process in 1.3% of the global area. The global map of the contribution of each removal process can be found in the Supporting Information Figures S2.6 – S2.8.

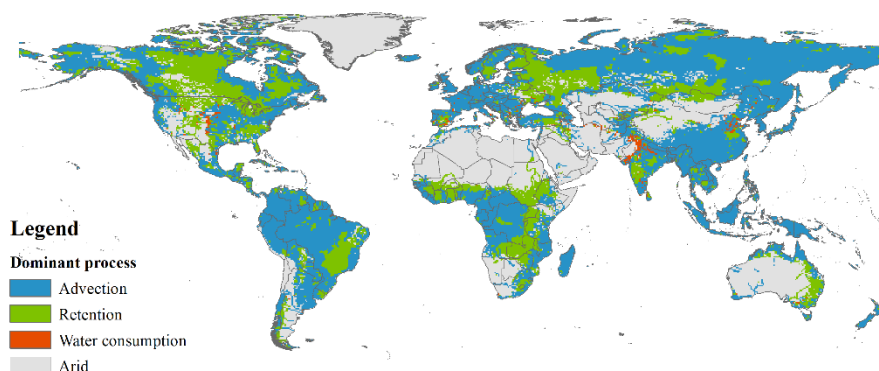


Figure 2.4 Dominant processes of net removal rate for cumulative FFs (fate factors) on a global scale. Because FFs of different emission routes only vary in the fraction of N transported from the emission to water ($fr_{e \rightarrow i}$) which is irrelevant for removal rates,

dominant processes are analyzed based on FFs of freshwater.

The overall statistical distribution of cumulative FFs and their main drivers (residence time, discharge, and aridity index, whose global maps can be found in Supporting Information Figures S2.10 - S2.12), are grouped according to the corresponding dominant process for each grid cell: advection, retention, or water consumption in Figure 2.5. The grid cells dominated by advection are mainly clustered in the interval of low residence time (the 95% quantile is 12.9 days) and their average residence time is 5.3 days. For these cells, the average discharge is 792.5 m³/s, which is much higher than the 263.6 m³/s and 16.9 m³/s for cells dominated by retention and water consumption respectively. Advection is also the main contributor to all grid cells with high discharge ($\geq 10^4$ m³/s). High discharge and low residence time are the typical hydrological features of large rivers, especially near the mouth. Therefore, most of the grid cells controlled by advection are distributed in the river basins of large rivers. Retention is the most significant process in grid cells where the residence time is high (the average residence time in retention-dominated cells is 92.5 days) and discharge is low, which means that retention controls the removal process in lakes, reservoirs, and near the source. Grid cells dominated by water consumption have a firm relationship with the aridity index (AI), and they are all distributed in the low-AI zone (AI < 1.24), showing that water scarcity plays an important role in these regions. In particular, the AI of 97% of these grid cells is lower than 1, which indicates that evaporation is higher than precipitation.

The cumulative FFs of cells dominated by retention are high, as its average is 99.5 days, while the averages of the cells controlled by advection and water consumption are 20.1 days and 16.2 days respectively. These findings agree with Helmes et al. (2012), as they found that most of the retention-dominated cells have a high residence time and the cells dominated by water use are distributed in the arid zone.

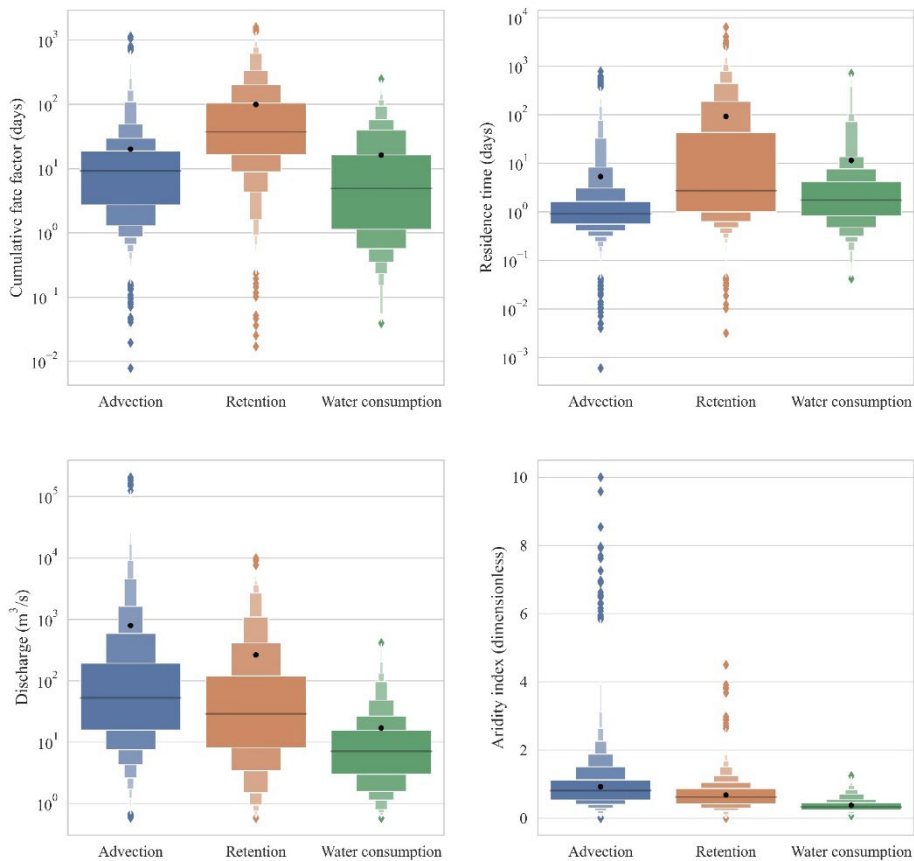


Figure 2.5 Letter-value plots of cumulative FFs (fate factors), residence time, discharge, and aridity index of N for different dominant processes. The black line in each letter-value plot denotes the median of the data, and the black dot indicates the average value. The widest box is the range of approximate 1/4 to 3/4 quantile, the lower box of the second widest is the approximate 1/8 to 1/4 quantile, and the next lower box is the approximate 1/16 to 1/8 quantile, recursively (Heike et al., 2017). Note that the width of the box does not denote the probability density of element and its value is arbitrary.

The FFs spatial variability is thus largely driven by the local hydrological conditions, especially residence time and the discharge. For instance, according to GLWD1 and the World Lake Database (Hersch, 2012), Zambia contains six major lakes (surface area

$\geq 1000 \text{ km}^2$) and three large water bodies (surface area ranging from 100 to $<1000 \text{ km}^2$), which favor long residence times, and it is a hotspot of regional FFs in our study. In contrast, its neighboring country, Mozambique, has an extensive river network with high discharges with only one major lake and four large lakes, which favor removal through advection and is in the lowest FF class. Examples of discharge driving FF spatial heterogeneity include the difference between the Amazon River ($209,000 \text{ m}^3/\text{s}$) versus the São Francisco River ($2,943 \text{ m}^3/\text{s}$) and Paraná River ($17,290 \text{ m}^3/\text{s}$) in South America. The higher advection rate in the Amazon River results in comparatively lower FFs. Similarly, river sub-basins tend to have lower discharge and thus a higher FF than the main downstream branch. An example of this latter phenomenon is the Missouri River, which, as an upstream branch of the Mississippi River, has a fraction of its discharge ($2,478 \text{ m}^3/\text{s}$ vs $16,790 \text{ m}^3/\text{s}$), and thus a higher FF.

While this analysis shows that the cumulative FFs are highly related to the hydrological condition, the regional FFs also depend on the amount and location of the emission sources (e.g. synthetic fertilizer use). Due to the high residence time and low discharge in cells with large lakes and reservoirs, emissions from the nearby upstream to these cells increase the risk of N enrichment and persistence. For instance, agricultural emissions upstream of lakes and reservoirs (e.g. Lake Qinghai and Lake Baikal) may result in over 300 days of N persistence in the region, while fertilizing the same amount downstream of these lakes, reservoirs, or large rivers (e.g. Amazon River and Nile River) may only let N reside for 10 days, owing to high removal rates, thus causing lower eutrophication impacts.

2.4 Discussion

Our research calculates N FFs of three different emission routes at a half-degree spatial resolution and reveals the influence of hydrological conditions on N persistence, which affects the vulnerability of freshwater bodies to eutrophication. The local hydrological conditions depend on geological features, climate, and the presence of dams. For

instance, large rivers with high discharge and low residence time always appear in humid regions with steep terrain. These areas thus tend to have low FFs, whereas a dam increases the residence time, hence the higher FFs in river basins with a dam. Emissions from anthropogenic sources (e.g. via industrial and agricultural activity) in those regions with high FFs may cause severe eutrophic impacts on downstream areas. Through our analysis of FFs, spatial patterns have for the first time been quantified for inland N at the sub-degree grided scale and build the foundation to allow LCA practitioners to assess the regional eutrophic impact of N over the globe.

We also highlight that FF temporal variations even in subsequent years can be quite substantial in urban regions with a massive population, as attested by the RSD of FFs between 1998 and 2000 (Supporting Information Figure S2.9). This reveals that the nutrient fate in freshwater systems is a dynamic process and reinforces the necessity of using dynamic models to derive FFs to complement current steady-state LCIA models.

2.4.1 Comparison with other models

This research builds on previous studies, and it provides FFs of inland N emitted both from the soil and directly to freshwater. Previous research of Cosme et al. (2018) extracted hydrological parameters from the Global NEWS 2 model (Mayorga et al., 2010), in which the residence time was also used to estimate denitrification, and constructed a FF model for the global coast. Cosme et al. (2018) aimed at modeling the persistence of dissolved inorganic nitrogen (DIN) in the receiving coastal large marine ecosystems, and also provided information of inland N fate at the watershed scale as a complementary result to N discharge toward the ocean. The basin-area-weighted riverine FF for DIN of Cosme et al. (2018) is 96 days, while Payen et al. (2021), who also applied NEWS2, calculated the global average of freshwater FF for DIN as 257 days. Compared to their results, our global average FF of TN (29.3 days) is lower. Hotspots partly agree, but not always. For example, both Payen et al. (2021) and we identified hotspots in the Mississippi River and Ob River, while these are not hotspots

according to Cosme et al. (2018); Payen et al. (2021) also identified hotspots in the Ganges River and the Hudson Bay, while these are not hotspots according to our FFs or the ones of Cosme et al. (2018). The discrepancy between our FFs and their FFs results from the difference in nitrogen indicators (DIN vs. TN), as well as the different mechanisms of nutrient models, methods of calculating FFs, and spatial delineations. For instance, van Vliet et al. (2019) showed that global TN export of NEWS2 (45 Tg year⁻¹) is higher than that of IMAGE-GNM (37 Tg year⁻¹) due to the difference in hydrological input data, spatial resolution, and the estimation of retention. Besides, the ratios between DIN and TN also exert large variation in different rivers. For example, the ratios have been found to be 50% for the Yangtze River (Yan et al., 2001) and 86% for the Mississippi River (Goolsby et al., 1999).

The model by Helmes et al. (2012) put forward an inland FF model for P for 0.5°×0.5° grid cells. Due to different hydrodynamic and biochemical processes, there is a clear difference between N and P cycles (e.g. N has a variety of redox forms, and undergo denitrification and exchange with the atmosphere, while most P in nature exists in solid or dissolved form). The difference between N and P is reflected in the retention, which in both cases is calculated based on regression methods. The retention rates of Helmes et al. (2012) are a fixed value in each interval (71.2 year⁻¹ if discharge < 0.0882 km³year⁻¹, 25 year⁻¹ if 0.4473 < discharge < 0.0882 km³year⁻¹, and 4.4 year⁻¹ if discharge > 0.4473 km³year⁻¹), while retention rates in our study are site-dependent, the average of which for these intervals are 92.1 year⁻¹, 32.4 year⁻¹, and 18.4 year⁻¹, respectively. Moreover, Helmes et al. (2012) did not consider domestic and industrial water consumption. Higher N retention rates together with domestic and industrial water consumption result in lower FFs in our study. Nonetheless, the distribution of low-to-high values of P cumulative FFs (Helmes et al., 2012) is consistent with our model on a global scale, especially for the hotspots in North America, Central Asia, and Turkey. Furthermore, our model's spatial differentiation of dominant removal processes is similar to Helmes et al. (2012).

2.4.2 Uncertainties

Current FF studies, including the one presented here, do not estimate sub-year variability, and thus ignore seasonal information. de Andrade et al. (2021) assessed the temporal and spatial variability of phosphorus FFs for freshwater in Bahia, Brazil, and concluded that FFs do not intensely vary monthly, although they recommended distinguishing two periods of higher and lower water availability. In contrast, their analysis suggests that FFs are highly site-dependent, thus it is important to regionalize eutrophication indicators. FFs in temporal regions, however, may be subject to much more pronounced seasonality, and thus the level of temporal variability on a global scale requires further study. Furthermore, in contrast to water consumption affecting only a few extreme grids cells, our results show that the cumulative FFs are related to hydrological features, retention, and other biogeochemical processes. Given that IMAGE-GNM and PCR-GLOBWB control these aspects, some uncertainties for these models are presented below.

2.4.2.1 Advection

The assumptions of the hydrological model PCR-GLOBWB introduce uncertainties in the estimation of advection. On the one hand, the reservoirs in PCR-GLOBWB are designated for hydropower generation and therefore it maximizes the available potential energy (Beusen et al., 2015), which can overestimate the real reservoir volume and could lead to an overestimation of FFs. On the other hand, PCR-GLOBWB divides multi-cell water bodies (i.e. lakes and reservoirs) by splitting the volume and combines multiple water bodies located within the same grid cell, ignoring the small water bodies if their total water volumes are lower than the volume of the river channel. This results in an underestimation of FFs due to an assumed lower water volume (774 out of a total of 6369 reservoirs were omitted in the year 2000) (Beusen et al., 2015).

Further improvement in simulating global gridded hydrological parameters in PCR-GLOBWB would provide a better assessment of eutrophication impacts.

2.4.2.2 Retention

The retention rate, as an argument in the inverse proportional function of FF, tends to have higher values when the water depth is underestimated (Eq. 2.11). Due to the proportional relationship between water volume and depth, the overestimated real reservoir volume in PCR-GLOBWB leads to an underestimation of the retention rate. Furthermore, the exclusion of small water bodies leads to an overestimation of the retention rate. In that case, FFs are inversely affected by the inaccurate estimation of retention removal rate. The empirical equation of Wollheim et al. (2006) is based on a first-order degradation process, assuming retention follows an exponential function of net uptake velocity and hydraulic load. However, there are also other options for empirical retention equations. For instance, Behrendt and Opitz (1999) and Venohr et al. (2005) assumed retention is a power function of surface water area, De Klein (2008) assumes that discharge plays a role in the retention process; while Seitzinger et al. (2002) only related the hydraulic load to retention. Empirical equations are limited in that they quantify retention ignoring chemical-mechanistic processes such as the interaction among different nutrient forms. Nevertheless, studies such as Vilmin et al. (2020) are increasingly incorporating mechanistic geochemical dynamics to better understand nutrient transport in the hydrosphere. With such information, N fate can be more precisely estimated by including the transformations among different N forms, including ammonium (NH_4^+), nitrate (NO_3^-), nitrite (NO_2^-), and organic nitrogen, together with increasing the temporal resolution of the model (Vilmin et al., 2020).

2.4.2.3 The exclusion of sludge

As we mentioned in the methods section, calculating the cumulative FFs for N only relates to the denitrification process in the soil and the hydrological conditions of the

water. Hence, the exclusion of sludge in IMAGE-GNM does not influence the calculation of the cumulative FFs. Nevertheless, the exclusion of sludge might affect the aggregation of regional FFs by underestimating the emission-weighting data for direct emissions to freshwater. This impact on the regional FFs is difficult to generalize as overestimation or underestimation due to the uneven distribution of the sludge's share of emission-weighting data.

2.4.3 Potential variation under the climate change

Despite increasing retention, throughout the 20th century, more nutrients have been exported to the coast (Beusen et al., 2016). Further into the future, this trend is set to continue due to increasing use of fertilizer and increasing population and wastewater discharge (Mogollón et al., 2018a; van Puijenbroek et al., 2019). However, under a warmer climate, more evaporation can lead to an acceleration of the hydrological cycle, which may lead to a higher water advection rate and more nutrient transport. Together with the stronger advection rate, predicted additional water extraction from surface and groundwater (Wada and Bierkens, 2014) may counteract the effect of more intensive nutrient emissions. More research into future scenarios is required to assess future FFs.

2.4.4 Implications for LCIA modeling

LCIA methods seek to characterize the fate of human emissions. Cosme et al. (2018) have shown that FFs contribute much more to the spatial variability of CFs than exposure or effect factors, which demonstrates the importance of regionalizing especially the FFs, as presented here. The application of a gridded FF model may improve LCIA methods with regards to previous spatially resolved models, as it includes more details of intra-basin heterogeneities. Additionally, this work complements existing P-related LCIA models, and thus both the N and P fate can be used to better assess global eutrophication. Our analysis shows the strong relationship between FFs and N removal processes, which is crucial to designing more sustainable

site selections for N emitting activities and to raise awareness on the potential environmental impacts of globalized manufacture, trade, and consumption in terms of the N cycle. For such implementation in LCIA, the FFs can be aggregated from the original half-degree resolution to an arbitrary regional scale by weighing according to the emissions, or in case of erosion, using the land use area. This will allow LCA practitioners to obtain the final fate for nutrients emitted during production in any region matching their inventory data.

2.5 Conclusion

We introduced N into the assessment of the environmental impacts on the global freshwater system as a co-limiting nutrient for eutrophication to complement present analyses based on P. Our spatially explicit approach provides global FFs of nitrogen for grid-based emissions both from the soil and directly to freshwater systems. Moreover, our study emphasizes the quantitative analysis of the connection between hydrological conditions and FFs. Our study revealed that FFs show conspicuous spatial heterogeneity because of differences in hydrological conditions and provided regionalized FFs which serve as midpoint indicators and can help LCA practitioners choose more sustainable production sites or suppliers.

Supporting Information

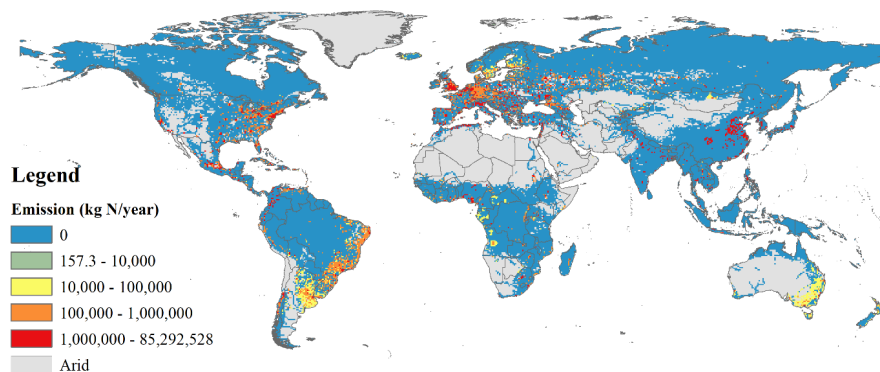


Figure S2.1 Global emission-weighting data of direct emission of N to freshwater

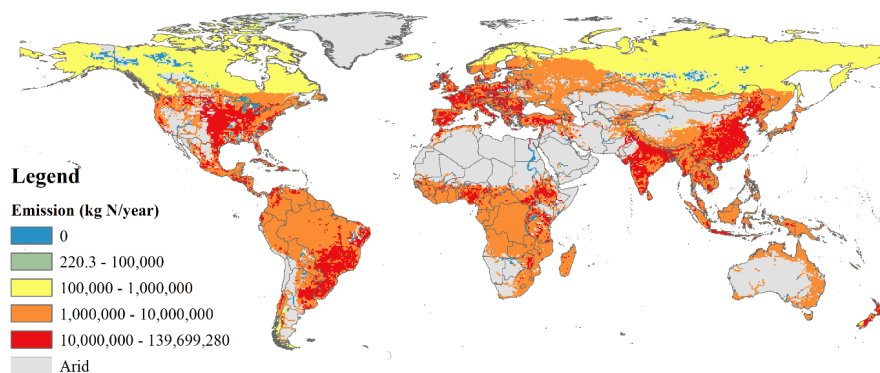


Figure S2.2 Global emission-weighting data of N of diffuse source to the soil

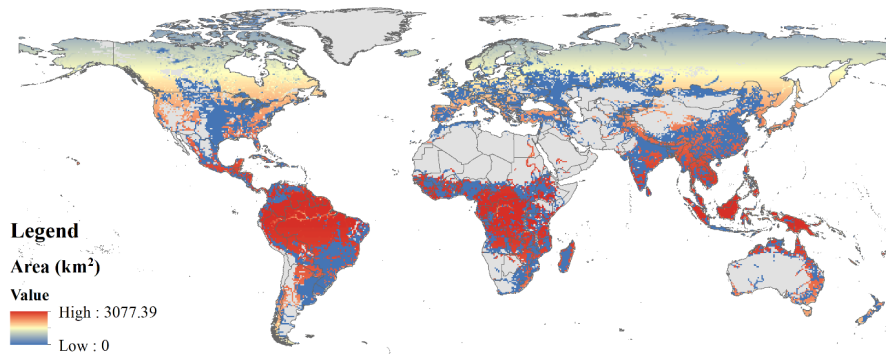


Figure S2.3 Global natural land area

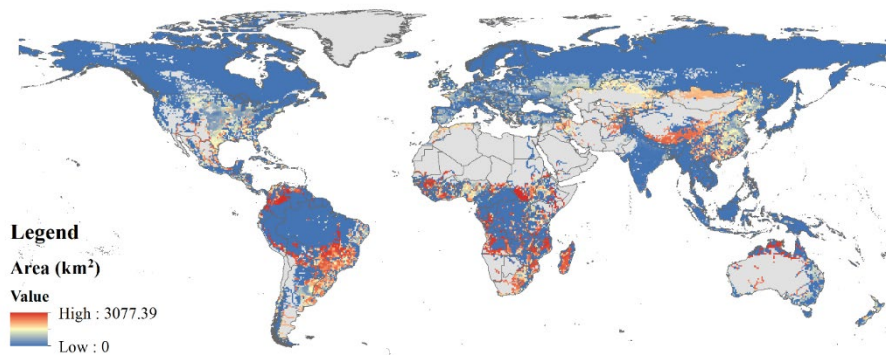


Figure S2.4 Global grassland area

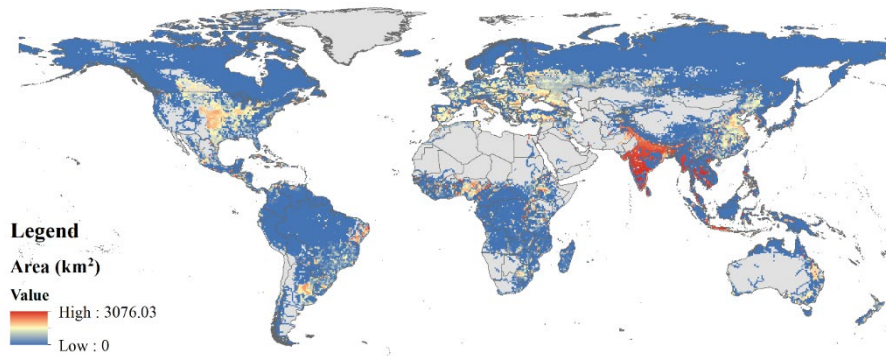


Figure S2.5 Global arable land area

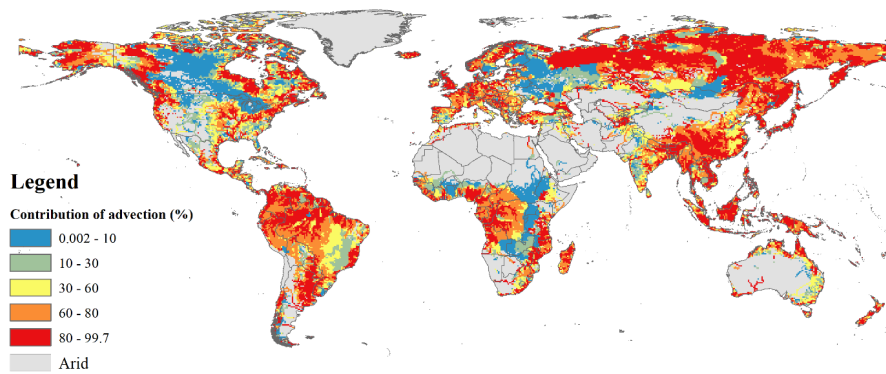


Figure S2.6 Global contribution of advection

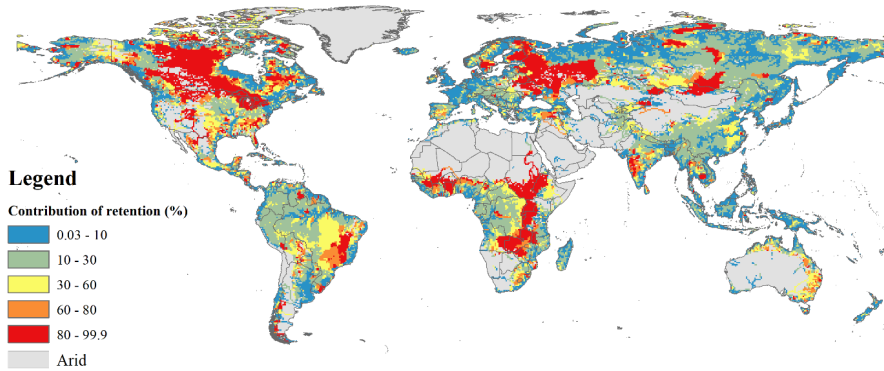


Figure S2.7 Global contribution of retention

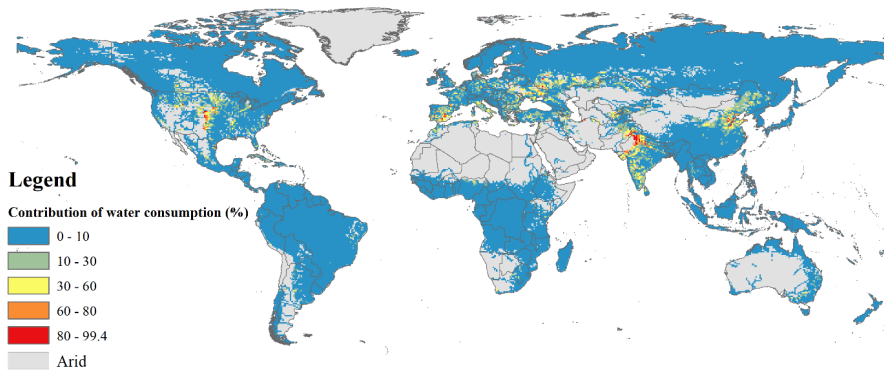


Figure S2.8 Global contribution of water consumption

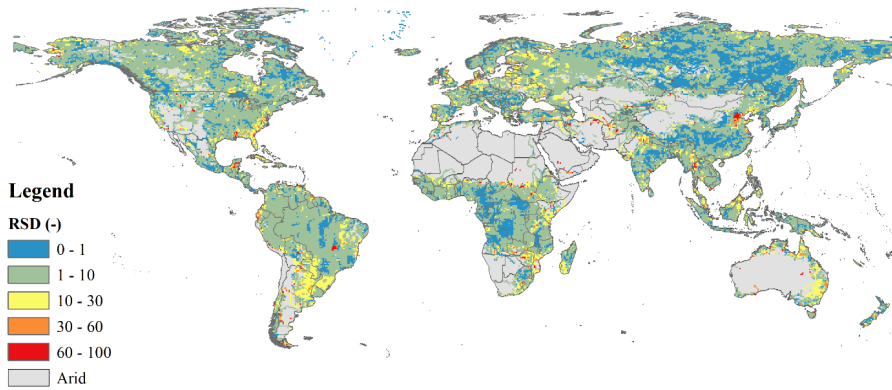


Figure S2.9 Relative standard deviation (RSD) of FFs between 1998 and 2000
(RSD is dimensionless shown as (-) in the legend.)

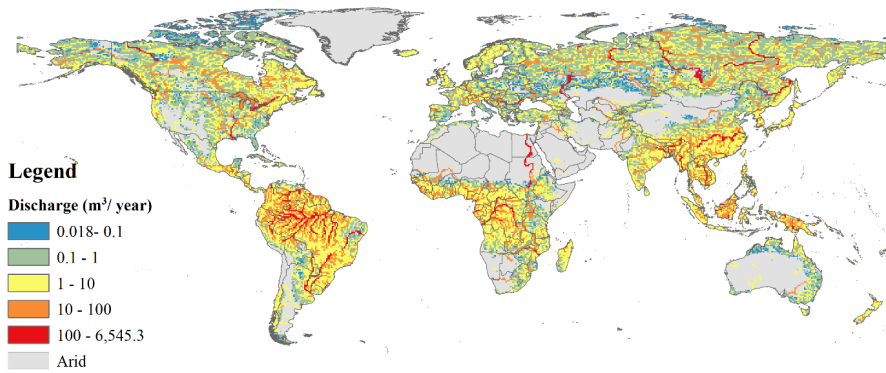


Figure S2.10 Global discharge

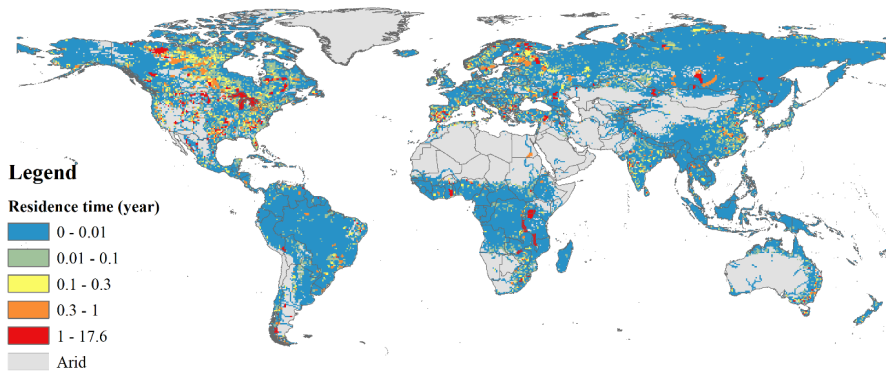


Figure S2.11 Global residence time

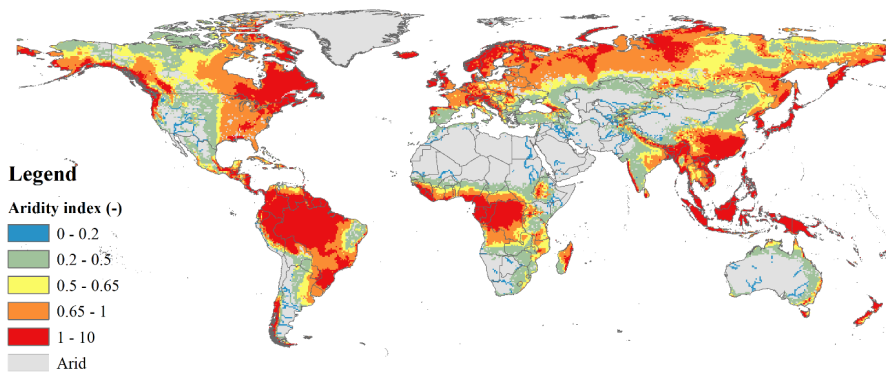


Figure S2.12 Global aridity index (AI, dimensionless shown as (-) in the legend.)

Table S2.1 Country-level fate factors (FFs)

Country	FFs for direct emission (days)	FFs for diffuse source (days kg N_{freshwater}/kg N_{emission})	FFs for erosion from natural land (days·kgN/(km²·year))
Åland	1.6	0.6	128.7
Afghanistan	17.5	2.8	2462.7
Albania	37.4	4.7	2761.7
Algeria	24.2	4.3	4346.5
Angola	17.8	4.6	240.1
Argentina	15.5	1	1802.0
Armenia	85.3	16.4	39715.2
Australia	30.5	1.9	989.4
Austria	30.8	4.9	8359.9
Azerbaijan	211.9	6.3	20848.3
Bahamas	No value	0.7	5.6
Brunei	0.9	0.3	6.0
Bangladesh	4.2	2.4	728.9
Belarus	47.7	3.8	1913.5
Belgium	7.4	2.4	1124.5
Belize	7.9	1.5	40.1
Benin	0.9	1.6	197.0
Bhutan	5.5	1.5	801.1
Bolivia	40.1	2.2	1242.0
Bosnia and Herzegovina	20.5	5.1	3990.3
Botswana	18.8	0.2	18.5
Brazil	52.7	4.5	1518.1
Bulgaria	60.5	7.1	12425.2
Burkina Faso	61.3	0.3	433.9
Myanmar	4.5	1.4	652.3
Burundi	No value	6.2	4607.4
Cambodia	3.1	1.6	156.6
Cameroon	9	2.4	788.7
Canada	26.3	7.9	1468.5

Country	FFs for direct emission (days)	FFs for diffuse source (days kg N_{freshwater}/kg N_{emission})	FFs for erosion from natural land (days·kgN/(km²·year))
Central African Republic	12.5	2.7	123.9
Chad	17.5	0.3	128.5
Chile	2.4	1.3	2420.0
China	20.2	13.3	12545.4
Colombia	10.2	2.8	2185.0
Comoros	No value	0.1	130.7
Republic of Congo	2.6	1.2	99.3
Democratic Republic of the Congo	16.7	2.8	583.4
Costa Rica	0.9	1.7	1863.2
Croatia	25.2	2.6	2505.2
Cuba	2.2	0.3	131.8
Cyprus	1.7	0	3.4
Czech Republic	43.7	11.4	19164.5
Côte d'Ivoire	No value	0	1064887.1
Denmark	6.1	1	408.7
Dominican Republic	33	5	6634.0
Ecuador	5.5	2.7	1148.7
Egypt	1.7	0	73.2
El Salvador	4.9	1.5	1672.4
Equatorial Guinea	0.6	0.6	41.6
Eritrea	67.7	0.4	851.1
Estonia	7.3	0.7	329.6
Ethiopia	38.2	3.4	4754.2

Country	FFs for direct emission (days)	FFs for diffuse source (days kg N_{freshwater}/kg N_{emission})	FFs for erosion from natural land (days·kgN/(km²·year))
Falkland Islands	0.9	0	93.2
Fiji	No value	0.1	23.7
Finland	13.7	3.1	179.7
France	4.6	1.2	1107.2
French Guiana	No value	1.7	39.7
Gabon	4.4	1.5	63.6
Gambia	1	0.1	173.2
Palestina	1.9	0.5	No value
Georgia	168.5	28.3	63093.3
Germany	20.3	1.9	2222.7
Ghana	34.7	3.5	1383.4
Greece	6.4	5.5	5488.6
Guadeloupe	0.9	0.2	4.5
Guatemala	2.3	3	3752.2
Guinea	29.9	2.3	608.0
Guinea-Bissau	No value	0.6	58.4
Guyana	1	1	31.5
Haiti	1.7	0.3	415.4
Honduras	27.2	7.6	8625.4
Hungary	24.9	1.1	3166.4
Iceland	2.2	1	203.0
India	14.6	3.3	3138.0
Indonesia	4.6	0.9	540.2
Iran	4.2	5.2	10877.7
Iraq	47.5	5	10289.7
Ireland	7	1.4	180.2
Israel	5.8	0.6	878.1
Italy	5	2.5	9311.5
Jamaica	0.9	0.2	105.9

Country	FFs for direct emission (days)	FFs for diffuse source (days kg N_{freshwater}/kg N_{emission})	FFs for erosion from natural land (days·kgN/(km²·year))
Japan	5.4	1.6	1095.4
Jersey	0.3	0	4.9
Jordan	15.2	1	1110.9
Kazakhstan	74.4	5.3	10956.0
Kenya	30.4	2.5	2671.5
Kyrgyzstan	66.9	44.1	84034.7
Laos	21.1	4.3	644.4
Latvia	9.9	0.5	416.3
Lebanon	22	0.8	458.7
Lesotho	132.8	17.4	25898.2
Liberia	3.4	0.7	59.1
Libya	2.6	0.2	95.8
Lithuania	12.8	1.6	628.8
Luxembourg	5.9	0.6	1211.5
Macedonia	41.5	11.8	25289.5
Madagascar	10.4	0.3	128.9
Malawi	53.5	5.1	1181.1
Malaysia	1.9	0.9	119.2
Mali	19.5	1.2	285.9
Mauritania	4.2	0.1	41.1
Mexico	52.9	8.2	12108.9
Moldova	27.7	2.9	26965.5
Mongolia	10.1	5.5	7502.5
Montenegro	10.1	18.1	2638.1
Morocco	31	5.7	17557.5
Mozambique	2.8	1.2	147.3
Namibia	7.1	1	88.1
Nepal	14.5	2.4	4746.9
Netherlands	8.2	1.4	258.4
New Caledonia	No value	0.3	29.6
New Zealand	9.9	3.2	6234.1

Country	FFs for direct emission (days)	FFs for diffuse source (days kg N_{freshwater}/kg N_{emission})	FFs for erosion from natural land (days·kgN/(km²·year))
Nicaragua	4	0.6	329.6
Niger	No value	0.2	490.6
Nigeria	5.8	0.7	947.3
North Korea	4	12.4	2479.0
Norway	4.5	5.9	772.0
Oman	0.3	0.1	3.1
Pakistan	12.9	3.8	12519.1
Vanuatu	No value	0.2	2.9
Panama	2.3	0.1	49.2
Papua New Guinea	1.7	0.8	99.2
Paraguay	20	1	303.1
Peru	23.2	5.4	3215.9
Philippines	10.6	1.1	545.1
Poland	20.7	1.1	1698.2
Portugal	16.3	4.3	4604.1
Puerto Rico	1.1	0.3	179.4
Reunion	0.4	0.1	116.3
Romania	27.1	3.2	8855.5
Russia	102.6	9.1	3113.9
Rwanda	39.9	5.1	22973.9
Saint Vincent and the Grenadines	0.6	0.1	1.4
Samoa	No value	0	No value
Saudi Arabia	9.9	0.1	12.7
Senegal	3.5	0.2	59.7
Serbia	49.5	7.5	29271.8
Sierra Leone	2.3	0.4	53.8
Slovakia	38.1	4.8	5591.0
Slovenia	26.2	5.2	1863.4

Country	FFs for direct emission (days)	FFs for diffuse source (days kg N_{freshwater}/kg N_{emission})	FFs for erosion from natural land (days·kgN/(km²·year))
Solomon Islands	No value	0.2	35.8
Somalia	12.3	0	44.6
South Africa	27.1	3.4	2145.9
South Korea	7.2	13.6	2656.1
Spain	84.4	10.1	18665.1
Sri Lanka	No value	1.7	369.6
Sudan	61.8	0.5	441.2
Suriname	1.2	2.7	34.5
Svalbard and Jan Mayen	0.4	0.1	11.9
Swaziland	24.8	2.7	3360.3
Sweden	13.8	5	545.0
Switzerland	20.5	4.8	7554.5
Syria	7.1	3.1	4566.1
Taiwan	2.2	0.9	1300.5
Tajikistan	42	11.6	10331.8
Tanzania	51.2	2.1	837.9
Thailand	9.9	3.8	1480.4
East Timor	1.1	0.2	587.1
Togo	5.9	5.5	2043.8
Trinidad and Tobago	1.2	0.2	3.9
Tunisia	2.4	3	6158.5
Turkey	83.9	39.7	46742.6
Turkmenistan	1.6	0.2	116.5
Uganda	74.2	1.6	3513.0
Ukraine	43.6	2.8	8658.4
United Kingdom	3.2	0.6	2672.1
United States	43.9	11.3	8761.3

Country	FFs for direct emission (days)	FFs for diffuse source (days kg N_{freshwater}/kg N_{emission})	FFs for erosion from natural land (days·kgN/(km²·year))
Uruguay	4.7	4.3	1777.1
Uzbekistan	37.1	5.5	5231.1
Venezuela	32.5	3.6	652.7
Vietnam	1.6	2.1	929.4
Virgin Islands, U.S.	0.8	0.2	1.3
Yemen	No value	0	5.2
Zambia	101.7	10.7	1661.8
Zimbabwe	37.8	5	1003.8

Chapter 3

A comparison between global nutrient retention models for freshwater systems

This chapter has been published as Zhou, J., Scherer, L., van Bodegom, P.M., Beusen, A.H.W., Mogollón, J.M., 2022. A Comparison Between Global Nutrient Retention Models for Freshwater Systems. *Frontiers in water* 4:894604.



Arthur Bensen

Abstract

Against the backdrop of increasing agricultural production, population, and freshwater/coastal eutrophication, studies are aiming to understand the behavior of nitrogen (N) and phosphorus (P) in the global freshwater system. Global nutrient models are typically used to quantify the nutrient amount and content in freshwater systems across different river orders and catchments. Such models typically use empirically derived nutrient retention equations for predicting nutrient fate, and these equations may be derived using data from a specific region or environment or for a specific context. Here we used IMAGE-GNM, a spatially explicit nutrient model at a half-degree resolution, to examine the performance of several well-known empirical equations by comparing the respective model outcomes with observed data on a global scale. The results show that 1) globally, the empirical retention equations work better for predicting N fate than P fate; 2) hydraulic drivers are the most important factor affecting the residual of total N and P concentrations, compared with the functional forms and the coefficients in the empirical equations. This study can aid in assessing the variability and accuracy of various retention equations from regional to global scales, and thus further strengthen our understanding of global eutrophication.

3.1 Introduction

During the 20th century, the global cycles of nitrogen (N) and phosphorus (P) have shown a rapid acceleration due to increasing nitrogen fixation and phosphate mining (Jenny et al., 2016). Over the 20th century, humans have almost doubled the global N and P delivery to freshwater systems from 34 to 64 Tg N yr⁻¹, and 5 to 9 Tg P yr⁻¹, respectively (Beusen et al., 2016). Due to a combination of N and P excessive nutrient loading, the global freshwater and coastal system has seen a major increase in eutrophication. Eutrophication can lead to the proliferation of algae blooms and hypoxia (Chislock et al., 2013; Müller et al., 2012), which consequently threatens the balance of environmental and ecological systems (Jenny et al., 2016; Vonlanthen et al., 2012; Schindler and Vallentyne, 2008). Toward the future, the rising trend of nutrient

accumulation in freshwater systems is set to continue due to the increase of fertilizer application and global population growth (Mogollón et al., 2018a). Moreover, warmer climates can lead to an acceleration of the hydrological cycle, which signifies both increasing evaporation and freshwater advection, and thus likely to exacerbate change in global nutrient cycles (Bouraoui et al., 2004; Statham, 2012). Thus, while global in-stream nutrient retention tends to vary slightly and stay stable under various future scenarios, N export to oceans is set to increase by up to 20% under future scenarios, unless human strictly takes sustainable practices in nutrient application and water use (i.e., Shared Socio-economic Pathway SSP1) (Beusen et al., 2022).

To better curb the increasing trend of eutrophication over the global aquatic system, the first step is to assess the fate of N and P, which requires regional to global nutrient models.

Despite the various modeling efforts, global estimates of nutrient exports are still highly variable. For instance, the estimated total phosphorus (TP) export of NEWS-2 (9 Tg yr^{-1}) is almost double the export of IMAGE-GNM (4 Tg yr^{-1} , Harrison et al. 2019), and total nitrogen (TN) of NEWS-2 (45 Tg yr^{-1}) is also higher than that of IMAGE-GNM (37 Tg yr^{-1} , van Vliet et al. 2019). van Vliet et al. (2019) and Grizzetti et al. (2015) reckoned that this issue results from the discrepancy in hydrological input data, spatial resolution, and the method used to calculate retention. Retention indicates the difference between nutrient input and output within a river segment or a lake. N retention includes the removal processes of denitrification, sedimentation, and uptake by aquatic vegetation (Saunders and Kalff, 2001), while P retention is affected by entrainment, sedimentation, sorption, as well as by uptake by plants and organisms (Reddy et al., 1999). Historically, retention is modeled through empirical equations based on regression analyses of localized nutrient input-output data (Behrendt and Opitz, 1999; Kelly et al., 1987). These regression analyses are based on localized studies (Kirchner and Dillon, 1975; Seitzinger et al., 2002). So far, current studies have never compared the performance of the various retention models globally. Identifying the best-performing retention models for global nutrient models can contribute to the

future knowledge of eutrophic impacts (e.g., nutrient loading/export to aquatic systems) (Jeppesen et al., 2009).

Kelly et al. (1987) proposed a mass balance model for N denitrification loss, and Howarth et al. (1997) employed this model to estimate N retention. Later on, Behrendt and Opitz (1999) found that this model can also be applied to P. They investigated 100 European rivers and developed a regression between retention and different hydraulic drivers, including hydraulic load and specific runoff. De Klein (2008) discovered large monthly variability in retention and the necessity to distinguish among drivers for N and P (e.g., P is highly related to temperature while N is not) after studying 13 catchments in the Netherlands and Germany. Furthermore, in contrast to N, P is susceptible to water body types due to its susceptibility to sedimentation and sorption (Reddy et al., 1999). Thus, the estimation of P retention should be based on different drivers for lakes vs. rivers. By analyzing 15 lakes in Canada, Kirchner and Dillon (1975) posited that the major driver of P retention was the areal water load (as opposed to the hydraulic load, the areal water load is related to specific runoff, Eq. 3.4), whereas Chapra (1975) argued that P retention could be better represented by apparent settling velocity in these lakes. Brett and Benjamin (2008) examined 305 input/output data of lakes and reservoirs in the USA and Canada and concluded that the main driver of lake P retention is residence time. In these studies, retention is dominated by hydrological drivers, i.e., hydraulic load and specific runoff. These drivers can only be converted from one into the other if the information of additional variables (i.e., water volume and depth) is provided. Such information is highly uncertain, which could potentially lead to biased estimates and increased uncertainties. Investigating this key feature was at the core of our study.

The aim of this study is to identify the best-performing retention model or set of regional retention models to assess the fate of global nutrients in freshwater systems. We adapted IMAGE-GNM to include a comprehensive set of retention equations. The retention models were examined by comparing the respective model outcomes with observed data. The model performance was also analyzed for different geographical

zones (“Geographical zone”, 2009), including the North Frigid Zone, the North Temperate Zone, the Torrid Zone, and the South Temperate Zone to discover the response of nutrient retention to hydrological conditions. The set of best-performing retention models can be applied to improve the accuracy of global nutrient models, which helps to better understand the global states of water quality.

3.2 Methods

3.2.1 Global nutrient model

In this study, we choose to use IMAGE-GNM (Beusen et al., 2015) as it is the best-fit nutrient model for our study among the most widely recognized nutrient models reviewed in MIPs (van Vliet et al., 2019). Of these, MARINA is a downscaled application of NEWS-2 to China and has not been employed for worldwide modeling (Strokal et al., 2016). HYPE has been used to estimate global hydrology (Arheimer et al., 2020), while for nutrients, this model was only developed at the regional scale, such as Europe (Strömbäck et al., 2019). Similarly, SPARROW was localized to the USA (McCrackin et al., 2013) and New Zealand (Alexander et al., 2002). Globally, NEWS-2 is differentiated at the watershed scale, while the resolution of IMAGE-GNM is gridded ($0.5 \times 0.5^\circ$). Thus, compared to NEWS-2, IMAGE-GNM captures the inner-basin information, which is unneglectable since the geographical variation of nutrients within large watersheds is highly uneven. This spatial delineation allows validating nutrient data since the measurement stations are scattered over the watersheds and cannot reflect the estimation of the whole watershed.

IMAGE-GNM is a dynamic distributed model that depicts nutrient flow and delivery processes in soils, freshwater systems, and export to coasts. A detailed description and the code (written in Python 2.7) of IMAGE-GNM can be found in Beusen et al. (2015). In this study, different retention equations were implemented into IMAGE-GNM. The simulated concentration of TN/TP in rivers and TP in lakes were compared with respective observed data. We distinguished between lakes and rivers when validating P estimates to account for the strong links between P fate and lake ecology (Brett and

Benjamin, 2008). For N, we deemed this distinction unnecessary since N retention can be entirely represented by the water discharge difference between these water bodies (Saunders and Kalff, 2001). Due to a lack of TN observations in global lakes, the performance of simulated TN in lakes was not assessed in this study.

3.2.2 Retention models

Load-weighted nutrient water body retention (R_L , dimensionless) indicates the proportion of retention load ($R_{N,P}$, kg yr⁻¹) to the load of nutrients transported to the freshwater system ($L_{N,P}$, kg yr⁻¹).

$$R_{L,N,P} = \frac{R_{N,P}}{L_{N,P}} = \frac{L_{N,P} - O_{N,P}}{L_{N,P}} \quad (3.1)$$

where $O_{N,P}$ (kg yr⁻¹) denotes the export of nutrients at the outlet of the water body.

In our study, we only included strictly empirical models of mostly pure hydrological nature. Some empirical models also account for ecological nature, namely hydro-ecological retention models, whereas in this study the only two models that may be considered hydro-ecological models are the model of Wollheim et al. (2006) (section 3.2.2.1.1 (1)) and De Klein (2008) (for P, section 3.2.2.1.2 (2)). In this study, however, we only focused on the hydrological part and represented ecological impacts by temperature factors. The hydrological drivers in retention models are represented by the empirical function of hydraulic drivers, including hydraulic load (Eq. 3.2) and specific runoff (Eq. 3.3). We elaborate on these functions raised in literature in sections 3.2.2.1-3.2.2.2 and summarize all models in Table 3.1.

$$H_L = \frac{D}{t_r} \quad (3.2)$$

$$q = \frac{Q}{A} \quad (3.3)$$

where H_L (m yr⁻¹) is the hydraulic load represented by quotient between the depth (D , m) and residence time (t_r , yr) of the water body; q (L km⁻² s⁻¹) is the catchment area-specific runoff, which equals the discharge (Q , L s⁻¹) divided by catchment area (A ,

km²).

The specific runoff can also be expressed as areal water load W_L (m yr⁻¹, Eq. 3.4), which denotes the annual value of the water column height per water surface area in the unit of specific flow:

$$W_L = \frac{q \times 8.64 \times 0.365}{W} \quad (3.4)$$

where q (L km² s⁻¹) is the specific runoff introduced in Eq. 3.3, W (%) is a ratio of the surface water area to the watershed area, and 8.64×0.365 is a coefficient to convert the unit from L km² s⁻¹ to m yr⁻¹.

3.2.2.1 Riverine retention models for TN/TP

3.2.2.1.1 Hydraulic-load-driven models

(1) Wollheim et al. (2006, 2008)

Current IMAGE-GNM employs Wollheim et al. (2006, 2008)'s equation as the retention model. Here, the retention $R_{L_{N,P}}$ is defined as a first-order degradation process (Eq. 3.5).

$$R_{L_{N,P}} = 1 - \exp\left(-\frac{v_f}{H_L}\right) \quad (3.5)$$

where v_f (m yr⁻¹) indicates the net uptake velocity expressing the biochemical features of a nutrient. v_f for P (Eq. 3.6) takes a basic value of 44.5 m yr⁻¹ (Behrendt and Opitz, 1999) and is modified by the temperature factor $f(T)$ (Eq. 3.8):

$$v_{f_P} = 44.5 \cdot f(T) \quad (3.6)$$

For N, v_f (Eq. 3.7) is initialized to 35 m yr⁻¹ (Wollheim et al. 2006, 2008) and modified by the temperature factor and concentration factor $f(C_N)$, which is proposed by Beusen et al. (2015):

$$v_{f_N} = 35 \cdot f(T) \cdot f(C_N) \quad (3.7)$$

where $f(C_N)$ represents the effect of concentration on denitrification resulting from electron donor limitation if excessive N is transported into the water (Mulholland et al.,

2008). $f(C_N)$ was calculated as an approximation of a hyperbolic function which contains the following points: 7.2 at $C_N = 0.0001 \text{ mg L}^{-1}$ and 1 at a turning point $C_N = 1 \text{ mg L}^{-1}$, and continues to decline mildly to 0.37 at $C_N = 100 \text{ mg L}^{-1}$ and keep constant for a higher concentration (Marcé and Armengol, 2009).

$$f(T) = \alpha^{T-20} \quad (3.8)$$

where α is 1.06 for P (Marcé and Armengol, 2009) and 1.0717 for N (Mulholland et al., 2008); T is average annual temperature ($^{\circ}\text{C}$).

(2) Kelly et al. (1987)

Kelly et al. (1987) proposed a simple mass balance model for the N denitrification losses in lakes and Howarth et al. (1997) used this mass transfer model to estimate the N retention of rivers. Behrendt and Opitz (1999) found this equation can be used to estimate phosphorus retention. Their studies have shown that this function form can be applied to both river systems and lakes.

$$R_{L,N,P} = \frac{S_{N,P}}{S_{N,P} + H_L} \quad (3.9)$$

where $S_{N,P}$ is an average mass transfer coefficient given in m yr^{-1} . Behrendt and Opitz (1999) estimated the mass transfer coefficient S_N for nitrogen (N) as 11.9 and S_P for phosphorus (P) as 16.1.

(3) Seitzinger et al. (2002)

Seitzinger et al. (2002) combined N observations from 10 rivers and 23 lakes in the USA. This study provided the equation of N retention as Eq. 3.10 and proved it applies to rivers, lakes, and reservoirs:

$$R_{L,N} = 88.45 \cdot H_L^{-0.3677} \quad (3.10)$$

3.2.2.1.2 Specific-runoff-driven models

(1) Behrendt and Opitz (1999)

Behrendt and Opitz (1999) investigated Dissolved Inorganic N (DIN) measurements

and provided two correlation equations for nutrients. While IMAGE-GNM calculates TN, DIN is the major component of TN. We, therefore, included these two equations in our research. Note that they defined “emission” as the inflow flux of nutrients to the aquatic system, which is equivalent to “load ($L_{N,P}$)” in IMAGE-GNM, while the term “load” used in their study indicated the nutrient exported at the outlet of the river, which equals the “output ($O_{N,P}$)” defined in IMAGE-GNM. Therefore, it necessitates a conversion from the output-weighted retention $R_{O_{N,P}}$ to load-weighted $R_{L_{N,P}}$ (Eq. 3.11).

$$R_{L_{N,P}} = \frac{R_{O_{N,P}}}{1 + R_{O_{N,P}}} \quad (3.11)$$

The first statistical equation is expressed by a power function of areal water load W_L :

$$R_{O_{N,P}} = a \times W_L^b \quad (3.12)$$

where a and b are statistical coefficients. For N, a equals 5.9 and b equals -0.75; for P, a and b are 13.3 and -0.93, respectively.

The second retention equation, in which the driving force is the catchment area-specific runoff q , can be expressed as:

$$R_{O_{N,P}} = c \times q^d \quad (3.13)$$

where c and d are statistical coefficients. For N, c is 6.9 and d is -1.10; for P, c and d are 26.6 and -1.71, respectively.

Behrendt and Opitz (1999) (W_L) and Behrendt and Opitz (1999) (q) were used to identify the retention equations driven by areal water load W_L and the catchment area-specific runoff q , respectively, in the following sections.

(2) De Klein (2008)

De Klein (2008) studied monthly TN retention for catchments whose areas ranged from 20.8 km² to 486 km². The results of this study showed that load-weighted nitrogen retention R_L is inversely related to surface water area-specific runoff (SR , m³ ha⁻¹ s⁻¹). The SR can be expressed as a ratio of specific runoff to the surface water area.

De Klein (2008) gave a retention equation based on the monthly time step. It was then aggregated to an annual scale by summing the monthly inputs and the estimation of

monthly exports. De Klein (2008) argued that the difference between monthly retention and annual retention of N was negligible, whereas, for P, the status remains uncertain. However, we assume that the equation still works for P at an annual time step.

Herein, the retention equation of N can be expressed as:

$$R_{LN} = 0.0246(SR)^{-0.57} = 0.0246 \left(\frac{e \cdot q}{W} \right)^{-0.57} \quad (3.14)$$

where e is a unit conversion coefficient of 10^7 , W (%) is the percentage of surface water area to watershed area (including land area and water area).

Besides SR , P retention is also determined by temperature:

$$R_{LP} = 0.253(SR)^{-0.20} \times 1.01^{(T_i - 22)} \quad (3.15)$$

where T_i is the average water temperature ($^{\circ}\text{C}$).

(3) Venohr et al. (2005)

Venohr et al. (2005) provided another group of statistical coefficients for TN retention based on the same dataset as Behrendt and Opitz (1999). Venohr et al. (2005) distinguished water bodies by assigning different coefficients for lakes, rivers, and reservoirs (Eq. 3.16):

$$R_{LP} = \frac{f \times W_L^g}{1 + f \times W_L^g} \quad (3.16)$$

where f and g are statistical coefficients. F is 1.9 and g is -0.49 for rivers; f is 7.279 and g is -1 for lakes and reservoirs.

3.2.2.2 Lake retention models for P

(1) Kirchner and Dillon (1975)

By analyzing nutrient budget information from 15 Canadian lakes, Kirchner and Dillon (1975) developed an empirical equation for the retention of phosphorus in lakes:

$$R_{LP} = 0.426 \exp(-0.271W_L) + 0.574 \exp(-0.00949W_L) \quad (3.17)$$

(2) Chapra (1975)

In contrast to Kirchner and Dillon (1975), Chapra (1975) argued that the retention of P can be more precisely related to both the areal water load W_L and the settling velocity

of P-contained particles (v), assuming the lake is at a steady state:

$$R_{LP} = \frac{v}{W_L + v} \quad (3.18)$$

where v (m yr⁻¹) is the apparent settling velocity of TP, which was estimated as 16 m yr⁻¹.

(3) Brett and Benjamin (2008)

Brett and Benjamin (2008) conducted a statistical reassessment of total phosphorus (TP) input/output data to determine which hydraulic driver is most strongly associated with lake phosphorus concentration and retention. They provided the best-fit equation as Eq. 3.19:

$$R_{LP} = 1 - \frac{1}{1 + 1.12t_r^{0.53}} \quad (3.19)$$

where t_r (yr) denotes the water residence time of lakes and reservoirs.

3.2.3 Sample data for validation

Water quality sample data, including TN and TP concentrations, were obtained from the Global Freshwater Quality Database (GEMStats, UNEP GEMS/Water Programme (2007)), Global River Chemistry Database (GLORICH, Hartmann et al. (2019)), and United States Geological Survey (USGS, Aulenbach et al. (2007)). We downloaded the datasets on September 17, 2021. The sample data from literature covers the main rivers of Africa and Asia, including the Nile River (El-Sadek, 2011; Sinada and Yousif, 2013), the Pearl River (Liu et al., 2009), the Yangtze River (Liu et al., 2018; Maotianet al., 2014; Sun et al., 2013a; Sun et al., 2013b), and the Yellow River (Chen et al., 2004; Tao et al., 2010). We used a DIN/TN ratio of 50% to transform dissolved inorganic nitrogen (DIN) into TN for the Yangtze River (Liu et al., 2018; Yan et al., 2001) and took a DIN/TN (the same as NO₃/TN, since nitrite NO₂ occupies less than 1% of DIN and the

Table 3.1 Summary of retention models proposed by previous studies

Approach	Driving force	Applicability	Nutrient	Original scale	Function form
Wollheim et al. (2006)	H_L $v_f (C_i, T_i)$	River and lake	N, P	Global	$R_{L,N,P} = 1 - \exp\left(-\frac{v_f}{H_L}\right)$
Kelly et al. (1987)	H_L	River and lake	N, P	North America and Norway	$R_{L,N,P} = \frac{S_{N,P}}{S_{N,P} + H_L}$
Seitzinger et al. (2002)	H_L	River and lake	N	Northeastern U.S.A.	$R_{L,N} = 88.45(H_L)^{-0.3677}$
Behrendt and Opitz (1999) (W_L)	W_L	River and lake	N, P	Europe	$R_{L,N,P} = \frac{a \times W_L^b}{1 + a \times W_L^b}$
Behrendt and Opitz (1999) (q)	q	River and lake	N, P	Europe	$R_{L,N,P} = \frac{c \times q^d}{1 + c \times q^d}$
De Klein (2008)	q	River and lake	N	The Netherlands	$R_{L,N} = 0.0246 \left(\frac{e \cdot q}{W}\right)^{-0.57}$
	q, T_i	River and lake	P	The Netherlands	$R_{L,P} = 0.253 \left(\frac{e \cdot q}{W}\right)^{-0.20} \times 1.01^{(T_i-22)}$

Venohr et al. (2005)	W_L	River and lake	N	Europe	$R_{LP} = \frac{f \times W_L^g}{1 + f \times W_L^g}$
Kirchner and Dillon (1975)	W_L	Lake	P	Canada	$R_{LP} = 0.426 \exp(-0.271W_L) + 0.574 \exp(-0.00949W_L)$
Chapra (1975)	W_L	Lake	P	Canada	$R_{LP} = \frac{v}{W_L + v}$
Brett and Benjamin (2008)	t_r	Lake	P	North America	$R_{LP} = 1 - \frac{1}{1 + 1.12t_r^{0.53}}$

Note: Driving forces are site-related variables to be determined by the observed or simulated data, whereas the non-driving-force parameters in the retention equation are constant coefficients provided by literature. Definitions of the variables as the driving force of retention: H_L (m yr^{-1}) is hydraulic load; W_L (m yr^{-1}) is areal water load; q ($\text{L km}^{-2} \text{ s}^{-1}$) is specific runoff; C_i (mg L^{-1}) is the nutrient concentration; T_i ($^{\circ}\text{C}$) is average annual temperature; t_r denotes the water residence time for lakes and reservoirs; v (m yr^{-1}) is the apparent settling velocity of total phosphorus.

ammonium concentration is low in rivers) ratio of 77% for the Nile River, the Yellow River, and the Pearl River (Turner et al., 2003). For computing TP, we used a ratio of 62% to transfer PO₄ into TP data (Turner et al., 2003).

We selected the data reported in the year 2000 since it is the last representative (most recent) year of IMAGE-GNM (Beusen et al., 2015). The samples include 9770 items of TN data from 1199 river stations, 19701 items of TP data from 2261 river stations, and 141 items of TP data from 23 stations of 7 lakes. The depth and residence time of lakes were derived from the World Lake Database (Herschey, 2012) except for Ashkui at narrows in Seal Lake and Wuchusk Lake, which lack measured data. For these two lakes, we applied the prediction of PCR-GLOBWB, the global hydrological model running on a grid cell level that has been integrated into IMAGE-GNM. Note that in the validation of lake retention equations, including Kirchner and Dillon (1975), Chapra (1975), and Brett and Benjamin (2008), we apply Wollheim et al. (2006)'s equation to calculate river retention in the cells that contain no lakes or reservoirs.

For validation, the cells with an invalid hydrological parameter (i.e., zero discharge and zero volume) were removed. To avoid errors raised by inadequate spatial data representation, basins with fewer than 10 grid cells were also excluded (Beusen et al., 2015). Consequently, 82% of the river sample items from 1157 river stations for TN and 91% of the river sample items from 2185 river stations for TP were included in the analysis (Figure 3.1). The validation was conducted based on a 0.5×0.5° grid-cell scale based on the resolution of predicted results of IMAGE-GNM. When stations were located within the same cell, the average of the samples was taken as observed data.

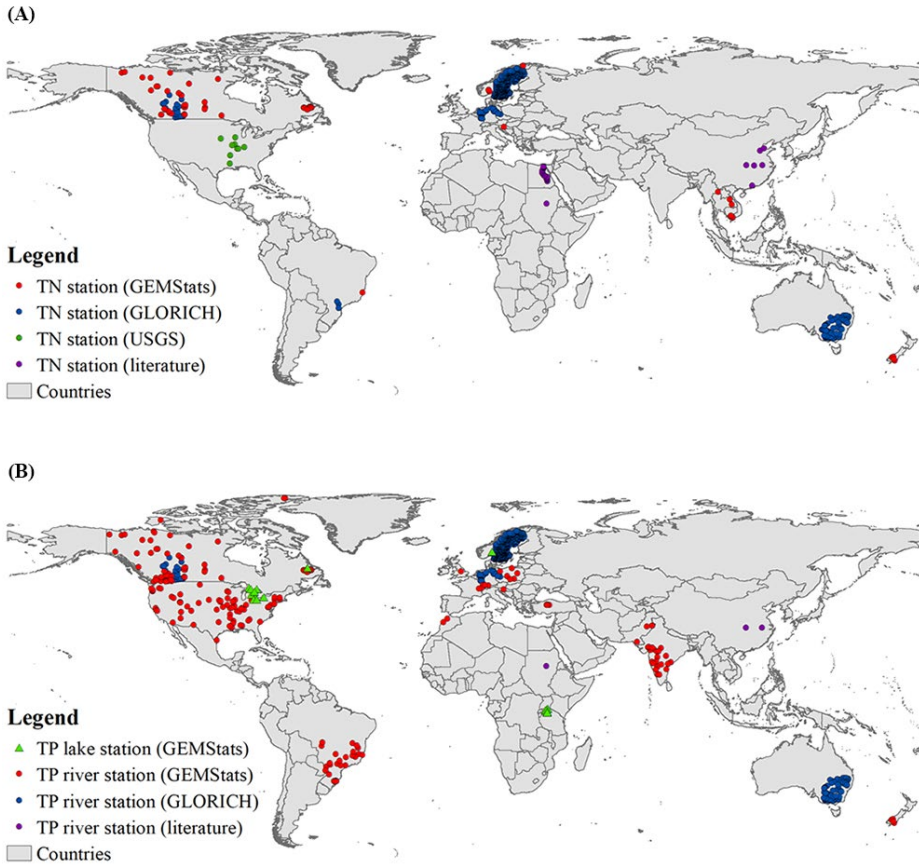


Figure 3.1 Sampling stations of (A) TN and (B) TP concentration over the globe. For N, all the stations are river stations. Note that (1) due to a lack of TN observations in global lakes, lake TN was not assessed in this study; (2) for TP, GEMStats has included USGS data. (3) in total, there are 1157 TN river stations including 63, 823, 261, and 10 stations distributed in North Frigid Zone, North Temperate Zone, South Temperate Zone, and Torrid Zone, respectively; for TP, the respective geographical zone contains 68, 1535, 493, and 89 river stations (2185 TP river stations globally).

3.2.4 Assessment of the model performance

We used the interquartile range ($IQR = Q_3 - Q_1$) to describe the dispersion and employed

Yule's coefficient (Yule's coefficient = $\frac{Q_3+Q_1-2Q_2}{Q_3-Q_1}$) to depict the skewness of simulated retention through non-parametric coefficient (Yule and Kendall, 1968); where Q_1 , Q_2 , Q_3 denote the 25th percentile, 50th percentile, and 75th percentile respectively.

We employed the mean-Normalized Root Mean Square Error (NRMSE) to evaluate the error between predicted and observed nutrient concentrations of each retention model.

$$NRMSE = \frac{1}{\bar{O}} \sqrt{\frac{\sum_{i=1}^n (O_i - P_i)^2}{n}} \quad (3.20)$$

where \bar{O} is the average of observations; n is the number of pairs of predicted-observed data; O_i and P_i are the observed value and predicted value of the i th cell, respectively.

The retention model that has a minimal NRMSE generates the lowest discrepancy between predicted values and observed values. NRMSE is a widely used criterion for the validation of nutrient concentrations (e.g., Beusen et al. 2015; Liu et al. 2018). However, NRMSE is quite sensitive to extremes, in particular to extremely high values. The Pearson correlation coefficient (r) is complementary to it and assesses the dynamic behavior of the model rather than the bias.

We used a logarithmic transformation to linearize the pairwise data and use r to evaluate the correlation between predictions and observations. Meanwhile, taking r of logarithmic data into account also lessens the likelihood risk of misjudging the performance of right-skewed residuals.

$$r = \frac{\sum_{i=1}^n (\log O_i - \overline{\log O_i})(\log P_i - \overline{\log P_i})}{\sqrt{\sum_{i=1}^n (\log O_i - \overline{\log O_i})^2} \sqrt{\sum_{i=1}^n (\log P_i - \overline{\log P_i})^2}} \quad (3.21)$$

Ideally, NRMSE is close to zero (on a range from 0 to unlimited) and r close to 1 (on a range from -1 to 1).

3.2.5 Significance of difference

We applied one-way Analysis of variance (ANOVA) to evaluate the significance of differences in performance among retention models. Here, as a measure of performance, the difference in simulated and observed concentration in a sampled grid cell was taken. The mean difference (i.e. whether a model consistently over- or underestimated retention and corresponding concentration) was evaluated.

To verify normality, the distribution of residuals of each model was judged based on probability plots. Then, we examined the homoscedasticity with the Brown–Forsythe test (Brown and Forsythe, 1974) due to its robustness and its maintenance of good statistical power (Derrick et al., 2018). TP showed heteroscedasticity and was analyzed with Welch’s ANOVA instead. To evaluate the differences in retention between specific pairs, we conducted a pairwise comparison using Tukey’s honestly significant difference (HSD) for homoscedastic data and a Games-Howell post hoc test for heteroscedastic data between pairs of samples.

The analysis was accomplished using Python 3.7. Details of packages/versions/functions are listed in Supporting Information Table S3.1.

3.3 Results

3.3.1 Validation

The plots of riverine simulation against observations show that the empirical equations perform better for TN than for TP (Figure 3.2 and Figure 3.3). Furthermore, the NRMSE of TN outcomes ranges from 1.62 to 2.31, which is much smaller than the NRMSE of TP whose interval is between 4.97 and 13.84. The Pearson's r of TN is higher than that of TP (Table 3.2 and Table 3.3).

The retention models of Behrendt and Opitz (1999) (q) generated the lowest NRMSE and a satisfactory Pearson's r (>0.5) for both N and P, being the best option for estimating riverine retention of TN/TP.

Among TN retention models, with the exception of Behrendt and Opitz (1999) (q) and

Seitzinger et al. (2002), the models' NRMSEs are higher than 2. The largest NRMSE (2.31) was generated by the retention model of Kelly et al. (1987) despite having the largest r value of 0.71. Behrendt and Opitz (1999) (q)'s r is 0.62, which shows an acceptable correlation between the simulated and observed concentrations. Hence, the retention model of Behrendt and Opitz (1999) (q) performs best for TN according to our analyses and validation dataset. Compared with Wollheim et al. (2006), which is the currently used retention equation in IMAGE-GNM, Behrendt and Opitz (1999) (q) can reduce the NRMSE by 41% for estimating riverine TN concentration globally. The retention model of Behrendt and Opitz (1999) (q) also simulated the lowest NRMSE (4.97) for P retention, followed by that of De Klein (2008) (6.40), whose Pearson's r is the lowest (0.26). Excepting the retention model of De Klein (2008), the difference in Pearson's r among the models is quite minor, ranging from 0.42 to 0.54. However, aside from Behrendt and Opitz (q) and De Klein (2008), the NRMSEs of the models exceed 10. The best-performing model, Behrendt and Opitz (1999) (q), can reduce the NRMSE of Wollheim et al. (2006) by 107%.

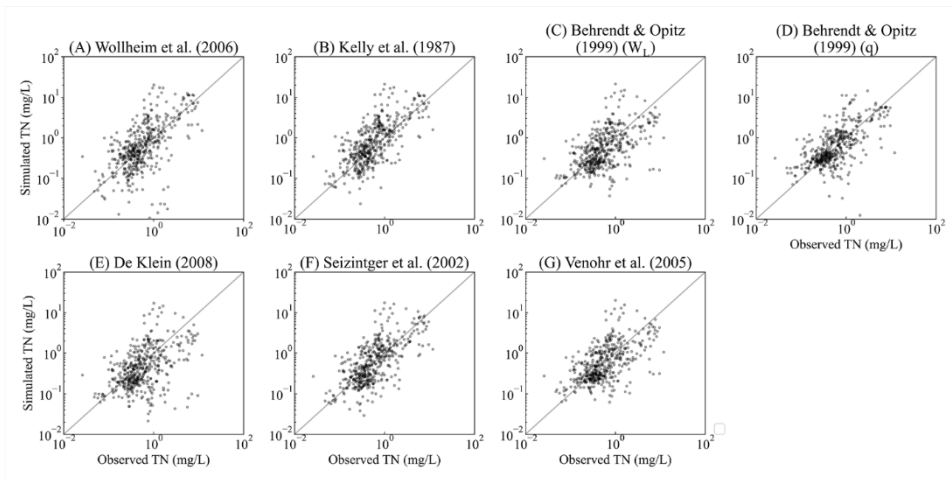


Figure 3.2 Validation of predicted values against observations of annual average concentration for riverine N (each dot represents the predicted values against average observed N concentration of the measurement stations within the same cell). The sample size is 449, the number of grid cells covered by measurement stations.

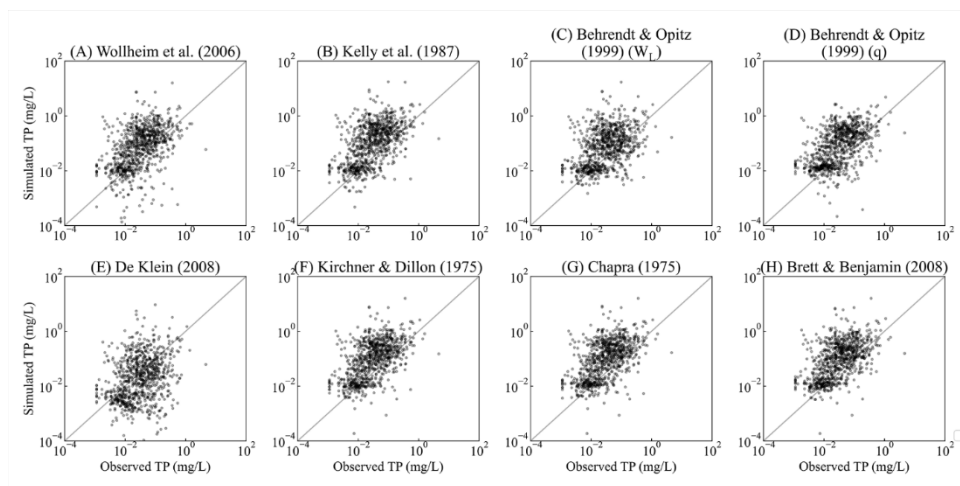


Figure 3.3 Validation of predicted values against observations of annual average concentration for riverine P (each dot represents the predicted values against average observed P concentration of the measurement stations within the same cell). The sample size is 849, the number of grid cells covered by measurement stations.

The comparison between simulated and observed TP concentrations in lakes is shown in Figure 3.4. Since the measurements vary considerably across the locations of stations within a lake, we plotted measurements as boxplots to show the variation. In Mjøsa and Wuchusk Lake, the simulations of all the models are higher than the observed TP concentration, while in other lakes, simulated TP is closer to the observations. De Klein (2008)'s residuals (i.e. the difference between simulated and average observed concentration in a lake) in Mjøsa and Wuchusk Lake are the smallest among empirical equations. Besides, De Klein (2008)'s simulations of other lakes do not deviate from the observed measurement intervals, yielding the best performing empirical equation. The NRMSE and Pearson's r of De Klein (2008) are 1.09 and 0.77 (Table 3.3). De Klein (2008) has the second-lowest NRMSE following Kelly et al. (1987) (0.89), but Kelly et al. (1987)'s r shows the second-worst performance (0.59). Behrendt and Opitz (1999) (q) has the highest Pearson's of 0.92 as well as the highest NRMSE (8.18). NRMSE and r of Wollheim et al. (2006) are 1.81 and -0.47, respectively, both of which perform worse than Kelly et al. (1987), Behrendt and Opitz (1999) (W_L), De Klein (2008), and

Brett and Benjamin (2008). Replacing the retention equation of De Klein (2008) with Wollheim et al. (2006) in IMAGE-GNM can reduce the NRMSE in lakes by 66%.

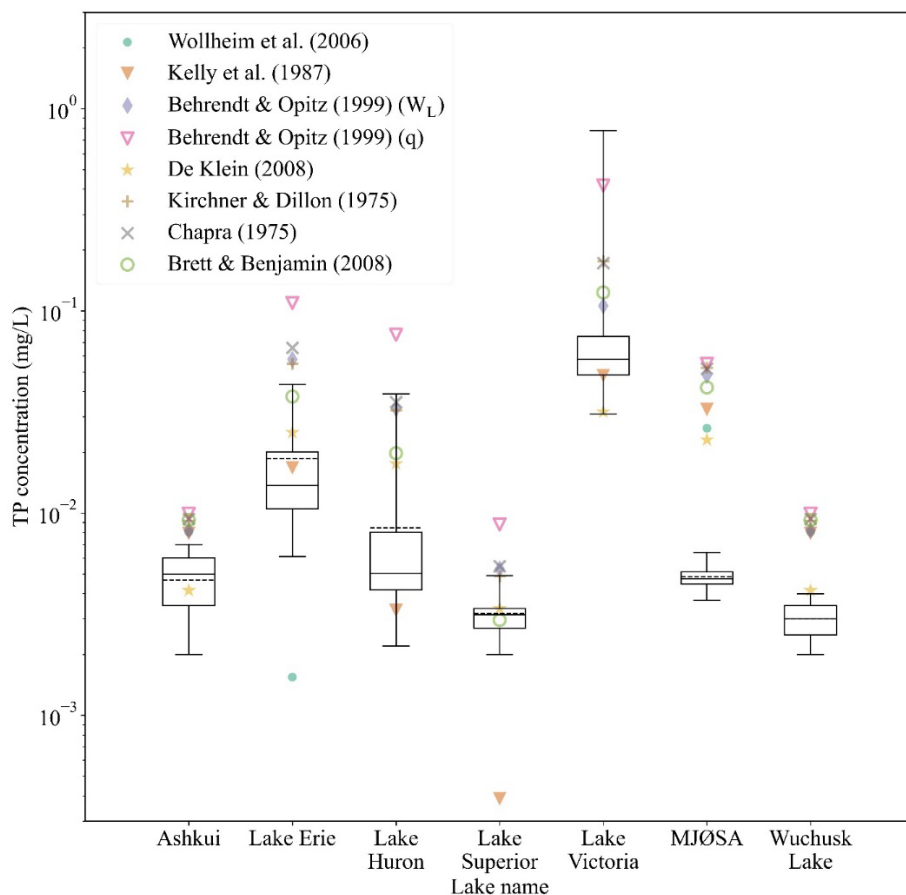


Figure 3.4 Simulated TP concentration of lakes compared with observed values. The boxplot shows the range of observed TP concentrations of each lake: the dark solid lines in the boxes are the median value of observations; the dark dash lines are the average of observations; the upper and lower borders of the boxes indicate 75th percentile and 25th percentile of observations; the whiskers denote upper and lower extremes of observations. IMAGE-GNM simulates lake concentration at the outlet cell of the lake, providing one value (average concentration) for each lake. Note that Wollheim et al.

(2006)'s simulation of Lake Huron, Lake Superior, and Lake Victoria is not shown in the log-scaled figure, as it predicted an extremely low concentration (< 0.0001 mg/L) for these lakes.

The performance of empirical equations differs by geographical zone (Table 3.2 and Table 3.3). For the N retention models, Behrendt and Opitz (1999) (q) obtained the lowest NRMSE in the North Frigid Zone, North Temperate Zone, and South Temperate Zone, which can lower the NRMSE by Wollheim et al. (2006) by 63%, 45%, and 32% in the respective regions. In the Torrid Zone, Venohr et al. (2005) performed the best, as it reduces the NRMSE by 88% compared with the currently used retention equation. For P, Behrendt and Opitz (1999) (q) is the best-performing retention model in North Temperate Zone and Torrid zone, reducing the NRMSE of Wollheim et al. (2006) by 132% and 146%, whereas the riverine retention model Wollheim et al. (2006) combined with the lake retention models of Kirchner and Dillon (1975) or Chapra (1975) provides the best fit of retention in the North Frigid Zone. Wollheim et al. (2006) is also recommended in the South Temperate Zone, as it has both the second-lowest NRMSE and the second-highest r . The best retention models of different geographical zones are presented in bold in Table 3.2 and Table 3.3 and listed in Supporting Information Table S3.2.

Table 3.2 Assessment of the performance of N retention models for rivers. The values of the best-performing models are shown in bold on a global or regional (geographical zone) scale. Note that only river samples were included due to a lack of lake sample data.

Region and Observation Type	Criteria	Wollheim et al. (2006)	Kelly et al. (1987)	Behrendt and Opitz (1999) (W_L)	Behrendt and Opitz (1999) (q)	De Klein (2008)	Seitzinger et al. (2002)	Venohr et al. (2005)
Global	NRMSE	2.29	2.31	2.12	1.62	2.02	1.93	2.04
	r	0.58	0.71	0.55	0.62	0.45	0.68	0.59
North Frigid Zone	NRMSE	0.57	0.51	0.42	0.35	0.49	0.48	0.43
	r	0.14	0.18	0.32	0.25	0.24	0.09	0.18
North Temperate Zone	NRMSE	2.35	2.33	2.10	1.62	1.99	1.85	1.97
	r	0.59	0.73	0.65	0.68	0.57	0.71	0.66
Torrid Zone	NRMSE	1.71	2.15	1.13	2.18	0.96	0.92	0.91

	r	0.05	-0.22	0.20	-0.31	0.16	-0.12	0.15
South	NRMSE	1.91	2.06	2.02	1.45	1.97	2.03	2.10
Temperate								
Zone	r	0.46	0.55	0.09	0.40	-0.02	0.49	0.19

Table 3.3 Assessment of the performance of P retention models for rivers and lakes. The values of the best-performing models are shown in bold on a global or regional (geographical zone) scale.

Region and Observation Type	Criteria	Wollheim et al. (2006)	Kelly et al. (1987)	Behrendt and Opitz (1999) (W_L)	Behrendt and Opitz (1999) (q)	De Klein (2008)	Kirchner and Dillon (1975)	Chapra (1975)	Brett and Benjamin (2008)
Lakes	NRMSE	1.81	0.89	1.59	8.18	1.09	2.70	2.73	1.47
Global	r	-0.47	0.59	0.83	0.92	0.77	0.87	0.87	0.84
Rivers	NRMSE	10.29	13.84	10.96	4.97	6.40	10.60	10.91	10.61

Global	r	0.42	0.54	0.42	0.52	0.26	0.54	0.54	0.54
North Frigid Zone	NRMSE	2.36	2.37	2.49	2.51	2.75	2.33	2.33	2.37
	r	0.32	0.28	0.05	-0.03	-0.67	0.35	0.35	0.23
North Temperate Zone	NRMSE	10.94	12.41	8.27	4.72	5.40	11.24	11.60	11.25
	r	0.39	0.56	0.48	0.55	0.33	0.56	0.55	0.55
Torrid Zone	NRMSE	11.40	27.35	26.48	4.64	14.22	11.52	11.54	11.50
	r	0.22	0.24	0.15	0.27	0.09	0.22	0.23	0.22
South Temperate Zone	NRMSE	4.90	7.99	6.96	5.67	3.03	5.56	5.81	5.57
	r	0.32	0.24	-0.05	0.31	-0.08	0.32	0.32	0.33

3.3.2 Retention model comparison

Figure 3.5 (TN) and Figure 3.6 (TP) show that different retention models generate similar hotspot distributions. The hydraulic-load-driven models (i.e., retention models of Kelly et al. (1987), Wollheim et al. (2006), and Seitzinger et al. (2002)) predicted relatively lower retention than specific-runoff-driven models (i.e., retention models of Behrendt and Opitz (1999), De Klein (2008), and Venohr et al. (2005)).

Despite different hydraulic driving forces among retention models, the hotspots of all the models are located in arid zones, South Africa, West Argentina, Mississippi River Basin, and Colorado River Basin. However, low retention values are quite distinct. For N, retention values under or equal to 0.1 cover over 50% of the global area in hydraulic-load-driven models (i.e., the retention models of Kelly et al. (1987), Wollheim et al. (2006), and Seitzinger et al. (2002)). In contrast, in specific-runoff driven models (i.e., the retention models of Behrendt and Opitz (1999), De Klein (2008), and Venohr et al. (2005)), low retention (≤ 0.1) occurs in only 24% to 30% of the global area. For P, regions with retention under or equal to 0.1 calculated by hydraulic-load-driven models (i.e., retention models of Kelly et al. (1987) and Wollheim et al. (2006)) occupy 58% and 66% of the global area, respectively. In contrast, low retention values (≤ 0.1) in specific-runoff driven models (i.e., the retention models of Behrendt and Opitz (1999)(WL), Behrendt and Opitz (1999)(q), and De Klein (2008)), occur in <36%. In particular De Klein (2008)'s model only generated 5% low-value retention globally.

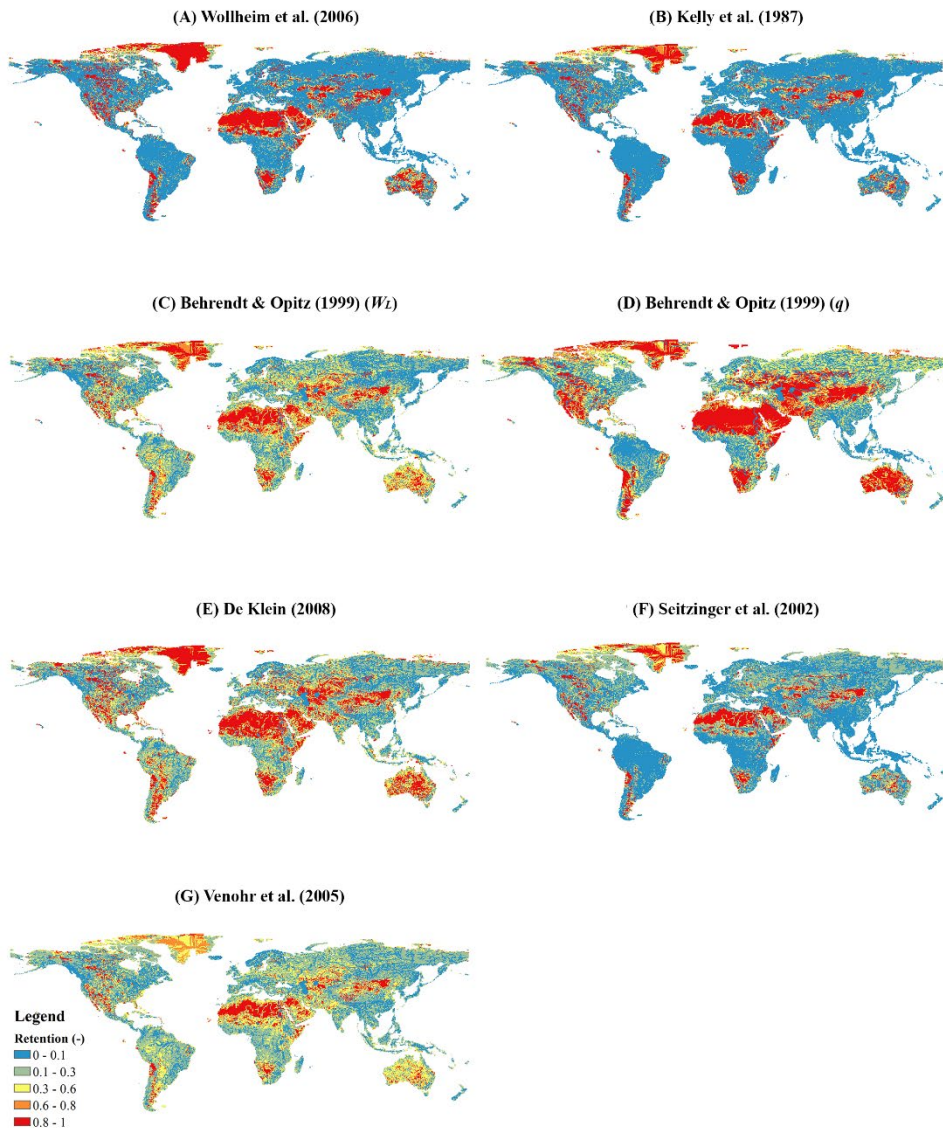


Figure 3.5 N retention for different models at a half-degree resolution (Retention is dimensionless, and the unit was labeled as “-”)

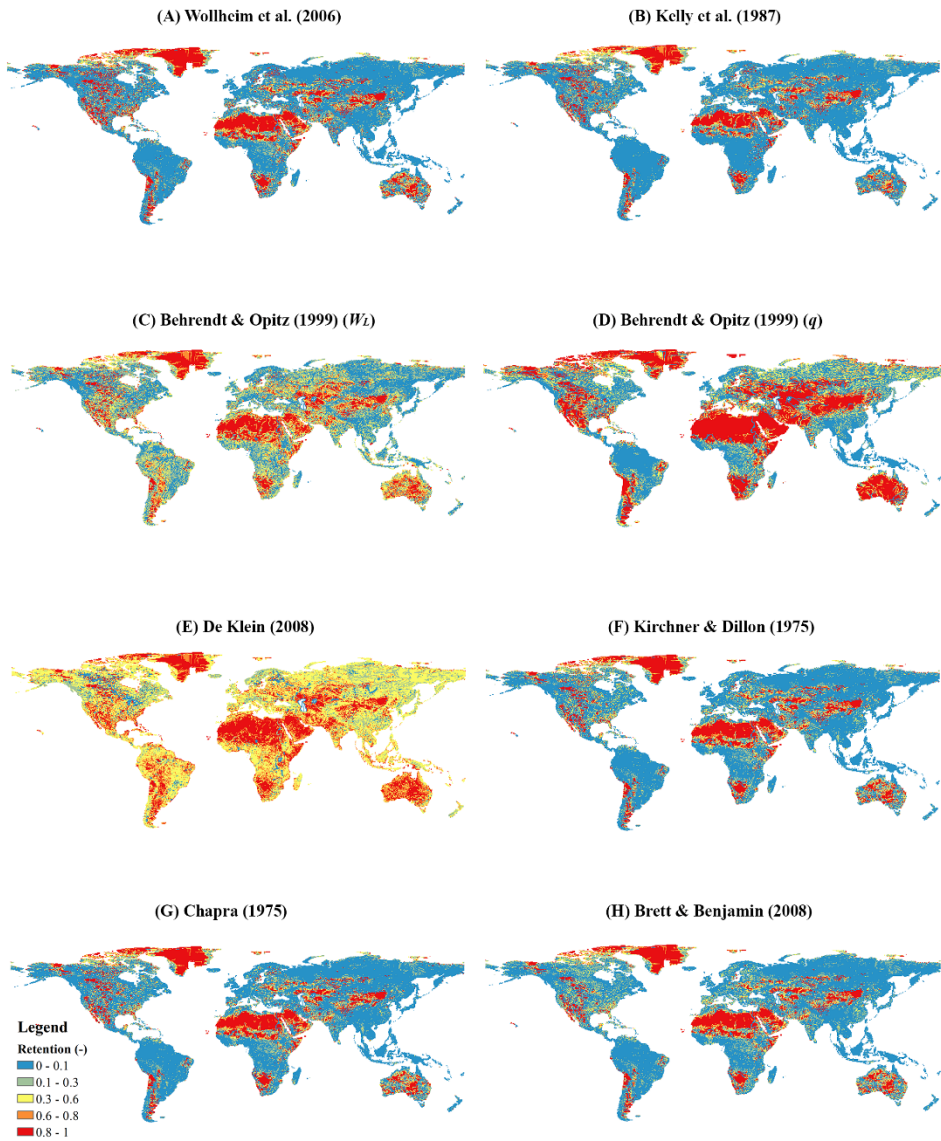


Figure 3.6 P retention maps for different models at a half-degree resolution (Retention is dimensionless, and the unit was labeled as “-”)

The dispersion (represented by IQR) and skewness (represented by Yule’s coefficient) between N and P retention showed only minor differences except for De Klein (2008)

(Table 3.4 and Table 3.5), which predicted a much smaller dispersion and skewness for P when compared with N.

For both N and P, the retention from hydraulic-load-driven models displayed larger skewness than specific-runoff-driven models. Yule's coefficient of retention predicted by hydraulic-load-driven models is larger than 0.5, while Yule's coefficients of specific-runoff-driven models range from 0 to 0.5. Thus, the retention simulated by models with a driving force of hydraulic load is more asymmetrically distributed than that of runoff-driven models. Nevertheless, the retention from all the models is positively skewed.

For N, the retention model of Behrendt and Opitz (1999) (q) predicted the largest average retention globally, followed by the simulation of De Klein (2008) and Behrendt and Opitz (1999) (W_L), while those models with a driving force of hydraulic load predicted relatively smaller average retention. The IQR of the simulation following Behrendt and Opitz (1999) (q) is the highest, revealing that the model simulates more dispersed retention than other models.

For P, the retention model of De Klein (2008) predicted the largest average retention globally, with the second and third largest average retention modeled by Behrendt and Opitz (1999) (q) and Behrendt and Opitz (1999) (W_L), respectively. In contrast, the retention models of Wollheim et al. (2006) and Kelly et al. (1987) with a hydraulic load driver simulated smaller average retention. Lake retention models including Kirchner and Dillon (1975), Chapra (1975), and Brett and Benjamin (2008) cause little impact on global riverine retention. Thus, the prediction of these models is close to that of Wollheim et al. (2006) on a global scale. Larger difference in IQR was found between different specific-runoff-driven models, as IQRs of modeled retention following Behrendt and Opitz (1999) (q) and De Klein (2008) are 0.893 and 0.382 respectively, while IQRs of hydraulic-load-driven models range from 0.234 to 0.398.

Table 3.4 Descriptive statistics of N retention of different retention models

Retention models	Wollheim et al. (2006)	Kelly et al. (1987)	Behrendt and Opitz (1999) (W_L)*	Behrendt and Opitz (1999) (q)*	De Klein (2008)	Seitzinger et al. (2002)	Venohr et al. (2005)
Average	0.273	0.203	0.328	0.430	0.386	0.228	0.285
5%	0	0	0	0	0	0	0
25%	0.024	0.011	0.081	0.081	0.099	0.068	0.102
Quartiles 50%	0.061	0.031	0.222	0.335	0.243	0.101	0.203
75%	0.413	0.201	0.505	0.804	0.639	0.214	0.378
95%	1.0	0.998	0.991	1.0	1.0	1.0	0.936
Dispersion (IQR)	0.389	0.190	0.424	0.723	0.540	0.146	0.276
Skewness (Yule's coefficient)	0.814	0.790	0.332	0.297	0.466	0.560	0.265

* W_L and q were used to identify different retention equations of Behrendt and Opitz (1999) as driven by areal water load W_L and the catchment area-specific runoff q , respectively.

Table 3.5 Descriptive statistics of P retention of different retention models

Retention models	Wollheim et al. (2006)	Kelly et al. (1987)	Behrendt and Opitz (1999) (W_L)	Behrendt and Opitz (1999) (q)	De Klein (2008)	Kirchner and Dillon (1975)*	Chapra (1975)*	Brett and Benjamin (2008)*
Average	0.278	0.219	0.354	0.437	0.553	0.263	0.263	0.257
5%	0.0	0.0	0.0	0.0	0.0	0.0	0.0	0.0
25%	0.028	0.015	0.067	0.029	0.358	0.027	0.027	0.029
Quartiles 50%	0.068	0.042	0.237	0.311	0.517	0.065	0.065	0.069
75%	0.426	0.249	0.600	0.922	0.740	0.384	0.358	0.327
95%	1.0	0.999	0.998	1.0	1.0	1.0	1.0	1.0
Dispersion (IQR)	0.398	0.234	0.533	0.893	0.382	0.357	0.331	0.298

Skewness (Yule's coefficient)	0.802	0.774	0.363	0.370	0.166	0.787	0.774	0.730
----------------------------------	-------	-------	-------	-------	-------	-------	-------	-------

* Kirchner and Dillon (1975), Chapra (1975), and Brett and Benjamin (2008) are lake retention models; for those cells without lake cells, Wollheim et al. (2006)'s equation is used to calculate river retention.

3.3.3 Difference score performance of retention models

Both TN and TP showed significant differences in their mean subtraction between simulated and observed concentration among the retention models. For TN, Tukey's HSD showed a clear distinction between hydraulic load-driven models on the one hand and specific-runoff-driven models on the other hand (Figure 3.7 (A), Supporting Information Table S3.3). The Games-Howell post hoc tests showed similar differences in model groups for TP (Figure 3.7 (B), Supporting Information Table S3.4). Particularly, the retention models of De Klein (2008) deviated strongly in performance, which may relate to the difference of their coefficients and the consideration of temperature in De Klein (2008).

Generally, the average difference between observed and simulated concentration is lower for specific-runoff-driven models than for hydraulic-load-driven models. Note that concentration is inversely proportional to the estimation of retention. A positive average difference between simulated and observed concentrations signifies an overestimation of concentration and thus an underestimation of retention. For both TN and TP, retention models, except for the TN equations of De Klein (2008), tended to underestimate retention, particularly in low-retention regions (retention ≤ 0.1).

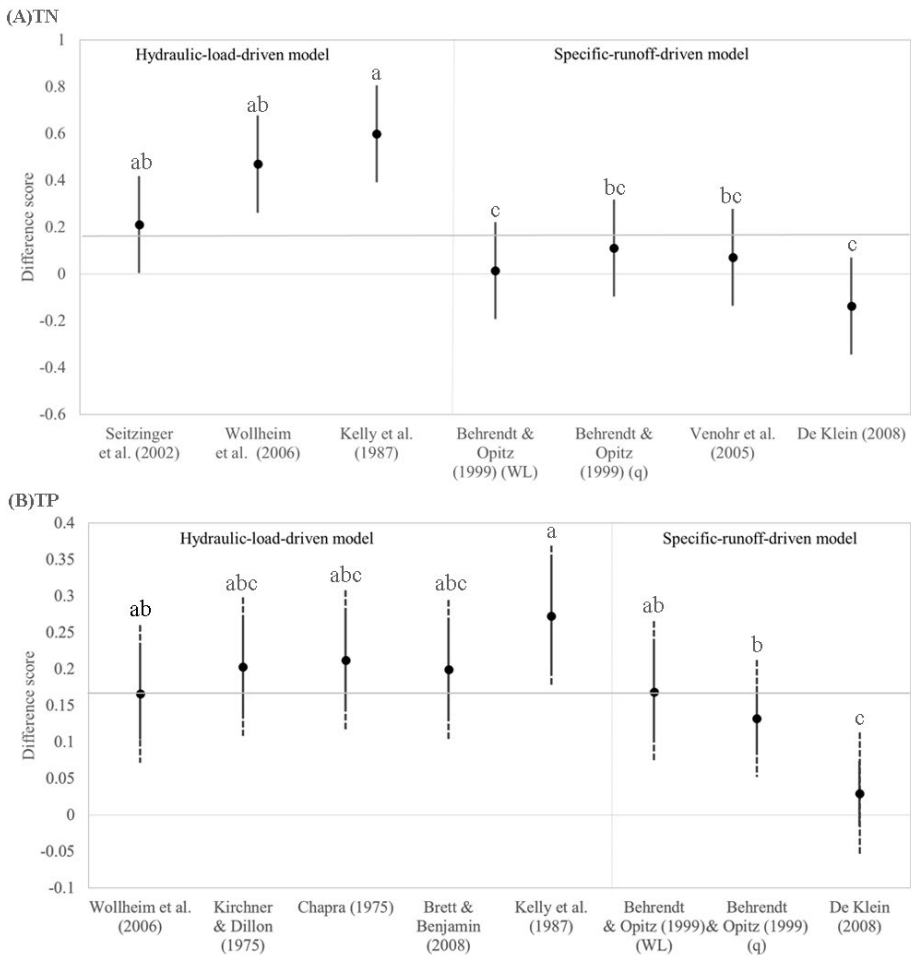


Figure 3.7 Difference score between simulated and observed concentration for (a) TN and (b) TP among different retention models. Black points are the average difference. The length of the “wings” (shown as black lines around the average) equals $SE \cdot q_{\alpha,k,v}$ with critical value $q_{\alpha,k,v}$ and standard error SE determined by Tukey’s HSD or Games-Howell post hoc test. The solid lines show the minimal $SE_{i,j} \cdot q_{\alpha,k,v}$ and the dashed lines of the wings indicate the range of pairwise $SE_{i,j} \cdot q_{\alpha,k,v}$ from the minimum to the maximum. Different letters a, b, c on top of the wings identify significant differences (p -value < 0.05) in concentration among the retention models.

3.4 Discussion

As far as we are aware, this is the first study to assess the performance of empirical retention equations for global nutrient models and to investigate the role of driving forces, function form, and equation coefficients. The strengths of this study include its analyses on the global and regional performance of retention equations using multiple criteria (NRMSE, Pearson's r , and relative bias (i.e., average difference score shown in Figure 3.7) and the comparison of model residuals for different water bodies based on abundant samples from diverse sources.

We applied NRMSE and Pearson's r as the performance criteria and used an ANOVA and a post hoc test to investigate the performance of (and differences between) retention models. The results revealed that the impact of function form and coefficients are inferior to the hydraulic driver. Since most of these models were developed based on a local dataset (Table 3.1), the coefficients and function forms were expected to represent the corresponding local systems better than the globe. However, our results show that some of these local studies perform better globally than those developed at global scales (i.e., Wollheim et al., 2008). Particularly, empirical retention equations whose driving force is hydraulic load predicted relatively lower retention than specific-runoff driven models. Hydraulic-load-driven models tended to underestimate retention and overestimate concentration, particularly for TN. The specific-runoff driven equations of Behrendt and Opitz (1999) (q) and De Klein (2008) provided the best fit for the simulation of riverine nutrient retention and P retention in lakes, respectively.

Our study reinforced the importance of temperature as a secondary driving force of P retention (D'angelo et al., 1991; Jensen and Andersen, 1992; Kim et al., 2003), since the retention models of De Klein (2008) lowered the difference between simulations and observations and is the only model that considered temperature. Our results were also in line with the discovery that riverine N and P retention depends on the specific runoff rather than hydraulic load (Behrendt and Opitz, 1999) and predicted P values disperse more than predicted N values using empirical equations to estimate retention (Hejzlar et al., 2009).

Using the best combination of retention models for geographical zones (Table S3.2), we simulated the global export to coastal waters of N and P are 30.5 Tg N yr⁻¹ and 5.8 Tg P yr⁻¹. For the global N export, our estimation is lower than those of NEWS-2 (45 Tg N yr⁻¹, Mayorga et al. 2010) and IMAGE-GNM (37 Tg N yr⁻¹, Beusen et al., 2016). The combination of retention models for various zones can better represent the realistic retention and results in a lower global export that is closer to observations. For P, our estimation falls between the global export of NEWS-2 (9 Tg P yr⁻¹, Mayorga et al., 2010) and IMAGE-GNM (4 Tg P yr⁻¹, Beusen et al., 2016). Moreover, the best combination of P retention models avoids the bias caused by Wollheim et al. (2006) to predict zero P loads in the high-retention regions.

Our assessment of lake P retention differs from the multiple comparison results of Brett and Benjamin (2008), who compared and optimized the retention equation for lake TP in the USA and Canada and regarded Brett and Benjamin (2008)'s equation, a residence-time-driven equation, as the best fit. We identify the reason as the difference of performance criteria and spatial coverage of sample data. Brett and Benjamin (2008) used the logarithm coefficient of determination r^2 as the performance criterion, which is equivalent to the square of Pearson's r of linearized log-transformed data. Indeed, the model of Brett and Benjamin (2008) got high r scores among all the models in our research, but their model performs worse than De Klein (2008) and Kelly et al. (1987) if we consider NRMSE. In conclusion, our use of multiple criteria shows the advantage of providing more information of both correlation and errors between simulations and observations.

3.4.1 Uncertainties of retention modeling

Uncertainty may arise from a lack of data availability and data representativeness. For instance, when assessing model performance in different geographical zones, retention models perform worse in the Torrid Zone than at the global level, which might be due to a misrepresentation of the nutrient states throughout the Torrid Zone (it covers only 1.5% of all TN samples and 3.4% of TP samples). In the South Temperate Zone, despite

a sufficient amount of data, the data lack representativeness, as most of the samples were collected in the Murray Darling Basin in Australia. We included NO₃/DIN and PO₄ data and used nutrient ratios to deal with a lack of data availability. However, the imposed nutrient ratio may introduce uncertainty into observation data as well. For instance, Turner et al. (2003), Meybeck (1982), and Goolsby et al. (1999) estimated global NO₃/TN ratios to vary from 59% to 86% and PO₄/TP ratios from 46% to 70% by investigating world's rivers. However, other literature (e.g., Liu et al. 2018; Yan et al. 2001) provided specific ratios for different rivers. To lower the uncertainty raised by these ratios, we used specific ratios firstly, and if no specific ratios were found, we employed the recommended global ratio from Turner et al. (2003). As more data become available, these retention models can be further evaluated and improved.

The ability of the model to reproduce the hydrological conditions is also crucial for the performance of modeled retention. For instance, although the Torrid Zone and the North Frigid Zone had almost the same amount of data, the performance of these two regions was quite different. Better retention predictions in the North Frigid Zone are related to more accurate PCR-GLOBWB discharge simulations in Europe, North America, and monsoon-dominated regions due to more precise meteorological forcing. In contrast, the least accurate results in the Torrid Zone are probably linked to the unsatisfactory simulation of discharge in African rivers since PCR-GLOBWB likely overestimates the groundwater recession rates and underestimates African inland delta evaporation (Sutanudjaja et al., 2018). In addition, due to faster rates of hydrological change in humid tropics, the hydrological condition is harder to describe precisely by a yearly-step model (Wohl et al., 2012).

On the other hand, the processing of water storage in PCR-GLOBWB introduced more uncertainties into the estimation of the hydraulic load than of specific runoff that was only affected by the discharge. Assuming reservoirs serve hydropower generation, PCR-GLOBWB overestimates the real reservoir volume by maximizing storage capacity under full power generation due to a lack of data from power plants on a global scale (Haddeland et al., 2006; Adam and Lettenmaier, 2008). However, PCR-

GLOBWB sometimes underestimates the total water volume by ignoring small reservoirs when combining multiple water bodies located within the same cell (Beusen et al., 2015). These uncertainties may explain why retention estimates from hydraulic-load-driven retention equations deviate more from observations than when based on specific-runoff-driven equations.

3.4.2 The effect of driving forces on P and N retention

The reason that specific-runoff-driven models perform better than hydraulic-load-driven models lies mainly in accuracy of the predictions on their driving force. IMAGE-GNM can better predict specific runoff that is composed of discharge and area since discharge was validated with observation in PCR-GLOBWB and area was obtained from geo-information (Van Beek et al., 2011). In contrast, hydraulic load works worse due to the uncertainties of reproducing water volume and water body depth.

Temperature has been shown to be an important driving force of P retention (D'angelo et al., 1991) to compensate for the difference between predicted and observed concentration but works secondary to hydraulic drivers, as Figure 3.7 shows those retention models considering temperature factor (i.e., Wollheim et al. (2006) and De Klein (2008)) lower the difference between predictions and observations within the models with the same hydraulic drivers. The effect of temperature works via influencing PO_4 release from sediments in streams and lakes (Fillos and Swanson, 1975; Holdren and Armstrong, 1980; Jensen and Andersen, 1992; Kim et al., 2003) and the physical properties of the water (Jeppesen et al., 2009). In contrast, N retention may also be affected by temperature, given NH_4 release from sediments (Shinohara et al., 2021), but the temperature effect on N is less substantial than P, since the N content ratio between sediments and other mediums (e.g., water) was found to be much lower than P (Downing and McCauley, 1992).

Future scenarios point to a global temperature increase due to greenhouse gas emissions (IPCC, 2018). Under a warmer climate, higher water temperature increases the time windows of biological activities and intensifies the interaction of the physical

environment and the biogeochemical properties in the hydrosphere (Jeppesen et al., 2009; Withers and Jarvie, 2008). This would likely lead to more nutrient release from aerobic sediments and an increase in nutrient concentrations in freshwaters.

3.4.3 Limitations and future improvement

River damming causes a decrease in the specific runoff and the hydraulic load, which leads to sediment trapping and an increase in nutrient retention (Maavara et al., 2015). While empirical equations capture the effects of changing hydrological parameters, they do not include biogeochemical mechanisms. These limitations act on both N and P. With respect to biogeochemical mechanisms, limitations relate to the lack of accounting for interactions among nutrient species, interactions with other elements, and for instance remobilization of P into water bodies due to the long-term accumulation of anthropogenic P retention in sediments. The errors between modeled and observed riverine P are larger than for N in our study. The larger error of P may result from the complexity of P transformations between unneglectable particle forms and dissolvable species, and the complex exchange between the water column and the sediment, which statistical regression equations of TP cannot reproduce or predict.

As such, model developers should search for ways to incorporate mechanistic geochemical dynamics into modeling nutrient retention in aquatic systems, so that models can better estimate N/P fate by distinguishing the specific forms and by including the transformations among different nutrient species. For instance, Vilmin et al. (2020) proposed a framework to describe the interactive processes between nutrient species and examined the model performance of N fate by splitting TN into ammonium (NH_4^+), nitrate (NO_3^-), nitrite (NO_2^-), and organic nitrogen. Future research into process-based biogeochemical dynamics is needed to better assess P retention.

3.4.4 Implications for the global assessment of nutrient retention

The global assessment of retention equations that was conducted in our study can improve the accuracy of global nutrient models: compared to the currently used

retention equation, applying the best-fit retention equation can reduce the NRMSE of riverine N, lake P, and riverine P in IMAGE-GNM by 41%, 66%, and 107%, respectively. By comparing the performance of empirical equations in different geographical regions, our study provided a possible way for model developers to further consider integrating regional retention modeling into global nutrient simulations. Further, the analyses of errors in performance, having distinguished the role of driving forces, function form, and equation coefficients, can constitute a step forward to the future development of empirical retention equations.

3.5 Conclusion

In this study, we used NRMSE to evaluate the error of model outcomes and Pearson's r of log-transformed data. We employed ANOVA and post hoc analyses to evaluate the under- or overestimates of different retention models.

Our results showed that global retention derived from different retention equations generates different patterns: the hydraulic-load-driven equations differ considerably from specific-runoff driven models and predicted relatively lower retention. The hydraulic driver is thus the most important factor that affects predicted TN/TP concentrations. Globally, empirical equations perform better for N than P. The retention models of Behrendt and Opitz (1999) (q) generate the lowest NRMSE for both N and P, being the best option for estimating riverine retention of TN/TP, while De Klein (2008)'s model is recommended for simulating P retention in lakes and reservoirs.

This global assessment allows model developers to choose empirical retention equations that best fit their region, thus improving the accuracy of modeling global nutrient fate and the N or P exports to coastal waters. Such improvements provide a better insight into the eutrophication in aquatic systems and support decision-makers to formulate environmental policies. The analysis on the driving force of retention constitutes a basis for the development of retention models for future nutrient fate and waterborne eutrophication-related studies.

Supporting Information

Table S3.1 Python packages, versions, and functions used for ANOVA and post hoc test. The analysis was accomplished by Python 3.7.

	Package	Version	Subpackage/M odule	Function
ANOVA	scipy	1.6.2	stats	f_oneway
Welch's ANOVA	pingouin	0.5.1	/	welch_anova
Tukey's HSD	statsmodels	0.12.2	stats.multicom p	MultiComparison , tukeyhsd
Games-Howell post hoc test	pingouin	0.5.1	/	pairwise_gamesh owell

Table S3.2 Best-performing retention models on a global and regional scale

Region and Observation Type	N	P
Lakes* Global	/	De Klein (2008)
Rivers* Global	Behrendt and Opitz (1999) (<i>q</i>)	Behrendt and Opitz (1999) (<i>q</i>)
North Frigid Zone	Behrendt and Opitz (1999) (<i>q</i>)	Wollheim et al. (2006) combined with the lake retention models of Kirchner and Dillon (1975) or Chapra (1975)*
North Temperate Zone	Behrendt and Opitz (1999) (<i>q</i>)	Behrendt and Opitz (1999) (<i>q</i>)
Torrid Zone	Venohr et al. (2005)	Behrendt and Opitz (1999) (<i>q</i>)
South Temperate Zone	Behrendt and Opitz (1999) (<i>q</i>)	Wollheim et al. (2006)

* The column names “Lakes” and “Rivers” indicate the classification of observed data, not the retention model types. The combination of riverine and lake retention model for P is used for validation with observed data of river stations.

Table S3.3 Multiple-comparison of the residual averages of N retention models by Tukey's HSD

Model 1	Model 2	Mean difference	p-value	Lower limit	Upper limit	Reject null hypothesis
Behrendt & Opitz (W_L)	Kelly et al.	0.585	0.001	0.170	1.000	TRUE
De Klein	Kelly et al.	0.736	0.001	0.321	1.151	TRUE
De Klein	Wollheim et al.	0.606	0.001	0.191	1.021	TRUE
Kelly et al.	Venohr et al.	-0.528	0.003	-0.943	-0.113	TRUE
Behrendt & Opitz (q)	Kelly et al.	0.489	0.009	0.074	0.904	TRUE
Behrendt & Opitz (W_L)	Wollheim et al.	0.454	0.021	0.039	0.869	TRUE
Venohr et al.	Wollheim et al.	0.398	0.070	-0.017	0.813	FALSE
Kelly et al.	Seitzinger et al.	-0.388	0.084	-0.803	0.027	FALSE
Behrendt & Opitz (q)	Wollheim et al.	0.359	0.141	-0.056	0.774	FALSE
De Klein	Seitzinger et al.	0.348	0.171	-0.067	0.763	FALSE
Seitzinger et al.	Wollheim et al.	0.258	0.520	-0.157	0.673	FALSE
Behrendt & Opitz (q)	De Klein	-0.247	0.568	-0.662	0.168	FALSE
De Klein	Venohr et al.	0.208	0.730	-0.207	0.623	FALSE
Behrendt & Opitz (W_L)	Seitzinger et al.	0.196	0.780	-0.219	0.611	FALSE
Behrendt & Opitz (W_L)	Behrendt & Opitz (q)	0.095	0.900	-0.320	0.510	FALSE
Behrendt & Opitz (W_L)	De Klein	-0.151	0.900	-0.566	0.264	FALSE
Behrendt & Opitz (W_L)	Venohr et al.	0.057	0.900	-0.358	0.472	FALSE

Model 1	Model 2	Mean difference	p-value	Lower limit	Upper limit	Reject null hypothesis
Opitz (W_L)						
Behrendt & Opitz (q)	Seitzinger et al.	0.101	0.900	-0.314	0.516	FALSE
Behrendt & Opitz (q)	Venohr et al.	-0.039	0.900	-0.454	0.376	FALSE
Kelly et al.	Wollheim et al.	-0.130	0.900	-0.545	0.285	FALSE
Seitzinger et al.	Venohr et al.	-0.140	0.900	-0.555	0.275	FALSE

*The family-wise error rate (FWER) is set to be 0.05, which means a 5% of probability rejecting the null hypothesis when it is true. If p-value \geq 0.05, it fails to reject the null hypothesis after adjustment for the multiple comparisons. Since Tukey's HSD generates constant SE and $q_{\alpha,k,v}$, lower and upper limit equal to Mean difference \pm SE \cdot $q_{\alpha,k,v}$.

Table S3.4 Multiple-comparison of the averages of P retention models by Games-Howell post hoc test

Model 1	Model 2	Mean difference	SE	t_w	Degree of freedom	p-value	Reject null hypothesis
Category 1: retention models applied to rivers and lakes							
Behrendt & Opitz (W_L)	De Klein	0.139	0.033	4.2	1381.2	0.001	TRUE
Behrendt & Opitz (q)	De Klein	0.103	0.021	4.9	1551.9	0.001	TRUE
De Klein	Kelly et al.	-0.243	0.039	-6.2	1215.6	0.001	TRUE
De Klein	Wollheim et al.	-0.136	0.031	-4.3	1436.4	0.001	TRUE
Behrendt & Opitz (q)	Kelly et al.	-0.140	0.037	-3.8	1051.1	0.004	TRUE

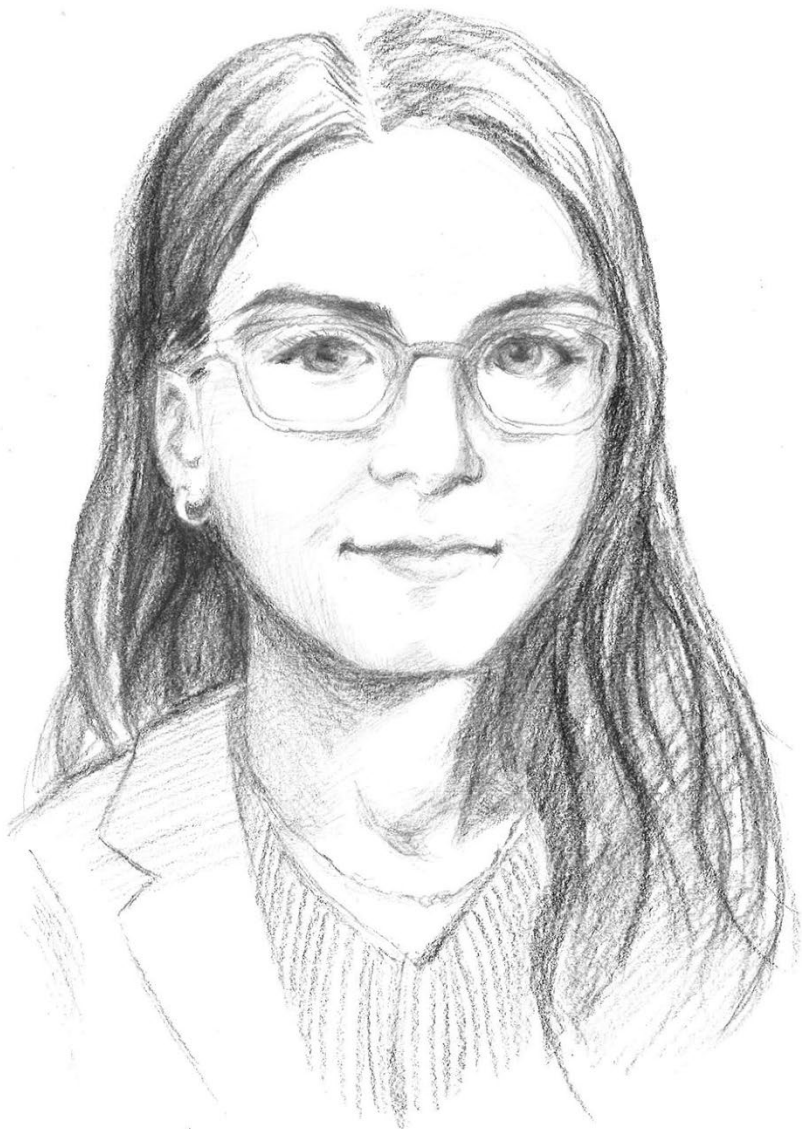
Model 1	Model 2	Mean difference	SE	t_w	Degree of freedom	p-value	Reject null hypothesis
Kelly et al.	Wollheim et al.	0.107	0.044	2.4	1574.6	0.232	FALSE
Behrendt & Opitz (W_L)	Kelly et al.	-0.104	0.045	-2.3	1620.4	0.294	FALSE
Behrendt & Opitz (W_L)	Behrendt & Opitz (q)	0.036	0.031	1.2	1156.7	0.900	FALSE
Behrendt & Opitz (W_L)	Wollheim et al.	0.003	0.039	0.1	1688.7	0.900	FALSE
Behrendt & Opitz (q)	Wollheim et al.	-0.034	0.029	-1.2	1196.5	0.900	FALSE
Category 2: retention models applied to lakes only							
Brett & Benjamin	Chapra	-0.013	0.039	-0.3	1694.9	0.900	FALSE
Brett & Benjamin	Kirchner & Dillon	-0.004	0.038	-0.1	1696.0	0.900	FALSE
Brett & Benjamin	Wollheim et al.	0.033	0.038	0.9	1695.1	0.900	FALSE
Chapra	Kirchner & Dillon	0.009	0.039	0.2	1694.6	0.900	FALSE
Chapra	Wollheim et al.	0.046	0.038	1.2	1692.1	0.900	FALSE
Kirchner & Dillon	Wollheim et al.	0.037	0.038	1.0	1695.3	0.900	FALSE

* If $p\text{-value} \geq 0.05$, it fails to reject the null hypothesis after adjustment for the multiple comparisons. Degree of freedom that varies between pairwise groups was derived from Welch's Anova. $q_{\alpha,k,v}$ is a constant due to the large degree of freedom. Since Games-Howell post hoc test generates variable $SE_{i,j}$, which t_w varies according to, we listed them here.

Chapter 4

Effects of nitrogen emissions on fish species richness across the world's freshwater ecoregions

This chapter has been published as Zhou, J., Mogollón, J.M., van Bodegom, P.M., Barbarossa, V., Beusen, A.H.W., Scherer, L., 2023. Effects of nitrogen emissions on fish species richness across the world's freshwater ecoregions. *Environ Sci Technol* 57, 8347–8354.



Laura Scherer

Abstract

The increasing application of synthetic fertilizer has tripled nitrogen (N) inputs over the twentieth century. N enrichment deteriorates the water quality and threatens aquatic species such as fish through eutrophication and toxicity. However, N impacts on freshwater ecosystems are typically neglected in Life Cycle Assessment (LCA). Due to the variety of environmental conditions and species compositions, the species' response to N emissions differs among ecoregions, requiring a regionalized effect assessment. Our study tackled this issue by establishing regionalized species sensitivity distributions (SSDs) of freshwater fish against N concentrations for 367 ecoregions and 48 combinations of realms and major habitat types globally. Subsequently, effect factors (EFs) were derived for LCA to assess the N effects on fish species richness at a 0.5×0.5-degree resolution. Results show good fits of the SSDs for all the ecoregions with sufficient data and similar patterns for average and marginal EFs. The SSDs highlight strong effects on species richness due to high N concentrations in the tropical zone and the vulnerability of cold regions. Our study revealed the regional differences in sensitivities of freshwater ecosystems against N content in great spatial detail and can be used to assess more precisely and comprehensively nutrient-induced impacts in LCA.

4.1 Introduction

Global food production has tripled in the past five decades to meet the demand of growing populations (FAOSTAT, 2008; Grüber et al., 1995). This has been achieved using large amounts of synthetic fertilizer for cultivating crops (Smil, 1999), importing excessive nitrogen (N) into local nutrient cycles (Bouwman et al., 2009; Galloway et al., 2004; Mogollón et al., 2018b). During the latter half of the 20th century, the global use of nitrogen fertilizers grew seven-fold (Smil, 1997), leading to a tripling of nitrogen inputs into freshwater systems (Zhang et al., 2021). This input reached approximately 120 Tg N yr⁻¹ in 2000. It represents a combination of fertilizer, manure, biological N₂ fixation, and nitrogen deposition. Future scenarios posit that N inputs will continue to rise due to population growth and the increasing proportions of proteins in human diets

(Beusen et al., 2022; Mogollón et al., 2018b; Smil, 2002).

The excessive release of nitrogen into the environment is adversely affecting ecosystems (Jenny et al., 2016; Schindler, Vallentyne, 2008; Vonlanthen et al., 2012). For instance, N enrichment can induce eutrophication in water bodies and toxicity to species. Eutrophication can cause hypoxia, the severity of which determines the survival of aerobic organisms in the water. Moreover, nitrate (NO_3^-) in drinking water is not only harmful to human health (Bryan and van Grinsven, 2013), but ammonia (NH_4), NO_3^- , and nitrite (NO_2^-) also perturb the pH and are toxic to fish (Russo and Thurston, 1977; Thurston et al., 1981; Westin, 1974). Many fish species are top predators, and their survival, diversity, and health are good indicators of the functioning of aquatic ecosystems (Villéger et al., 2017; Whitfield and Elliott, 2002).

Life cycle assessment (LCA) can be used to characterize the impact of eutrophication on biodiversity (Payen et al., 2019). LCA is a tool for assessing the environmental impacts of products across their life cycles and can help analyze the trade-offs between economic activities and the environment (Hunkeler, 2014; Muralikrishna and Manickam, 2017). Within the life cycle impact assessment (LCIA) phase of an LCA, characterization factors (CFs) express the relative magnitude of a certain environmental impact per unit of the characterized activity (Rosenbaum et al., 2018). As an endpoint-level component of CFs, effect factors (EFs) describe the sensitivity of the species community to environmental pressure (Potting and Finnveden, 2015). Such EFs can be used to assess N effects on freshwater biodiversity (Payen et al., 2019). Cosme and Hauschild (2017) estimated the effect of marine eutrophication-induced hypoxia on species. They used dissolved oxygen (DO) as an intermediate factor (exposure factor) connecting N with effects on species. Azevedo et al. (2013) investigated the patterns of biodiversity along phosphorus (P) concentration gradients in lakes and streams based on limited data from peer-reviewed papers. LC-IMPACT (Azevedo et al., 2020), ReCiPe2016 (Huijbregts et al., 2017), and Jwaideh et al. (2022) applied EFs derived from the P-species sensitivity distributions of Azevedo et al. (2013) that directly link to the fate of the nutrient (i.e., without exposure as an intermediate factor). However,

Cosme and Hauschild (2017) focused on marine ecosystems and only considered the hypoxia induced by N yet ignored the effect of N toxicity on species, while Azevedo et al. (2013) and the following phosphorous EF studies have not accounted for N. Furthermore, both of these studies were conducted at a very coarse scale of distinguishing the effects only for four or five biogeographical regions globally. In various cases, N contributes strongly to freshwater eutrophication. Globally, 26% of the area with undesirable periphyton growth is limited by N compared with 74% for P. When considering acceptable and undesirable periphyton growth, even 66% of the area is limited by N compared with 34% for P (McDowell et al., 2020). However, N effects on the ecosystem have not been explored globally (Payen et al., 2019; Zhou et al., 2022b).

Hydro-climatic and morphological conditions specific to catchments/ecoregions dictate patterns of fish distribution (Schipper and Barbarossa, 2022). Therefore, the response of fish assemblages to human stressors is contingent on these environmental conditions (Larentis et al., 2022; Schipper and Barbarossa, 2022). For instance, variation in water temperature may change dissolved oxygen demand for respiratory purposes for organisms (Kramer, 1987). Meanwhile, biotic sensitivity to such hypoxia differs between species. Therefore, N-induced eutrophication has divergent effects on diverse species composition across distinct ecoregions (Clark et al., 2017; Ekau et al., 2010; Larentis et al., 2022). Regionalized EFs of fish biodiversity loss are therefore required to describe the N impact on fish diversity across different ecoregions.

This study aimed to explore the regionalized effects of N on global freshwater ecosystems. Based on 41 years of fish occurrence data (covering 13,920 freshwater fish species) and N concentration simulations from the Integrated Model to Assess the Global Environment – Global Nutrient Model (IMAGE-GNM) (Beusen et al., 2015), we calculated the fish species sensitivity distribution (SSD) over 367 ecoregions and provide EFs of potential N-induced species loss at a half-degree resolution. This study is the first to reveal the statistical relationships between N content and species loss in the global freshwater system.

4.2 Methods

4.2.1 Global nutrient model

Measurement data for nutrients in global rivers and lakes are rare, especially for N. Worldwide total N (TN) sampling stations only occupy less than half of water quality stations (e.g., 4,685 N sampling stations out of over 18,000 river stations from the GLObal RIVer CHEMistry Database, GLORICH (Hartmann et al., 2019)) and cover few regions (e.g., only 83 countries are covered by N stations in the global water quality database, GEMStat (UNEP GEMS/Water Programme, 2007)).

The use of a global nutrient model can fill the gap of a lack of spatial N information, as it can predict the unknown N concentrations in water bodies without sampling (Beusen et al., 2016; Kroeze et al., 2012; Mayorga et al., 2010). Among recognized global nutrient models, IMAGE-GNM is a spatially explicit, dynamic model with the finest resolution (0.5×0.5 degree) that has been validated with sampling station data (van Vliet et al., 2019). The validation of Zhou et al. (2022a) found a NRMSE of 2.29 and a Pearson correlation coefficient (r) of 0.58 of IMAGE-GNM generated estimates vs. 9,770 records of total nitrogen observed data from 1,199 global river stations. Of these, the North Frigid Zone performed best in terms of NRMSE (0.57) but had a low r (0.14); the North Temperate Zone performed best in terms of r (0.59) but had a high NRMSE (2.35); the Torrid Zone had a relatively low NRMSE (1.71) but the lowest r (0.05); and the South Temperate Zone generated a relatively high r (0.46) but the second highest NRMSE (1.91) (The scale of these regions can be found in “Geographical zone” (2009)). In this study, we employed IMAGE-GNM to provide global N concentration estimates from 1970 to 2010 (Beusen et al., 2016, 2015; Bouwman et al., 2009), as these are the most recent years that are accessible from IMAGE-GNM. A detailed model description of IMAGE-GNM can be found in Beusen et al. (2015).

4.2.2 Freshwater fish species inventory

We compiled point occurrence data for freshwater fish species following the same

methodology as in Barbarossa et al. (2021, 2020). First, we retrieved occurrence data from the Global Biodiversity Information Facility (GBIF) (GBIF.org, 2019), FishNet network (Fishnet2, 2019), SpeciesLink (splink, 2019), Portal da Biodiversidade (ICMBio, 2019), and the Atlas of Living Australia (ALA) (PLAN, 2008). An overview of these source data can be found in Table S1 of Barbarossa et al. (2020). Second, we coupled the fish occurrence data to freshwater fish species names and associated synonyms, which were derived from Fishbase (we used the R package “rfishbase 4.0.0” (Boettiger et al., 2012) and set FISHBASE_VERSION as “19.04”) and Tedesco et al. (2017). Based on these datasets, we harmonized freshwater fish species names and excluded the occurrence records without year and geographic information. This step selected 13,774 unique freshwater fish species with scientific names and 825 species with synonyms. Third, we merged these occurrence records by assigning the scientific names for those with synonyms and removing the duplicates. In total, we obtained 13,920 freshwater fish species and 5,427,740 occurrence records from 1970 to 2010. Details can be seen in Supporting Information Figure S4.2.

4.2.3 Species sensitivity distributions

EFs ($\text{PDF} \cdot \text{m}^3 \cdot \text{kg}^{-1}$, described in section 4.2.4) are used within life cycle impact assessment (Rosenbaum et al., 2007) and typically expressed as the potentially disappeared fraction (PDF) of species, i.e., the relative species richness as a fraction of the total, per unit of an increase in stressor. EFs reflect both the sensitivity of the species (PDF between 0 and 1) and the size of the system being affected (here: volume). EFs can be derived from species sensitivity distributions (SSDs), which represent the continuous relationship between PDF and a stressor. In this case, PDF (dimensionless, Eq. 4.1) depends on the loss of species richness under the influence of N concentration levels ($\text{mg} \cdot \text{L}^{-1}$) compared to the maximum species richness that can be observed within ecological units. N can stress ecosystems through both eutrophication and toxicity. As an ecological unit, we used freshwater ecoregions, which are deemed a characteristic, geographically distinct combination of natural communities (Abell et al., 2008). Thus

we set ecoregions as the smallest ecological units to model EF (Supporting Information Figure S4.1, 426 freshwater ecoregions over the globe, data from Freshwater Ecoregions of the World (FEOW)). We also employed a coarser biogeographical classification by combining the realms and the major habitat types as a supplement to some ecoregions that lack occurrence records (49 realm-major habitat types globally, of which 48 have sufficient data to support regressions). The ecoregions and realm-major habitat types were rasterized before the derivation of SSDs. When the number of pairs of PDF-N concentration data was three or fewer, we deemed it insufficient for fitting SSD curves.

$$PDF = 1 - \frac{SR_{i,j}}{SR_{i,max}} \quad (4.1)$$

where $SR_{i,j}$ is the species richness of ecoregion i at the N-concentration level j and $SR_{i,max}$ is the maximum species richness in ecoregion i .

We extracted the species richness by counting the number of fish species that can survive at a given N concentration level for each ecoregion/ realm-major habitat type. We assume that the fish species are tolerant to the prevailing N-induced hypoxia/toxicity up to the N concentration at which they are observed within an ecoregion, whereas fish species richness gradually decreases with increasing N concentration by exceeding the species' tolerance levels. This follows a similar approach to Gade et al.⁶¹ for terrestrial acidification. To keep consistency with current LCA practices, the lower tolerance threshold was not considered. The lower tolerance threshold ensures organisms do not starve from a lack of nutrients. This threshold is beyond the scope of this study and may contain a functionally distinct ecosystem from the reference system (Payen et al., 2019). Therefore, we only consider the upper threshold of the stressor.

By matching the species occurrences with N concentration of the same year and location (by pixels of 0.5×0.5 degree), we derived the N tolerance thresholds for each species within each ecoregion/ realm-major habitat type.

We can predict SSD curves with a logistic function (Eq. 4.2) to fit the data pairs of PDF (calculated in Eq. 4.1) and N concentration. This function is widely used in LCIA method development (Azevedo et al., 2013; Gade et al., 2021; Roy et al., 2014; Scherer et al., 2022).

$$PDF = \frac{1}{1 + \exp\left(\frac{(a - \log_{10} C_N)}{b}\right)} \quad (4.2)$$

where a and b are empirical coefficients, a indicates the N concentration at which 50% of the species have disappeared, and b can be interpreted as the slope of the SSD. C_N ($\text{mg}\cdot\text{L}^{-1}$) is the N concentration.

We evaluated the performance of the regression using the pseudo- R^2 value and the normalized root mean square error (NRMSE). Normal R^2 values for linear regressions have been shown to be inappropriate for non-linear fits (Spiess and Neumeyer, 2010). We, therefore, selected Cox-Snell pseudo- R^2 , one of the most commonly used R^2 for non-linear regressions (Smith and McKenna, 2013). This index compares the likelihood ratio of the fitting function model to a null model that contains only the intercept. NRMSE discloses the magnitude of the errors normalized by the average value through division. We regarded as a good fit a Cox-Snell pseudo- $R^2 > 0.5$ and $\text{NRMSE} < 1$, following Scherer et al. (2022) and nutrient model research (Nakhaei et al., 2021; Zhou et al., 2022a).

4.2.4 Effect factors

Two main approaches can be used to calculate EFs: marginal and average.

In this study, we employed both approaches to show different perspectives of the N effects on fish biodiversity. The marginal approach (EF_{marginal} , $\text{PDF}\cdot\text{m}^3\cdot\text{kg}^{-1}$, Eq. 4.3) denotes the instantaneous change of effect due to the current stressor and is calculated as the derivative of the SSD (i.e., Eq. 4.2) at the current state.

$$EF_{marginal} = 1000 \cdot \frac{dPDF}{dC_N} = 1000 \cdot PDF^2 \cdot \left(\frac{b \cdot \exp\left(\frac{a - \log_{10} C_N}{b}\right)}{C_N \cdot \ln(10)} \right) \quad (4.3)$$

where 1000 is the coefficient to convert the unit of the reciprocal of C_N from $L \cdot mg^{-1}$ to $m^3 \cdot kg^{-1}$.

The average approach ($EF_{average}$, $PDF \cdot m^3 \cdot kg^{-1}$, Eq. 4.4) represents the long-term change of effect, comparing the current state with a desired reference state. This could be a state without anthropogenic interference, a political target, or a zero effect, and in this study, we took the year 1900 as the reference year, with the N concentrations taken again from IMAGE-GNM. The average approach has also been used to assess the effect of future states under different greenhouse gas concentration trajectories (de Schryver et al., 2009; Scherer et al., 2022).

$$EF_{average} = 1000 \cdot \frac{PDF_{current} - PDF_{ref}}{C_{N,current} - C_{N,ref}} \quad (4.4)$$

We calculated globally marginal and average EFs based on the gridded N concentration at the current state (represented by the year 2010) at a resolution of 0.5×0.5 degrees and the SSDs for the corresponding ecoregion/realm-major habitat type. EFs were derived from ecoregion-level SSDs first, and the realm-major habitat type was employed only if the species-stressor information was not sufficient for the ecoregions.

In those regions with zero N concentration, EFs were set to no value because no SSD could be derived. We also regarded N concentration $< 0.0001 \text{ mg} \cdot L^{-1}$ as zero N concentration due to the uncertainty in measurements and modeling.

4.3 Results

4.3.1 Species sensitivity distributions and potentially disappeared fractions

Among the 426 ecoregions, SSD curves could be derived for 367 ecoregions, and all of them performed well (Cox-Snell pseudo- $R^2 > 0.5$ and NRMSE < 1). Data from 22

ecoregions were insufficient to fit SSD curves (PDF-N concentration data pairs ≤ 3), and 37 ecoregions did not have any data. The minimum Cox-Snell pseudo- R^2 was 0.57, found for Lake Tanganyika (NRMSE = 0.36) and the maximum NRMSE equalled 0.55, found for Chuya (Cox-Snell pseudo- $R^2 = 0.75$). In total, the 367 analyzed ecoregions occupy 95% of the global area. Among them, 357 ecoregions had a Cox-Snell pseudo- $R^2 > 0.8$ and NRMSE < 0.4 (The maps of Cox-Snell pseudo- R^2 and NRMSE can be found in Supporting Information Figure S4.3 and S4.4). Ecoregion-level SSD curves of 6 of the large ecoregions of different continents are shown in Figure 4.1 as examples.

For those 59 ecoregions without ecoregion-level regression, we provided the realm-major-habitat-type-level SSDs. With these SSDs, we can fill the gaps of 58 of these ecoregions (Cox-Snell pseudo- $R^2 > 0.5$ and NRMSE < 1). The remaining ecoregion Bermuda, which belongs to Nearctic-Oceanic Islands, had data for neither the ecoregion level nor the realm-major habitat type level. The 58 SSD plots for the realm-major habitat type can be found in Supporting Information 3, and an overview of regression coefficients, criteria, area, etc. of ecoregions and realm-major habitat type are listed in Supporting Information 4 in Zhou et al. (2023).

Figure 4.1 illustrates the PDF of the current state (2010). The regions with zero N concentration and consequently no value for PDF occupy 14% of the global area. These regions are remote and included several lakes and arid zones (e.g., Sahel Desert and Australian deserts). In the regions with non-zero N concentration, about 15% of the area is at severe risk of potential disappearance of the local fish communities (PDF > 0.8). Among these, the high PDF of ecoregions might mainly be caused by high N emissions to freshwater over the years due to a large increase in population density (e.g., Lower Yangtze River in China and Southern Deccan Plateau in India), while the high PDF of a few regions in polar freshwater systems might result from the uncertainty raised by a lack of observational data, e.g., fish biodiversity of Lena and Taimyr showed high sensitivities to N content since all the occurrence was recorded at low N concentrations. The changes in PDF and N concentration can be found in Figure S4.5 and Figure S4.6 in Supporting Information.

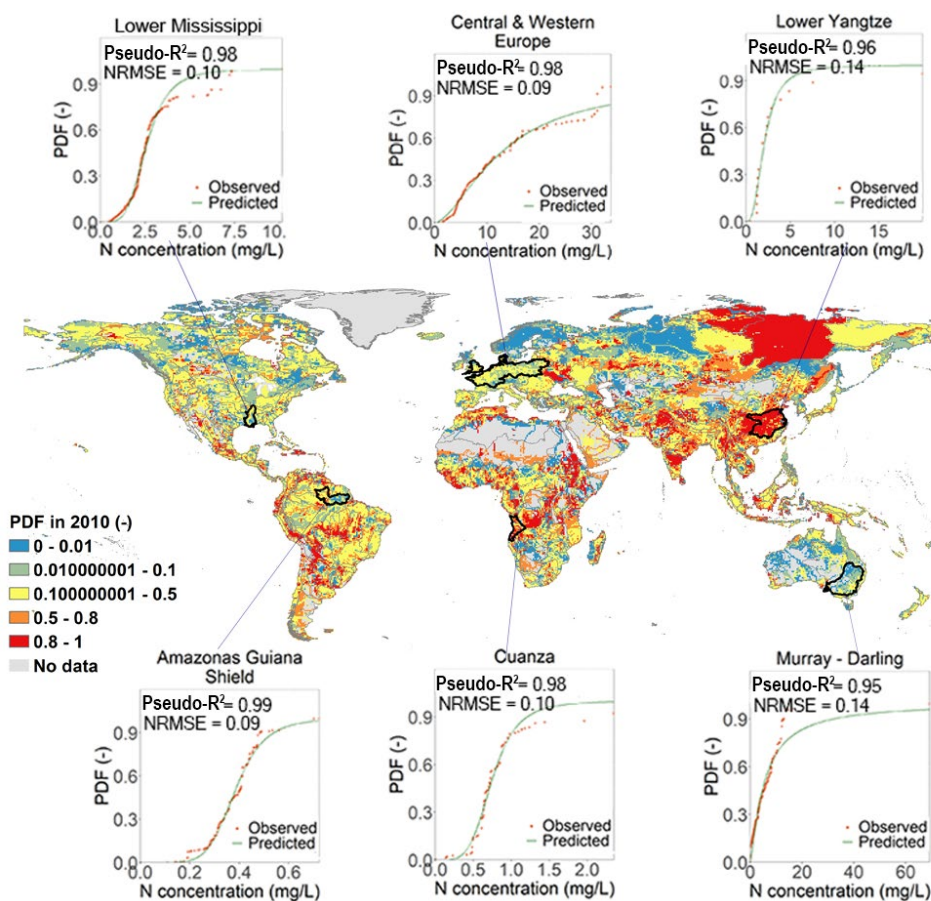


Figure 4.1 Potentially disappeared fraction (PDF) of the current fish species diversity (2010) at a 0.5×0.5° resolution and species sensitivity distributions (SSDs, following Eq. 4.2) for examples of large ecoregions in 6 continents. Note that the right limit is contained, while the left limit is not contained in the segment; e.g., 0 – 0.01 means 0 < PDF ≤ 0.01.

4.3.2 Effect factors

Marginal EFs and average EFs showed similar spatial patterns (Figure 4.2 and Figure 4.3). High values for marginal and average EFs (>100,000 PDF·m³·kg⁻¹) occurred in less than 1% of the non-zero N concentration area and were distributed in, e.g., Taimyr, Arabian Interior, Baluchistan, Borneo Highlands, and Sangha. Despite the similarity,

marginal EFs include slightly more areas with high values ($>100,000 \text{ PDF}\cdot\text{m}^3\cdot\text{kg}^{-1}$) and low values ($\leq 100 \text{ PDF}\cdot\text{m}^3\cdot\text{kg}^{-1}$), i.e., 33% had low values and 1.2% high values, while the average EF had 29% and 0.6% of low and high values, respectively.

The reason for more areas with high values for marginal EFs is that the current state is at a stage of a rapid increase of PDF, while the average EFs smoothen the change of effect by taking the difference between the current and desired state. In particular, the marginal EF showed an accelerated species sensitivity at $\text{PDF} \leq 0.5$ (occupying 70% of the area).

The higher percentage of low values in marginal EFs was caused by situations where PDF approaches 0 and 1, as, at these stages, little change of species richness can happen under the perturbation of N content in water. When the current PDF is close to 1, average EFs can show higher values than marginal EFs, as long as N concentrations varied from 1900 to 2010 in those regions. For instance, an average EF $> 100 \text{ PDF}\cdot\text{m}^3\cdot\text{kg}^{-1}$ can be found in some pixels in the Middle and Lower Yangtze River, Southern Deccan Plateau, and Amazonas High Andes, compared to their marginal EF close to 0. The average EF of some regions in Lena was lower than $100 \text{ PDF}\cdot\text{m}^3\cdot\text{kg}^{-1}$ due to little increase in N concentration during the past 110 years.

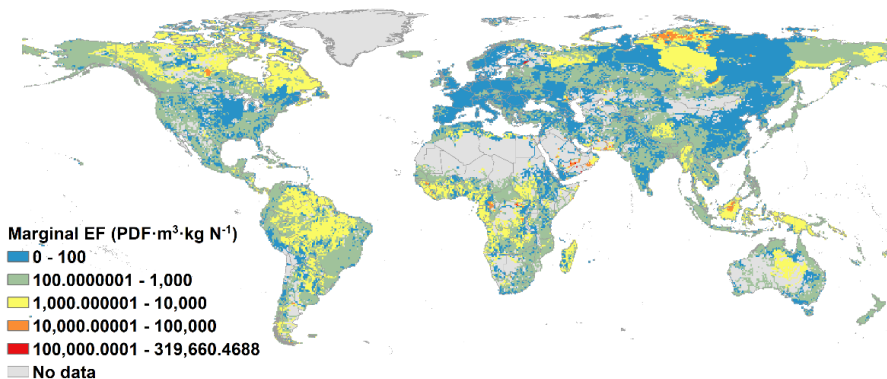


Figure 4.2 Marginal effect factors (EFs) at a $0.5\times 0.5^\circ$ resolution. The boundaries of the background map represent countries. Note that the right limit is contained, while the

left limit is not contained in the segment; e.g., 0 – 100 means $0 < EF \leq 100$.

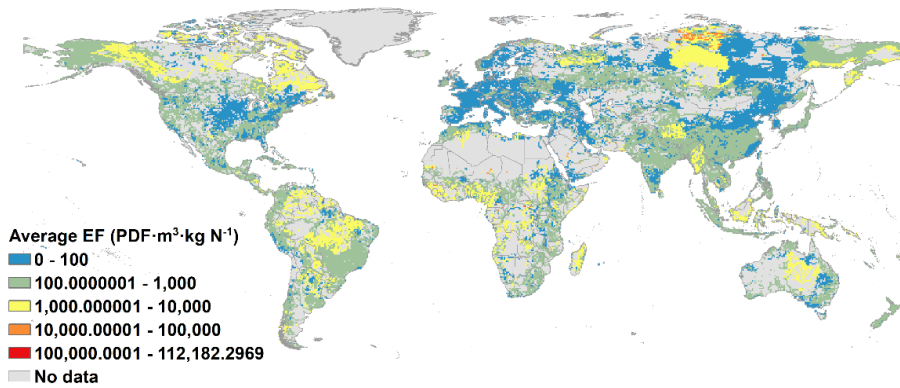


Figure 4.3 Average effect factors (EFs) at a $0.5 \times 0.5^\circ$ resolution. The boundaries of the background map represent countries. Note that the right limit is contained, while the left limit is not contained in the segment; e.g., 0 – 100 means $0 < EF \leq 100$.

4.4 Discussion

This study is the first to showcase a regionalized (ecoregion-level) relationship between freshwater species loss and N concentrations. Such information can provide more local support for assessing eutrophication and ecotoxicity impacts on local biodiversity.

Our study also provides the EFs at a much finer resolution (0.5×0.5 degree) than common in previous studies, such as Cosme and Hauschild (2017), LC-IMPACT (Azevedo et al., 2020), and ReCiPe2016 (Huijbregts et al., 2017). It allows for providing more detailed information on the local ecosystems and supports future research on assessing the impacts of nutrient emissions on biodiversity, for instance, when integrated into life cycle impact assessments.

Since no study established EFs or sensitivity to N inputs for freshwater species, we compared the spatial variability of our results with EFs for marine eutrophication (Cosme and Hauschild, 2017) and freshwater fish sensitivity to P (Azevedo et al., 2013).

In all these studies, N and P emissions tie to densely populated regions and induce eutrophication (and toxicity) downstream in both freshwater and marine ecosystems. In line with marine EFs for N estimated by Cosme and Hauschild, (2017), our EFs for N for freshwater fish are higher in tropical regions than in temperate zones. Our results also agreed with their patterns of EFs increasing from the polar to the tropical regions for most regions of Eurasia, Africa, and South America; differently, higher EFs of our study in the polar region than in the temperate zone are observed for North America and North Asia. However, in these polar regions (e.g., Western Hudson Bay, Lena, and Taimyr), our results agree with Azevedo et al. (2013), who posit that heterotrophic species are more sensitive in cold regions since these species are adapted to low nutrient concentrations. These differences among studies may result from more uncertainty in SSDs for polar regions due to fewer species occurrence data there. These findings highlight the need to better assess the effects of high concentrations on species loss in the tropical zone, while at the same time, the vulnerability of species in cold regions should also be considered.

Our result on the PDF of the current state reflects the environmental threshold of N content for losing freshwater fish species. It shows a similar spatial pattern to the regional boundaries for N surplus (Schulte-Uebbing et al., 2022), which were also derived from IMAGE-GNM. A consensus on the most severe N exceedances exists in India/Pakistan, eastern China, the Nile Basin, areas in Saudi Arabia, and along the Peruvian coast. From our results and the comparison with other studies, it follows that using a finer scale allows for describing the nutrient effects on species in more detail but also influences the reflection of the realistic species sensitivity. Using broader regions erases the geographical distinction of natural communities' responses to the various environments in smaller regions and therefore overestimates the effect for hyposensitive ecosystems and underestimates the effect for hypersensitive ecosystems. Thus, we recommend calculating the SSDs for ecoregions, unless the ecoregions cannot derive SSDs due to a lack of data and have to apply the realm-and-major-habitat-level SSDs.

An underlying assumption of this study is that fish species loss is tied to N increase. However, the individual N limitation may also be affected by the co-limiting effects of N and P under influence of eutrophication (Du et al., 2020; McDowell et al., 2020). N effects may be overestimated by our method, since the disappearance of fish species in some areas is co-affected by other stressors such as P. As McDowell et al. (2020) found, 66% of the freshwater is limited by N. Even though the loss of species induced by P limitations or other stressors might have influenced the species occurrence at a certain N concentration at some locations, the species might still be observed at the same N concentration at other locations within the same ecoregion and would, therefore, be considered tolerant. This approach undermines the effect of co-stressors. For future studies, we suggest evaluating the effects on fish species richness by simultaneously considering other human pressures and especially the co-limitation effects due to P emissions. Observations may, e.g., be coupled to models of global P fate (Beusen et al., 2015), land-use change interactions (Comte et al., 2021), global warming impact (Barbarossa et al., 2021; Comte et al., 2021), and water consumption threats to freshwater fish communities (Pierrat et al., 2022). Such a coupling will help to further disentangle the direct impacts of nitrogen load and will help in understanding whether and how its effects interact with other biodiversity threats.

Furthermore, the species-sensitivity relations could be refined by increasing the number of species observations and the quality of global N predictions. Another source of uncertainty lies in potential sampling bias for our underlying point occurrence dataset. For instance, the present study encountered the same problem of lacking occurrence data as the previous studies in cold regions, where the species sensitivity could be overestimated due to the underestimation of species richness. The accessibility to more species occurrence records can lower the uncertainty in some ecoregions due to lack of data, e.g., Lena and Taimyr in Polar freshwater systems. The accuracy of IMAGE-GNM is tied to the uncertainty introduced in N concentration predictions and it can be affected by various reasons such as model inputs, retention models, and hydrological parameters. The predictions of N concentration can be upgraded by using a mechanistic model, such

as IMAGE-DGNM (Vilmin et al., 2020). The current version of IMAGE-DGNM has been applied for several watersheds, and a future version of global N modeling can better support the research on N-induced impact on fish biodiversity (Vilmin et al., 2020).

Last but not least, we used 1900 as the reference year, as it is the earliest simulated year in IMAGE-GNM, but ideally, the reference state could reflect the pre-industrial levels.

In conclusion, our study quantified the regional relationships between N enrichment in freshwater and fish species loss, which complements the current freshwater eutrophication studies based on P in LCA. The regionalized freshwater SSDs and EFs reveal the sensitivities of ecosystems to nutrient emissions at a fine resolution. They can be applied to assess the spatially differentiated biodiversity impacts of N emissions over the world in LCA.

Supporting Information

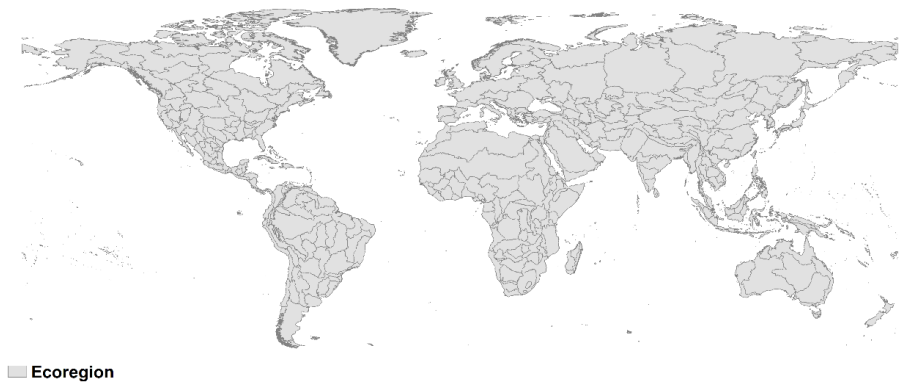


Figure S4.1 Freshwater ecoregions

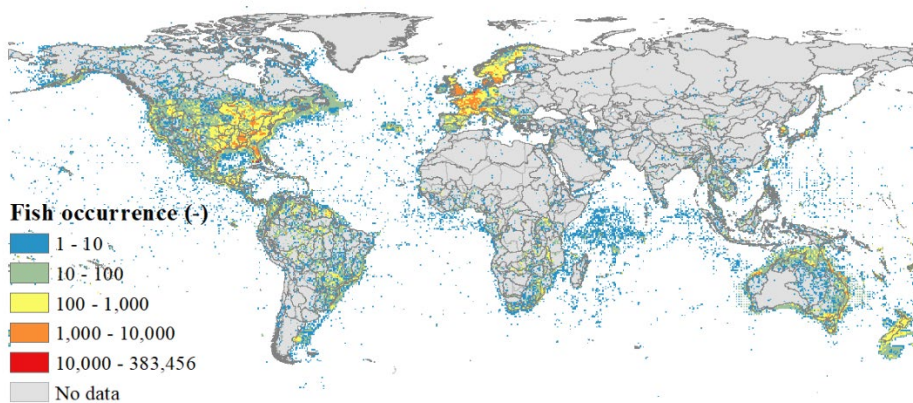


Figure S4.2 Occurrence records of freshwater fish species at a resolution of 0.5°×0.5°. The polygons illustrate freshwater ecoregions. We collected the occurrence records of freshwater fish species from 1970 to 2010, counted the numbers of the records during these 41 years, and rasterized them to a 0.5°×0.5° resolution. Fishes defined as freshwater species can be observed in freshwater, coastal, and marine ecosystems during their different life stages. We excluded the occurrences recorded in coastal and marine ecosystems when we matched the occurrence records with N concentration data in the freshwater.

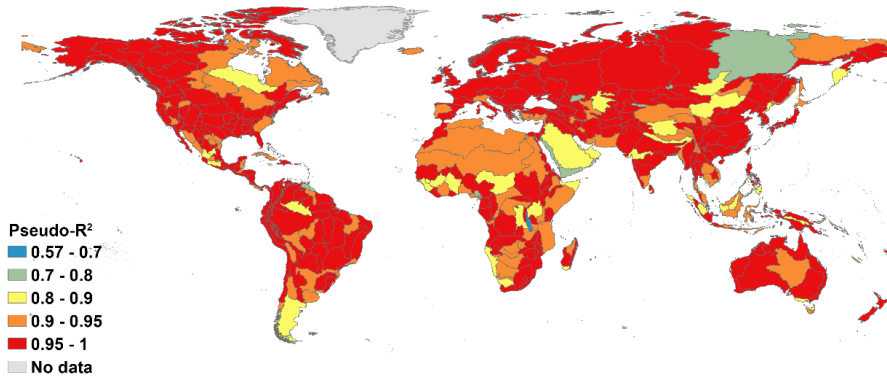


Figure S4.3 Cox-Snell pseudo- R^2 of species sensitivity distributions (SSDs) at the ecoregion level

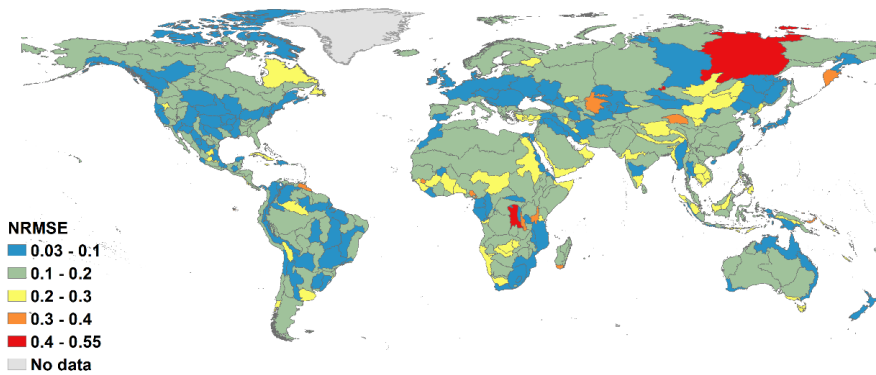


Figure S4.4 Normalized root mean square error (NRMSE) of species sensitivity distributions (SSDs) at the ecoregion level

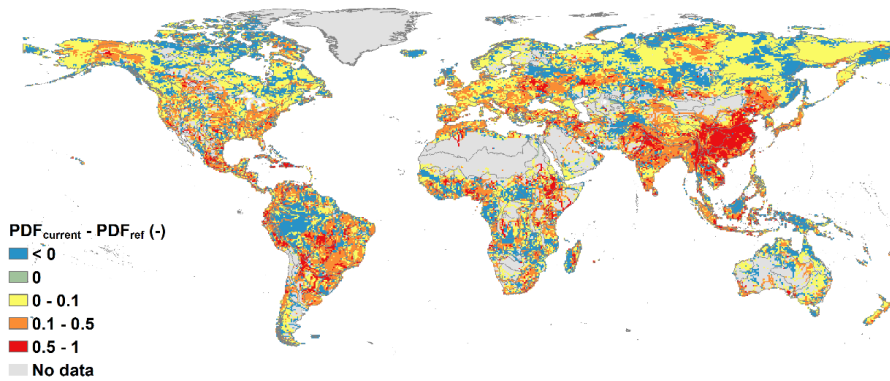


Figure S4.5 Change in the potentially disappeared fraction of species (PDF) between the current and reference states. In some grid cells, PDF decreases from the reference year 1900 to the current year 2010 along with a decrease of N concentration. This results from changes in hydrological conditions (e.g., change in discharge and/or runoff, land use change (e.g., conversion from agricultural land to natural land), and the inconsistency of the dataset whether there is ice cover or not (e.g., Iceland). In such cases, we set the average EF for these regions to “no value”

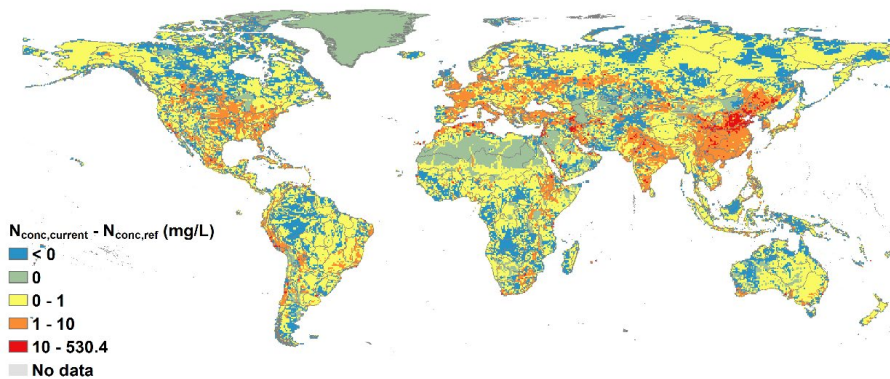


Figure S4.6 Change in N concentrations between the current and reference states

Chapter 5

Global regionalized characterization factors for phosphorus and nitrogen impacts on freshwater fish biodiversity

This chapter has been published as Zhou, J., Mogollón, J. M., van Bodegom, P. M., Beusen, A. H. W., Scherer, L., 2024. Global regionalized characterization factors for phosphorus and nitrogen impacts on freshwater fish biodiversity. *Sci Total Environ* 912, 169108.



Abstract

Inefficient global nutrient (i.e., phosphorus (P) and nitrogen (N)) management leads to an increase in nutrient delivery to freshwater and coastal ecosystems and induces eutrophication in these aquatic environments. This process threatens the various species inhabiting these ecosystems. In this study, we developed regionalized characterization factors (CFs) for freshwater eutrophication at 0.5×0.5-degree resolution, considering different fates for direct emissions to freshwater, diffuse emissions, and excessive erosion due to land use. The CFs were provided for global and regional species loss. CFs for global species loss were quantified by integrating global extinction probabilities. Results showed that the CFs for P and N impacts on freshwater fish are higher in densely populated regions that encompass either large lakes or the headwater of large rivers. Focusing on nutrient-limited areas increases country-level CFs for P in 51.9% of the countries and 49.5% of the countries for N compared to not considering nutrient limitation. This study highlights the relevance of considering freshwater eutrophication impacts via both P and N emissions and identifying the limiting nutrient when performing life cycle impact assessments.

5.1 Introduction

Humans have altered the phosphorus (P) and nitrogen (N) cycle by harvesting P and N from the geosphere and the atmosphere, respectively, and using them to boost agricultural production (Jenny et al., 2016). Mineral and synthetic fertilizers have contributed to a five-fold increase in global food production, boosting and supporting the 2.5-fold population growth during the past five decades. The long-term use of fertilizer and phosphate mining has doubled phosphorus (P) and tripled nitrogen (N) inputs to the global environment (Bouwman et al., 2009; FAOSTAT, 2008; Zhang et al., 2021). This has led to problems such as eutrophication (Jenny et al., 2016; Schindler and Vallentyne, 2008) and species toxicity (Kroupova et al., 2018). These issues negatively affect aquatic ecosystems and can also be harmful to human health (Bryan

and van Grinsven, 2013; Vonlanthen et al., 2012). The rising global food demand and its concomitant fertilizer requirements indicate that eutrophication in freshwater systems is likely to continue increasing in the near future (Beusen et al., 2022; Mogollón et al., 2018a, 2018b; Nedelciu et al., 2020).

Life Cycle Assessment (LCA) is one approach used to evaluate the environmental impacts of eutrophication (Muralikrishna and Manickam, 2017). Ecosystem quality, represented by biodiversity, is one of the core areas of protection regarding which impacts are assessed. Characterization factors (CFs) link emissions to biodiversity loss (Payen et al., 2019). In freshwater ecosystems, fish biodiversity is considered a good indicator of ecosystem health (Villéger et al., 2017; Whitfield and Elliott, 2002) and this indicator has previously been used in LCA (de Visser et al., 2023.; Pierrat et al., 2022). Due to the various environmental conditions (including the prevalence of nutrient limitations) and species compositions, impacts of P and N emissions on fish species vary spatially, which requires regionalized CFs for impact assessment.

In 2017, the United Nations Environment Programme (UNEP) launched the third phase of the Global Life Cycle Impact Assessment Method (GLAM) project as a part of the "Life Cycle Initiative" to standardize and review life cycle methods globally (Payen et al., 2019). GLAM advocates for the use of spatially explicit models with global coverage to develop regionalized CFs. Specifically for eutrophication, an additional recommendation from an earlier GLAM phase was to improve the modeling of physical and biogeochemical processes (Payen et al., 2019). Moreover, GLAM recommended the consideration of global as opposed to just local or regional species loss (Verones et al., 2019), for which global extinction probabilities (GEPs) have just recently been developed (Verones et al., 2022).

Our study aims to follow the GLAM recommendations and develop regionalized CFs for freshwater eutrophication (with a 0.5×0.5 -degree spatial resolution and yearly time step) by using the Integrated Model to Assess the Global Environment – Global Nutrient Model (IMAGE-GNM) (Beusen et al., 2015). We coupled the local nutrient

fate and concentrations from IMAGE-GNM to 41 years of freshwater fish species data (13,920 freshwater fish species) to estimate the impact at the local ecosystem level. Next, we employed GEPs (Verones et al., 2022) to extrapolate the regional species loss to global species loss. Our study provides practical indicators for economic actors to estimate the P and N impacts on the global freshwater ecosystem and serves as a roadmap for impact assessment of eutrophication in other ecosystems.

5.2 Methods

5.2.1 Characterization factors

In LCA, CFs connect the life cycle inventory (e.g., emissions) to impacts (e.g., on the ecosystem). Ideally, CFs are composed of multiple sub-factors following a cause-effect chain: fate, exposure, effect, and damage factors (Rosenbaum et al., 2015). In the case of eutrophication, fate factors (FFs) describe the fate of contaminants from emissions due to human activities eventually transported to the (aquatic) environment. In this study, we calculated FFs for 2010 by employing the approach of Zhou et al. (2022b), who distinguished emission routes into direct emissions to freshwater, diffuse emissions excluding erosion, and erosion caused by land use (their FFs were developed for the year 2000). While exposure factors (XFs) have sometimes been used in the past to represent impacts from eutrophication, such as hypoxia (Cosme and Hauschild, 2017), excessive nutrients also affect species in other ways, such as changes in the energy transfer in food webs (Wang et al., 2021), and noxious toxins produced by harmful algae (Chorus and Welker, 2021). Eutrophication-induced algae blooms also prevent predators from seeking prey by shading and diminishing light penetration (Lehtiniemi et al., 2005). Predators thus become more susceptible to nutrient increases compared with autotrophs, leading to decreases in cross-taxon congruence (Wang et al., 2021). These phenomena highlight the importance of considering the comprehensive effects of nutrients on biodiversity loss along with hypoxia when assessing the impacts of nutrient emissions. Therefore, we followed the widely used approach of deriving CFs directly from the fate to effect without considering exposure (e.g. LC-IMPACT

(Azevedo et al., 2020), ReCiPe2016 (Huijbregts et al., 2017), and Jwaideh et al. (2022).

Damage to biodiversity is often expressed through the potentially disappeared fraction (PDF) of species. In contrast to previous studies (Rosenbaum et al., 2015) that assessed impacts through the potentially affected fraction, we directly linked the nutrient concentration levels (kg/m^3) to PDF by regressing species sensitivity distributions (SSDs) for P following the method of Zhou et al. (2023) to calculate EFs for P ($\text{PDF} \cdot \text{m}^3/\text{kg P}$) and N ($\text{PDF} \cdot \text{m}^3/\text{kg N}$).

By linking fate and effect factors, we derived CFs for impacts on regional species loss (Eq. 5.1). Additionally, we employed Global Extinction Probabilities (GEPs) (Verones et al., 2022) of freshwater fish for CFs that assess the global impacts of freshwater eutrophication (Eq. 5.2). GEPs denote a scaling factor for potential regional species loss with respect to potential global extinctions (Verones et al., 2022). GEPs are available for 20 species groups across marine, terrestrial, and freshwater ecosystems. We selected the GEPs for freshwater fish to match the species group used in the EFs of the regional CFs, as recommended by Verones et al. (2022).

We estimated eight types of CFs for the combination of different emission routes and the marginal vs. average methods in assessing EFs (i.e., marginal and average CFs for direct emissions to freshwater, diffuse emissions excluding erosion, erosion caused by land use transition from natural land to arable land, and that to pasture). Detailed descriptions of FFs, EFs, and GEPs can be found in Zhou et al. (2023, 2022b) and Verones et al. (2022).

$$\text{CF}_{\text{regional},e \rightarrow i} = \sum_j \text{FF}_{e \rightarrow i \rightarrow j} \times \frac{\text{EF}_j}{V_j} \quad (5.1)$$

$$\text{CF}_{\text{global},e \rightarrow i} = \sum_j \text{FF}_{e \rightarrow i \rightarrow j} \times \frac{\text{EF}_j}{V_j} \times \text{GEP}_j \quad (5.2)$$

In Eq. 5.1 and Eq. 5.2, $\text{CF}_{\text{regional},e \rightarrow i}$ and $\text{CF}_{\text{global},e \rightarrow i}$ denote the cumulative CFs for regional species loss and global species loss in the source grid cell i (at a half-degree resolution) from an emission source e (erosion, diffuse sources excluding erosion, and

direct emissions to freshwater), respectively, and the subscript j indicates the downstream receptors of source cell i connected by advection. V_j is the water volume of the receptor j (m^3). The unit of CFs for erosion is $\text{PDF}\cdot\text{year}/(\text{m}^2\cdot\text{year})$, while that for diffuse sources excluding erosion and direct emissions to freshwater is $\text{PDF}\cdot\text{year}/\text{kgX}$, where X represents P or N.

For the additional erosion caused by land use, we subtracted the initial CFs of arable land/pasture and natural land to express the eutrophication impact of human activities ($\text{CF}_{\text{erosion}\rightarrow i, \text{landuse}}^*$, $\text{PDF}\cdot\text{year}/(\text{m}^2\cdot\text{year})$, Eq. 5.3).

$$\text{CF}_{\text{erosion}\rightarrow i, \text{landuse}}^* = \text{CF}_{\text{erosion}\rightarrow i, \text{landuse}} - \text{CF}_{\text{erosion}\rightarrow i, \text{natural land}} \quad (5.3)$$

5.2.2 Model and data

SSDs were estimated by coupling the fish occurrence data to nutrient concentration levels within the same locations (i.e., in half-degree pixels) for each year (from 1970 to 2010). We compiled the occurrence data for freshwater fish species following the approaches of Barbarossa et al. (2021, 2020). In total, we acquired 13,920 freshwater fish species and 5,427,740 occurrence records from 1970 to 2010.

We used results from IMAGE-GNM (Beusen et al., 2022) from the year 2010 (the latest non-scenario year) for nutrient loadings, emissions, and concentrations for total P (TP) and total N (TN) to derive FFs, EFs, and emission-weighting data (see Eq. 5.4 below). IMAGE-GNM was designed to be spatially explicit and dynamic, with a resolution of 0.5×0.5 degrees and a yearly time step (Beusen et al., 2016, 2015). This model uses a mechanistic approach to make predictions on nutrient transport processes, based on the hydrological cycle. The hydrological patterns were simulated by incorporating the PCRaster GLOBal Water Balance model (PCR-GLOBWB) (Sutanudjaja et al., 2018). For this study, we applied the hydrological and nutrient estimates of IMAGE-GNM from 1970 to 2010 for generating SSDs for P (SSDs for N were derived from Zhou et al. (2023)).

5.2.3 Freshwater nutrient limitation

In a specific water body, eutrophication can be limited by P or N, or co-limited by both nutrients, depending on the ratio of P and N content and their concentrations. Following McDowell et al.(2020), we assess the locations affected by nutrient over-enrichment and undesirable periphyton growth, which are directly tied to hypoxic “dead zones” and the loss of higher trophic species, such as fish (Wurtsbaugh et al., 2019).

According to McDowell et al. (2020), the nutrient limitation and the algal growth state are determined by a Redfield N:P ratio of 7:1 (by mass) and concentration thresholds for P and N in non-arid zones. Non-arid zones were defined as regions where discharge is nonzero. McDowell et al. (2020) differentiated limitations and the algal growth state into four types. We added a fifth type of acceptable periphyton growth without defining the limiting nutrient when both P and N concentrations are zero:

- 1) If the TN:TP ratio ≥ 7 and TP concentration < 0.046 mg/L, or if TP concentration equals zero and TN is nonzero, the cell has acceptable periphyton growth and is P-limited (type 1).
- 2) If the TN:TP ratio ≥ 7 and TP concentration ≥ 0.046 mg/L, the cell has undesirable periphyton growth and is P-limited (type 2).
- 3) If the TN:TP ratio < 7 and TN concentration < 0.800 mg/L, or if TN concentration equals zero and TP is nonzero, the cell is considered to have acceptable periphyton growth and to be N-limited (type 3).
- 4) If the TN:TP ratio < 7 and TN concentration ≥ 0.800 mg/L, the cell has undesirable periphyton growth and is N-limited (type 4).
- 5) If TN and TP concentrations are both zero, the cell is assigned to have no periphyton growth (type 5).

By implementing this spatial information on nutrient limitation, more precise CFs can be derived to assess the impacts of freshwater eutrophication. That is, CFs for P can be

applied where the cells are limited by P, and those for N can be used for regions limited by N.

5.2.4 Aggregation of CFs

To match the freshwater eutrophication CFs with life cycle inventory data, the grid-level CFs can be aggregated to any scale through Eq. 5.4 and Eq. 5.5. We provided CFs aggregated to the country level, the common level of inventory data, using two methods: (1) considering only the P/N-limited regions; (2) considering the entire region.

$$CF_{r,e} = \frac{1}{\sum_i E_{e \rightarrow i \in r}} \cdot \sum_i CF_{e \rightarrow i \in r} \cdot E_{e \rightarrow i \in r} \quad (5.4)$$

$CF_{r,e}$ (PDF·year·kg⁻¹) indicates the aggregation of nonzero CFs (i.e., we excluded CFs that are zero) for direct emissions to freshwater and diffuse emissions excluding erosion over a region r . In method 1, r only includes the P/N-limited regions within the country; in method 2, r indicates the whole country. $E_{e \rightarrow i \in r}$ (kg year⁻¹) is the emission-weighting data of the emission route e in the source cell i that belongs to the region r .

All nonzero $CF_{i \in r, erosion, landuse}^*$ were summed over a region r weighted by the area of the land use type ($A_{i \in r}$, m²) to provide $CF_{r, erosion, landuse}^*$.

$$CF_{r, erosion, landuse}^* = \frac{1}{\sum_i A_{i \in r}} \sum_i CF_{i \in r, erosion, landuse}^* \cdot A_{i \in r, landuse} \quad (5.5)$$

We also calculated the proportion of emission-weighting data (direct emissions and diffuse sources) and area (arable land and pasture) for nutrient-limited regions across all countries. It equals the ratio of emission-weighting data or area between nutrient-limited regions and the whole country. If it remains unknown where in a country a nutrient is emitted and which nutrient is limiting, one could calculate the average of P and N impacts, weighted by such proportions. For ease of use, we also provide country-level CFs that already incorporate such weights.

5.2.5 Global impact of eutrophication on freshwater fish species

We calculated the global freshwater fish species loss due to eutrophication from global nutrient emissions and agricultural land use in 2010 to test the application of the developed CFs. The impacts were obtained from the product of inventory data (direct or diffuse emissions, or land occupation area and time) and the respective CFs:

$$I_{emission} = \sum CF_{i,emission} \times E_i \quad (5.6)$$

$$I_{erosion} = \sum CF_{i,erosion} \times A_i \times t \quad (5.7)$$

where $I_{emission}$ and $I_{erosion}$ (PDF·year) represent the total impact on freshwater fish species, taking the sum of the impact of each source cell i ; $CF_{i,emission}$ (PDF·year·kgX⁻¹, where X represents P or N) and $CF_{i,erosion}$ (PDF·year/(m²·year)) indicate the CF for P and N emissions and for erosion, respectively, choosing the average CFs for global rather than regional species loss; E_i (kgX) denotes the emissions, for which we considered here the global emissions over a year; A_i (m²) is the land use area occupied, for which we considered here the total agricultural land use area; and t (year) is the occupation time, for which we considered one year. The emissions or land use areas were retrieved from IMAGE-GNM. The impact was aggregated over the world, considering the nutrient limitation.

5.2.6 Regionalized characterization factors

The gridded CFs for global freshwater species loss show similar hotspots for P and N (Figure 5.1, Figure S5.1 and S5.2 in Supporting Information). Results showcase only slight differences between using the average or marginal methods to assess effects. For the diffuse emissions and the direct emissions to freshwater, high CFs are located in densely populated regions that encompass either large lakes or the headwater of rivers, most of which are in tropical and temperate zones. For erosion, high CFs belong to those areas with intensive agriculture and animal husbandry. Compared with pastureland, more erosion per area occurs in arable land and thus leads to higher CFs.

High values for all the emission routes are found in the Andes Mountains (the upstream of the Amazon River), the Sierra Madre do Sul - Sierra Madre Occidental (the upstream of San Diego River and Marikina River), Great Salt Lake, Lake Tanganyika, and the Himalayas and Dangla Mountains (Yalu Cangbu River and Mekong River Basin).

Low CFs for P and N are found in high latitudes, such as the north of Canada, northern Europe, the south of Argentina, the east of Russia, and the northeast of China. These regions are sparsely populated and thus less affected by human activities, or they are located on the coasts where most contaminants disperse from freshwater to offshore environments.

Compared with CFs for regional species loss (Figure S5.3 and S5.4 in Supporting Information), CFs for global species loss show similar spatial patterns in tropical and temperate zones. Nevertheless, for direct emissions, CFs for global species loss seldom have hotspots in polar regions while CFs for regional species loss have hotspots in North Russia and North Canada. This difference results from considering or not considering GEP (Figure S5.13 in Supporting Information). In addition, CFs for global species loss show a larger variation between polar and temperate regions than CFs for regional species loss.

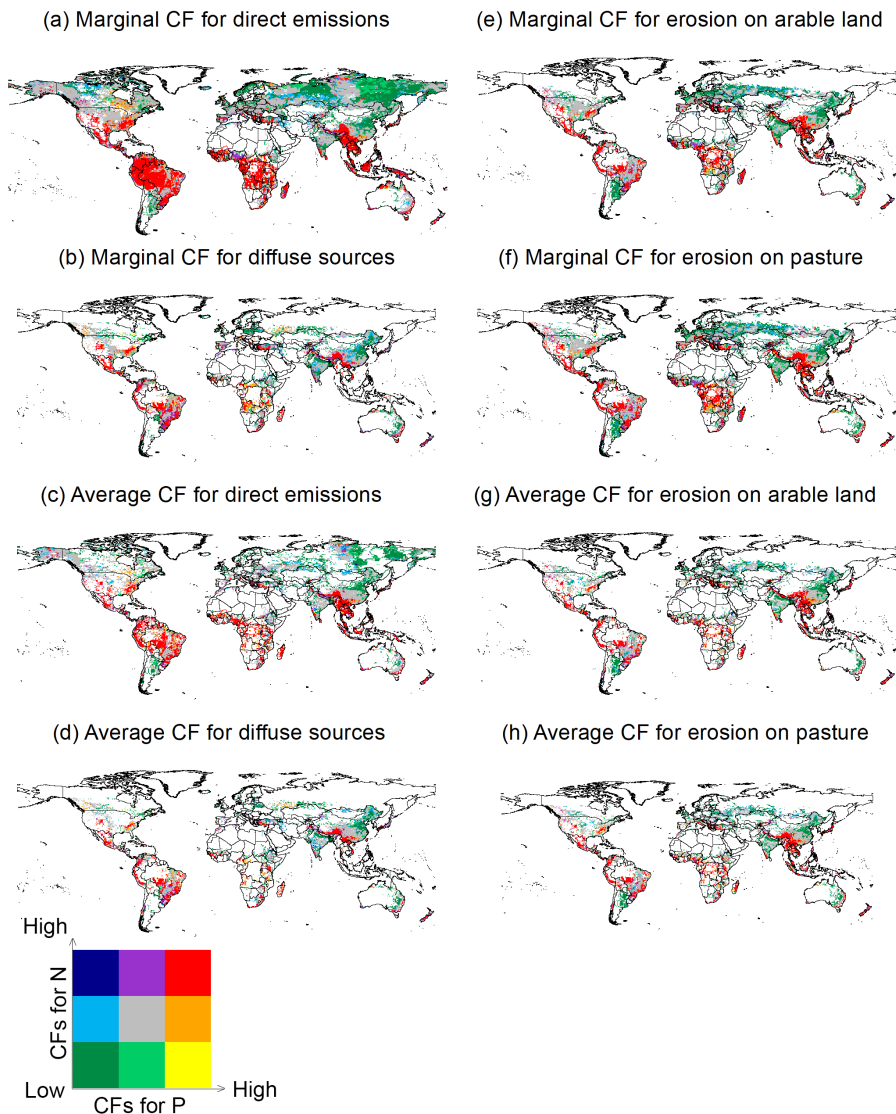


Figure 5.1 Comparison of characterization factors between P and N at a half-degree resolution. Low CFs and high CFs indicate CFs < first quartile (Q25) and CFs > third quartile (Q75), respectively, and medium CFs are between low and high CFs.

5.3 Results

5.3.1 Nutrient limitation

Excluding the 7.8% of global arid regions without freshwater, the non-arid regions

limited by P and N occupy 52.3% and 36.5%, respectively, while 3.4% are covered by negligible P and N concentrations (Figure 5.2). Among these, 23.5% of the area limited by P and 11.7% of the area limited by N is susceptible to undesirable rates of periphyton growth. Undesirable eutrophication ties up with densely populated regions, while acceptable nutrient freshwater concentrations are distributed in sparsely populated areas such as the polar region and arid zones. The US, China, and countries in north and west Europe, east South America, and central Africa belong to P-limited regions with undesirable periphyton growth. These regions are affected by P contained in runoff, domestic and industrial wastewater from populated urbans and sludge in arable land. Australia, the countries in north Africa and west Asia are more affected by N limitation as they represent regions with historically relatively small proportions of arable land.

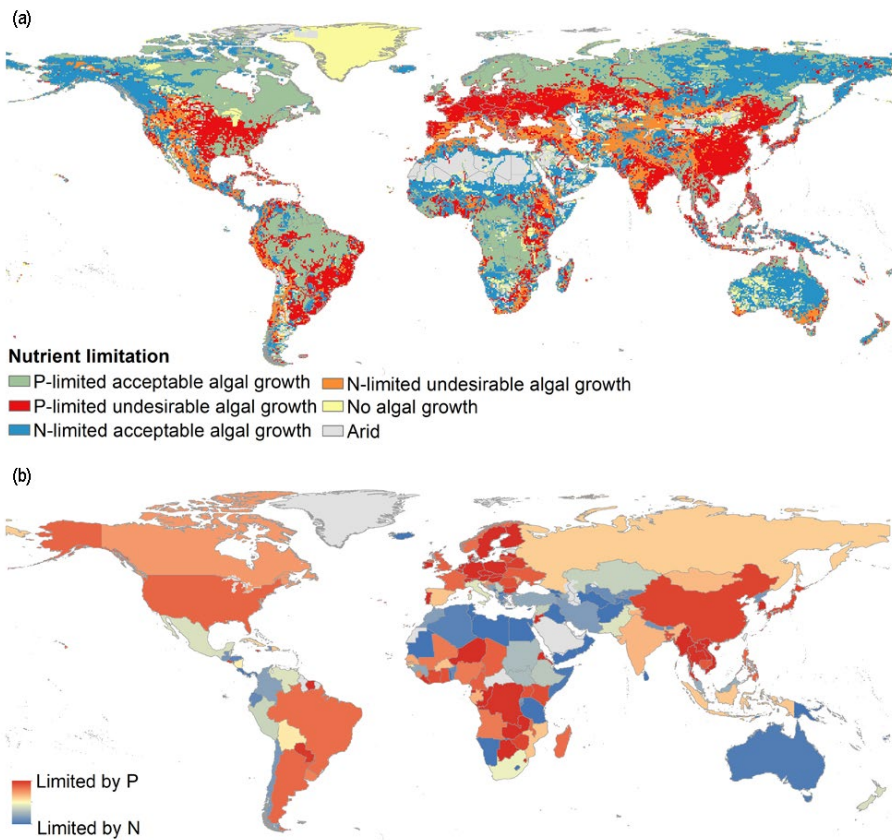


Figure 5.2 Nutrient limitation for algal growth based on the Redfield ratio: (a) on the gridded scale, (b) on the country scale. Acceptable and undesirable algal growth in panel (a) was determined based on the current P and N concentrations. Panel (b) shows the proportion of P-N limitation that is weighted by direct emissions in those countries where average CFs for this emission route are available.

5.3.2 Aggregation of characterization factors

The influence of considering nutrient limitation on country-level CFs varies across countries for all emission routes, while the hotspots (e.g. Cameroon) and low-CF countries (e.g. Libya) (Figures S5.5 - S5.12 in Supporting Information) maintain a similar pattern independent of nutrient limitation. Considering nutrient limitation leads to about half-half increase vs. decrease in country-level CFs. Take the average CFs for direct P emissions as an instance; the inclusion of nutrient limitation makes more countries have higher country-level CFs (56 countries higher vs. 52 countries lower than not considering nutrient limitation), whilst the opposite applies to direct N emissions (54 countries higher vs. 55 countries lower).

On a global scale, the inclusion of nutrient limitation leads to lower CFs for diffuse P emissions (by 2% to 3%) and higher CFs for other emission routes (by up to 30%). Yet, considering nutrient limitation makes CFs for N higher (by 25% to 62%) (Figure 5.3). The average CFs for all emission routes are higher than marginal CFs, independent of considering nutrient limitation.

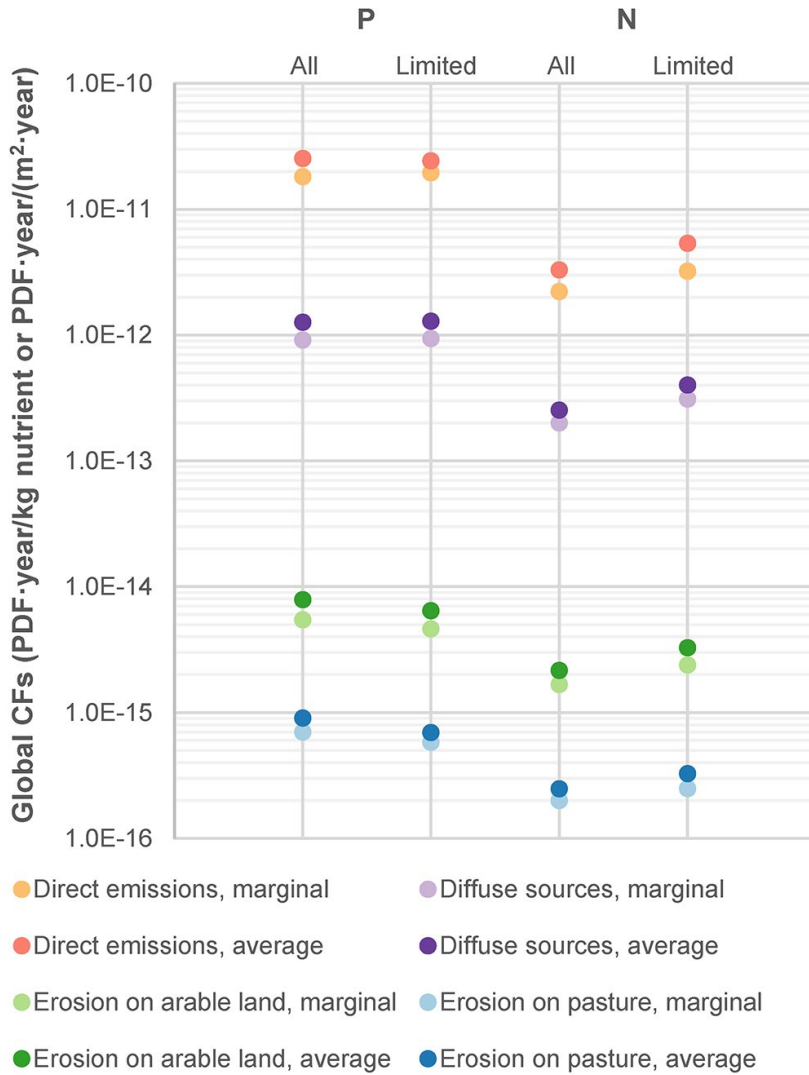


Figure 5.3 Globally aggregated characterization factors (CFs) for P and N impacts on global species richness. The unit of CFs for direct and diffuse emissions is PDF·year/kg nutrient, where nutrient represents P or N, while the unit of CFs for erosion is PDF·year/(m²·year). CFs consider either all regions (All) or only regions limited by the respective nutrient (Limited).

5.3.3 Global impact of eutrophication on freshwater fish species

Considering nutrient limitation in CFs, we calculated the impact of global P and N emissions as well as erosion enhanced by agricultural land use during the year 2010 on freshwater fish species richness as 0.138 PDF·year (Table 5.1). Among all the emission routes, erosion on arable land contributes the most to the impacts, while diffuse emissions are the second strongest contributor. Direct emissions rank third and still contribute considerably, while the erosion on pastureland has the least influence. Regarding nutrients, P leads to more than double the species loss than N. The difference in impacts is particularly evident for erosion. In summary, P is the paramount nutrient for freshwater eutrophication (causing an impact of 0.098 PDF·year), but the impact of N should not be neglected (0.040 PDF·year).

Table 5.1 Global species loss over the world considering the nutrient limitation. The unit is PDF·year.

	Impact of direct emissions	Impact of diffuse emissions	Impact of erosion on arable land	Impact of erosion on pasture	Sum
P	0.019	0.026	0.047	0.006	0.098
N	0.012	0.013	0.013	0.002	0.040

5.4 Discussion

In this study, we used two methods for deriving EFs (average and marginal) and compiled the CFs for four emission routes at multiple spatial scales: global, country level, and half-degree grid level. These CFs can be used with emissions and land use areas from life cycle inventories to assess the nutrient-induced impacts on freshwater fish biodiversity. Our improvements include providing CFs that cover eutrophication more comprehensively than just hypoxia (Cosme and Hauschild, 2017) with a much finer resolution for both FFs and EFs than previous studies (Cosme et al., 2018; Payen et al., 2021; Verones et al., 2020). We note that our CFs for N also encompass the potential impact of N-induced toxicity (Kroupova et al., 2018), which is a different

impact category to eutrophication (Chislock et al., 2013; Dodds and Smith, 2016; Payen et al., 2019; Smith et al., 2006). However, N overloads have been deemed to predominantly affect the aquatic ecosystem through eutrophication (Chislock et al., 2013; Dodds and Smith, 2016; Wang et al., 2021), while direct toxicity contributes little to the influence because it only occurs at a very high concentration of certain forms of N, such as ammonia and nitrite (Jones et al., 2014; Kroupova et al., 2018; Thurston et al., 1981).

Compared with previous studies that only consider P-related freshwater eutrophication and N-related marine eutrophication in CFs, our study is the first to incorporate both P and N simultaneously and consider which of the two nutrients is limiting where. The information about nutrient limitation can guide users in the choice to assess the impacts of either P or N emissions. The CFs allow LCA practitioners to estimate the nutrient impact on freshwater fish species richness more accurately. This method can also serve as a prototype that may be adapted for eutrophication impact assessment related to marine or terrestrial ecosystems.

Based on the approach outlined above (considering nutrient limitation), the global impact of eutrophication on freshwater fish species is 0.138 PDF·year. The dominance of erosion as a contributor to the impacts of freshwater eutrophication is consistent with the findings of Scherer and Pfister (2015). Since the fate within the freshwater is relatively short (in the order of dozens of days) but the emissions and erosion are spread throughout the year, the exposure duration can be assumed to be roughly one year. This means that 13.8% of the fish species potentially disappear due to freshwater eutrophication. This result approximates 15.6% (= 24.8%×63%) of freshwater fish species threatened with extinction due to pollution, as estimated by Miranda et al. (2022). This agreement shows the validity of using our CFs to reproduce the influence of freshwater eutrophication on the global ecosystem.

The model for nutrient transport and fate is crucial for determining CFs and can be a large source of uncertainty. For instance, 0.5% of the 0.5×0.5 degree grid cells have a

diffuse N loading from surface runoff that exceeds diffuse emissions, since IMAGE-GNM does not isolate the influence of long-term retention of N in the soil surface from the short-term loads in surface water due to new emissions. The isolation of these processes might be possible by using a process-based mechanistic model such as the IMAGE-Dynamic Global Nutrient Model (DGNM) (Vilmin et al., 2020), which models water column and sediment dynamics, and the exchanges between them. A future version on a global scale can form a better basis for developing CFs (Vilmin et al., 2020).

A large amount of data and high spatial resolution allowed distinguishing nutrient-species relationships across 425 ecoregions, which is substantially beyond the previous knowledge of only four geographical zones (Cosme et al., 2017). This resolution could even be improved for the effect factors by considering the background concentration at different locations within the ecoregions. More regionalized environmental indicators can help to better assess impacts at local scales. Our study showcases the advantages of finer spatial resolutions, and we recommend the continuation of this practice when developing new CFs in the future. Next to spatial differentiation, the temporal dynamics in emissions from human activities should be considered in future studies (Potting and Hauschild, 2006; Seppala et al., 2001).

In conclusion, we developed regionalized CFs for freshwater eutrophication at a fine spatial resolution and proposed a method to consider nutrient limitation in CFs. This work provides life cycle impact indicators and a roadmap for considering nutrient limitation to finetune CFs for multiple emission routes to assess the eutrophication impact on regional and global species richness for LCA practitioners. This roadmap and the consideration of comprehensive nutrient-species effects can be further used for developing regionalized CFs for eutrophication in other ecosystems.

Supporting Information

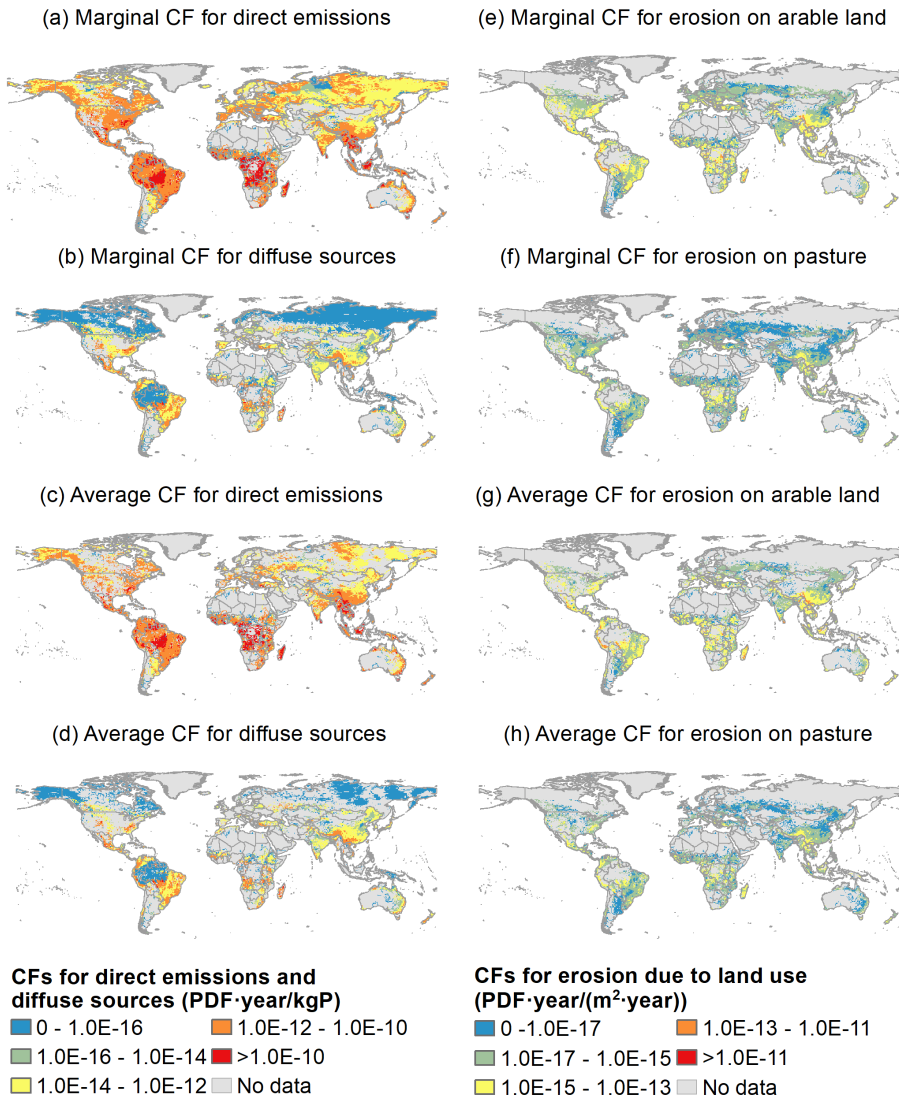


Figure S5.1 Characterization factors for freshwater fish species due to P emissions at a half-degree resolution

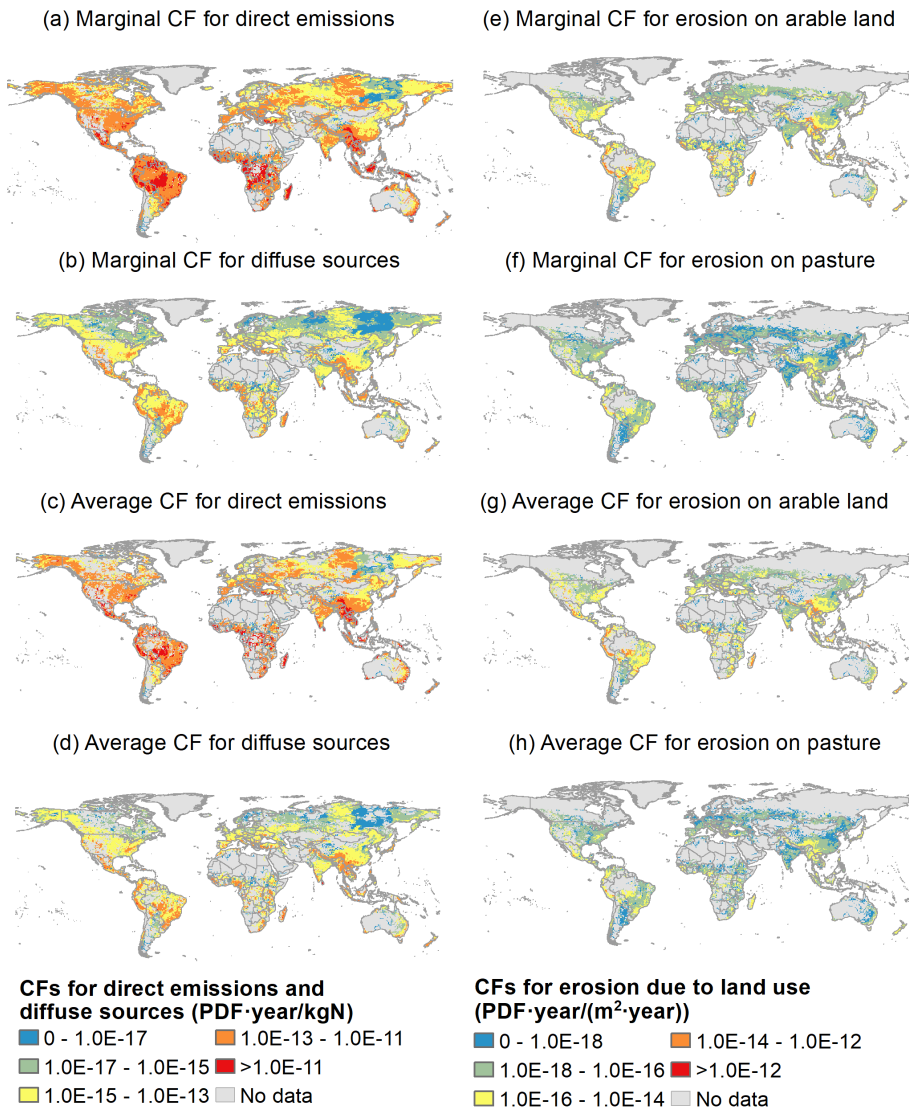


Figure S5.2 Characterization factors for freshwater fish species due to N emissions at a half-degree resolution

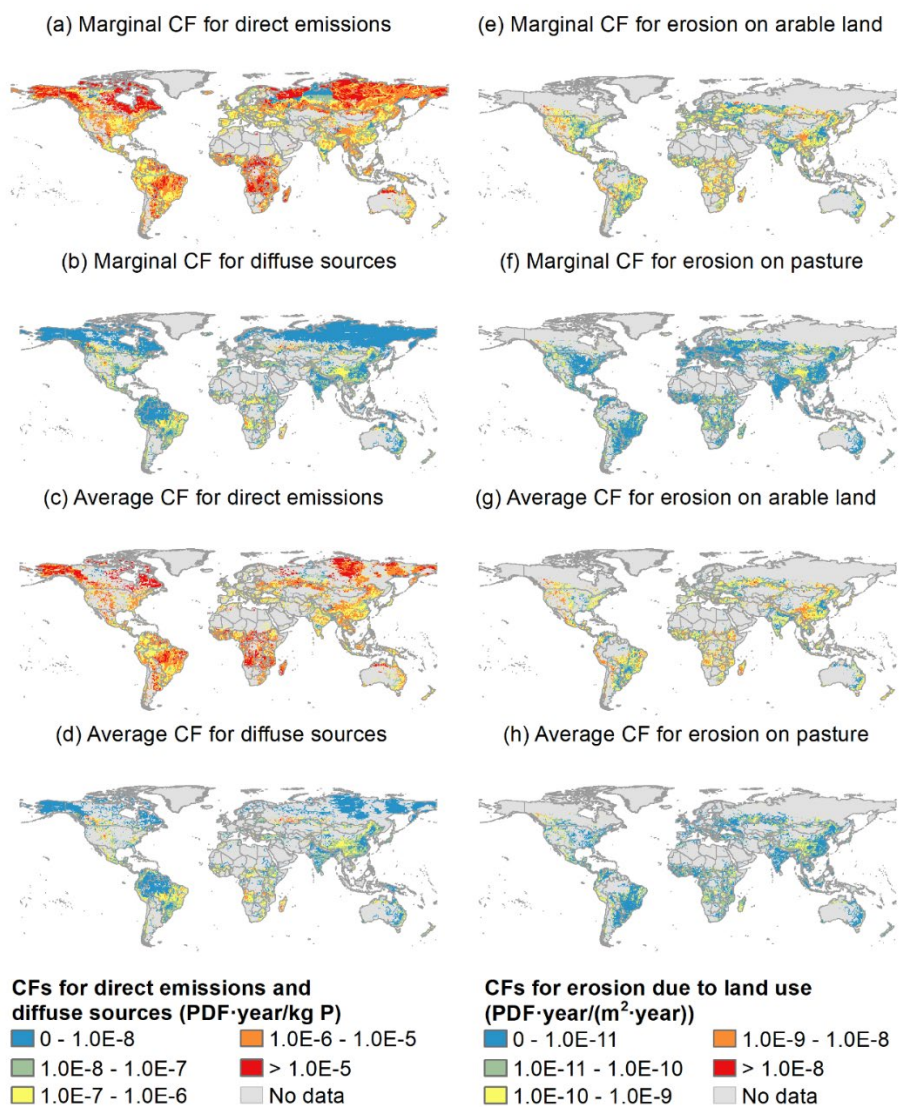


Figure S5.3 CFs for regional freshwater fish species loss due to P emissions at a half-degree resolution

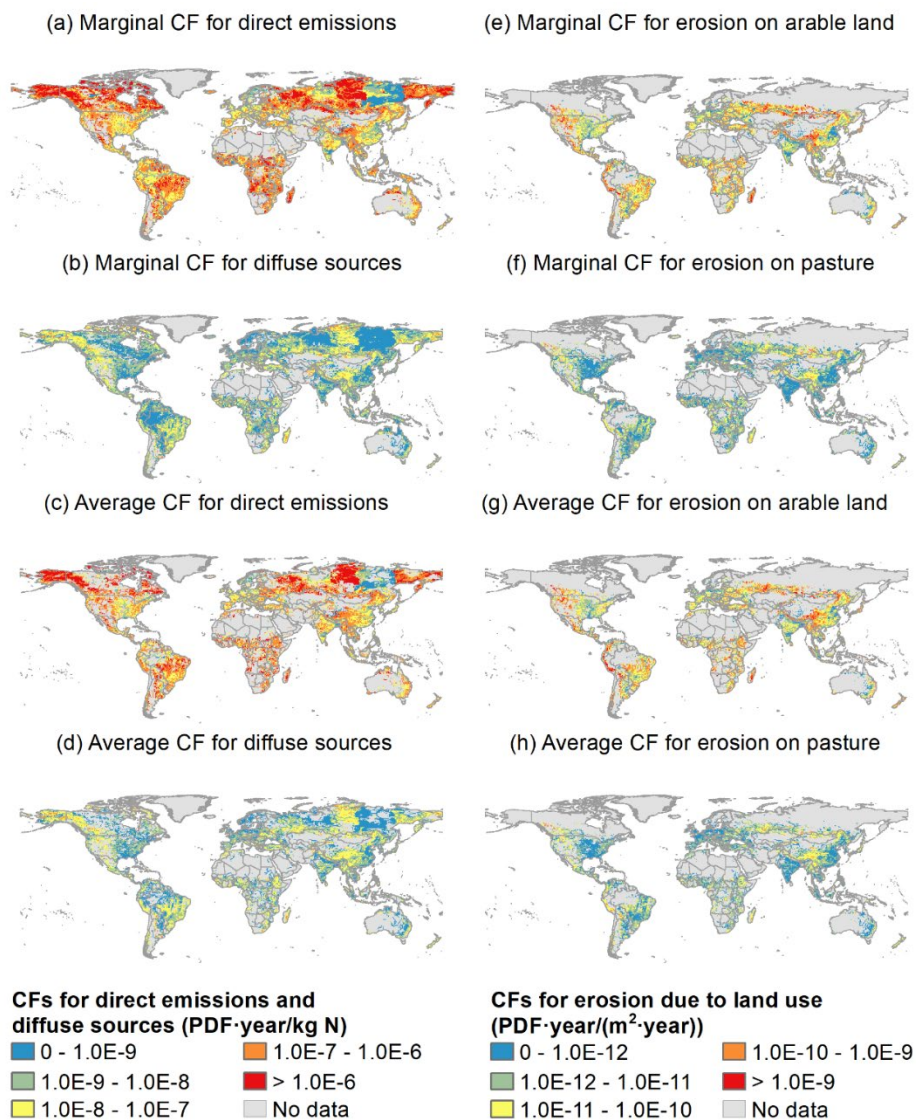


Figure S5.4 CFs for regional freshwater fish species loss due to N emissions at a half-degree resolution

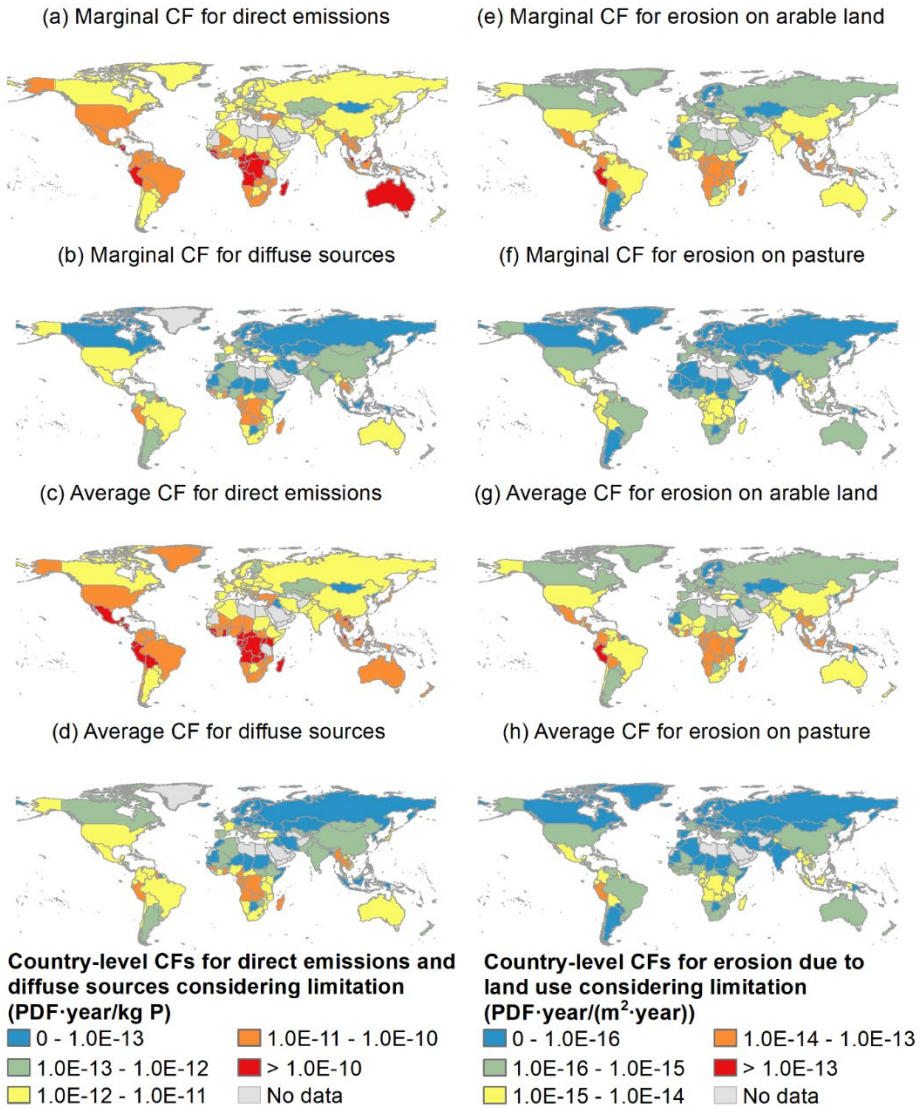


Figure S5.5 Country-level CFs for global species loss due to P emissions considering P-limited regions only

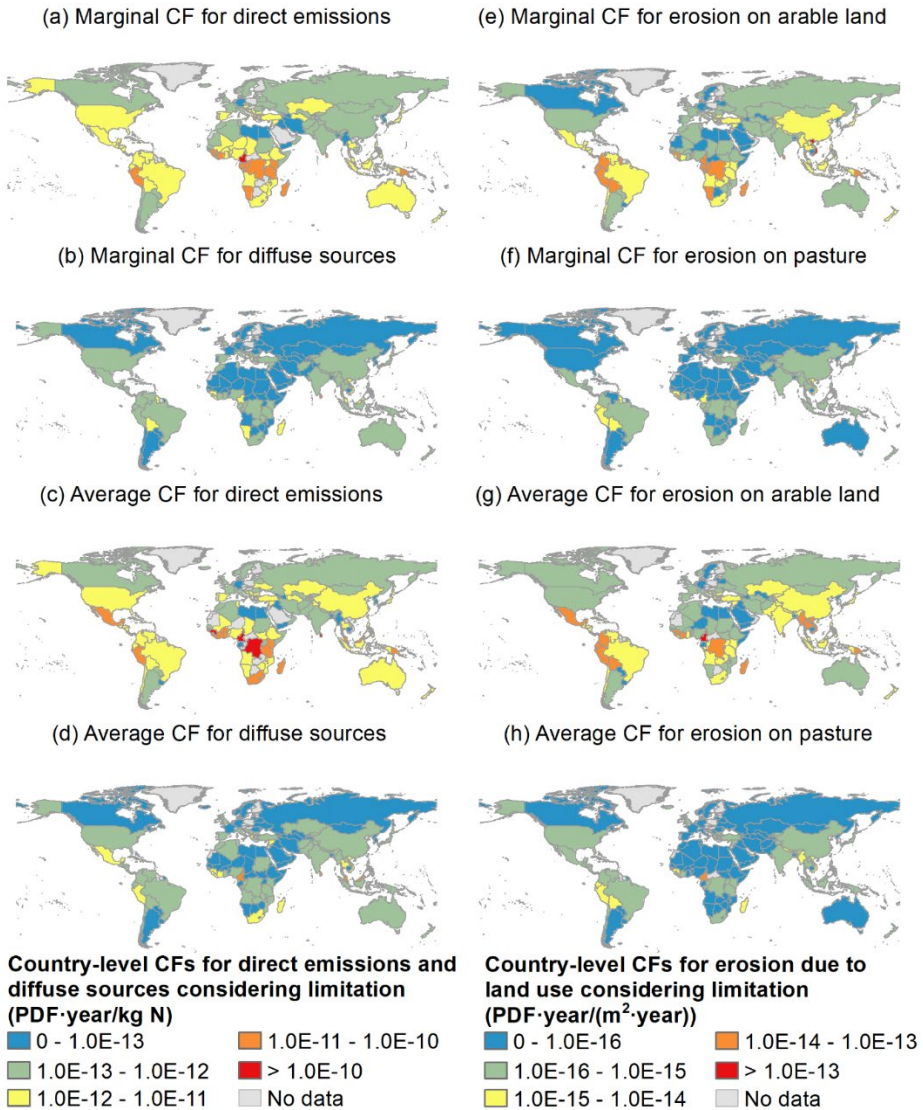


Figure S5.6 Country-level CFs for global species loss due to N emissions considering N-limited regions only

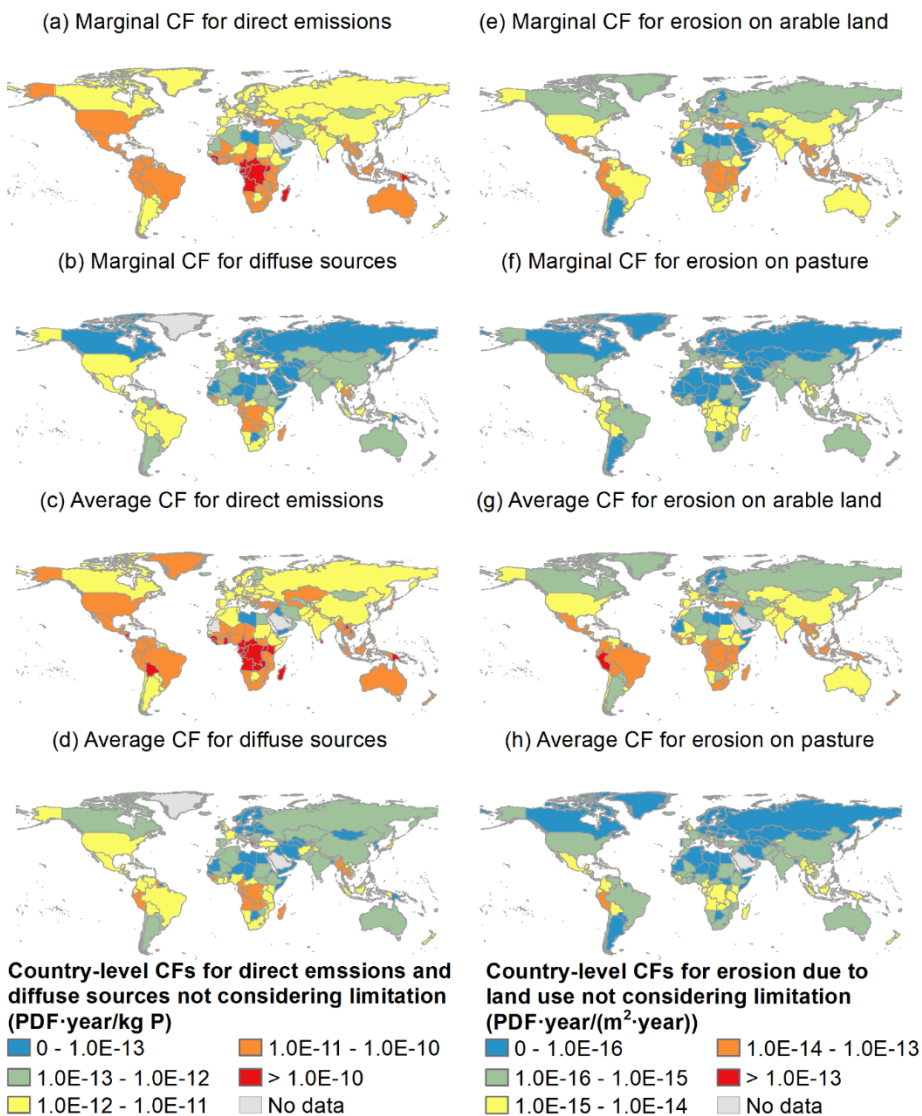


Figure S5.7 Country-level CFs for global species loss due to P emissions not considering the nutrient limitation

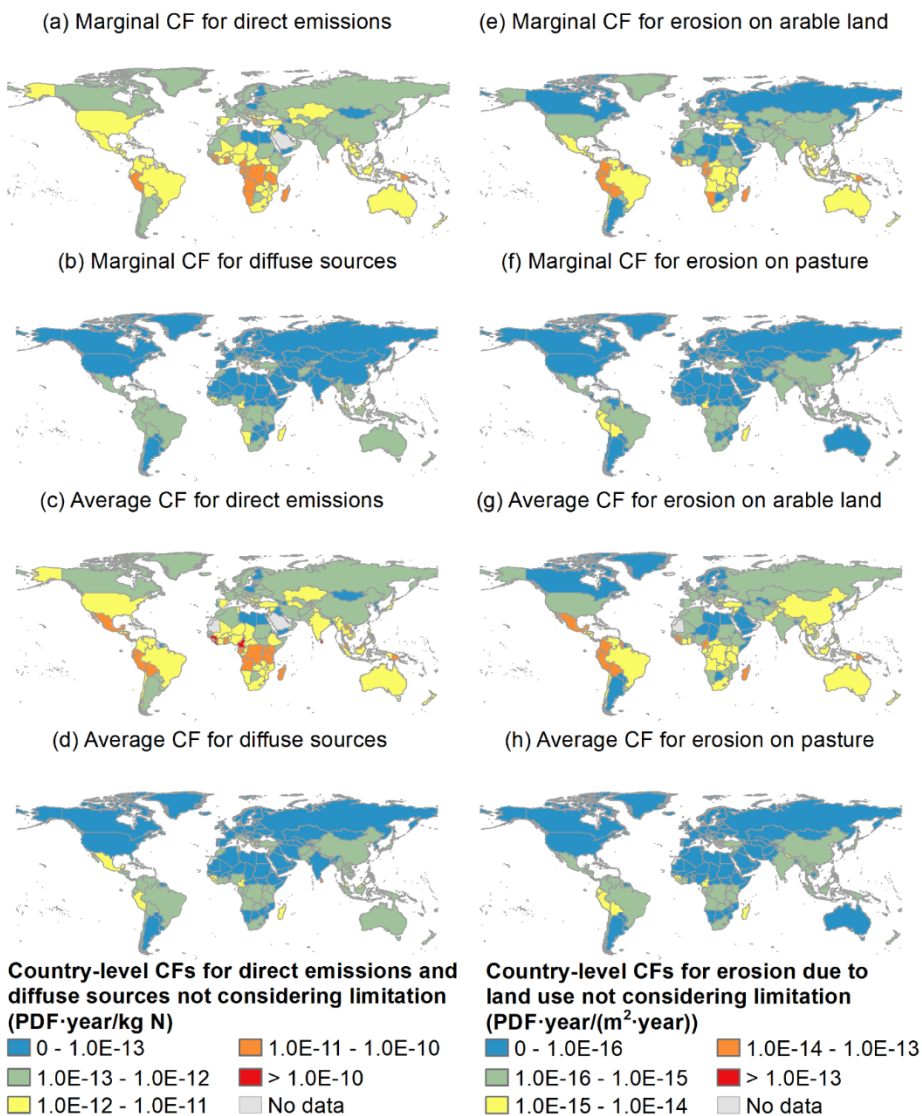


Figure S5.8 Country-level CFs for global species loss due to N emissions not considering the nutrient limitation

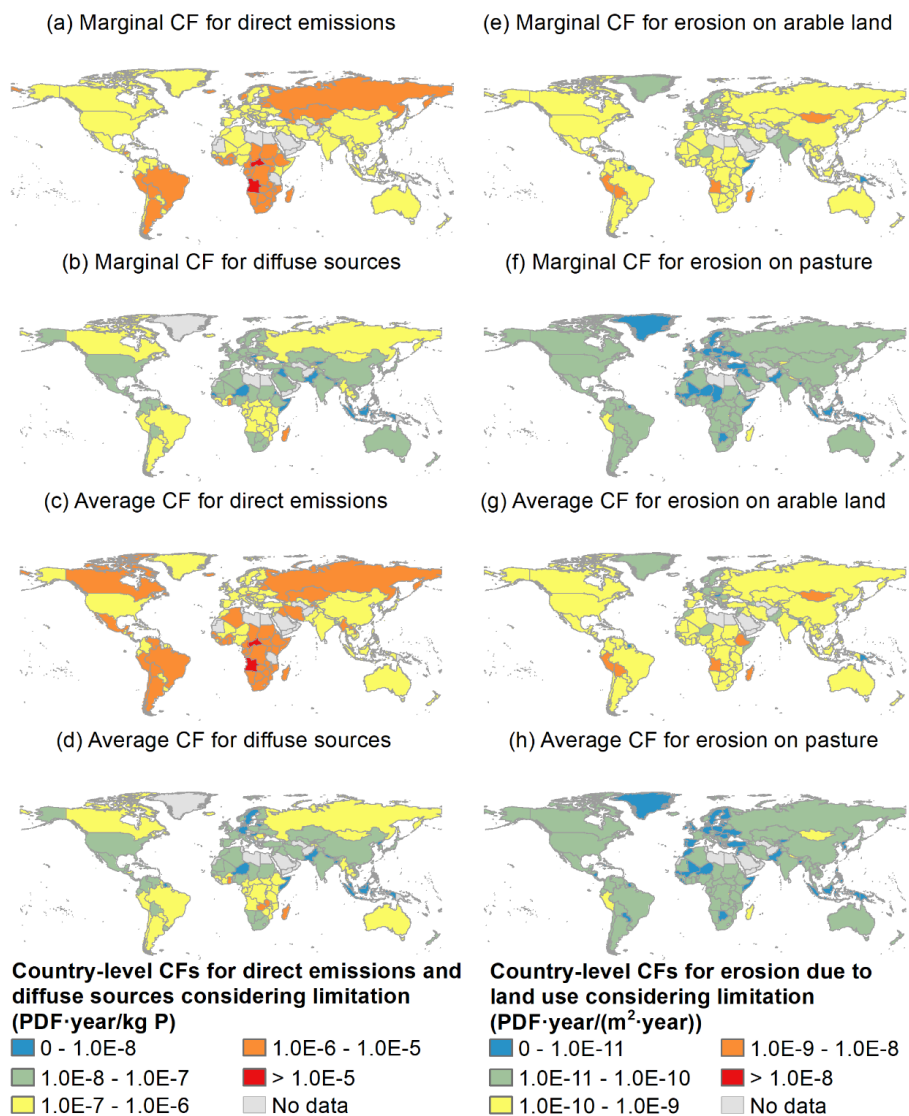


Figure S5.9 Country-level CFs for regional species loss due to P emissions considering P-limited regions only

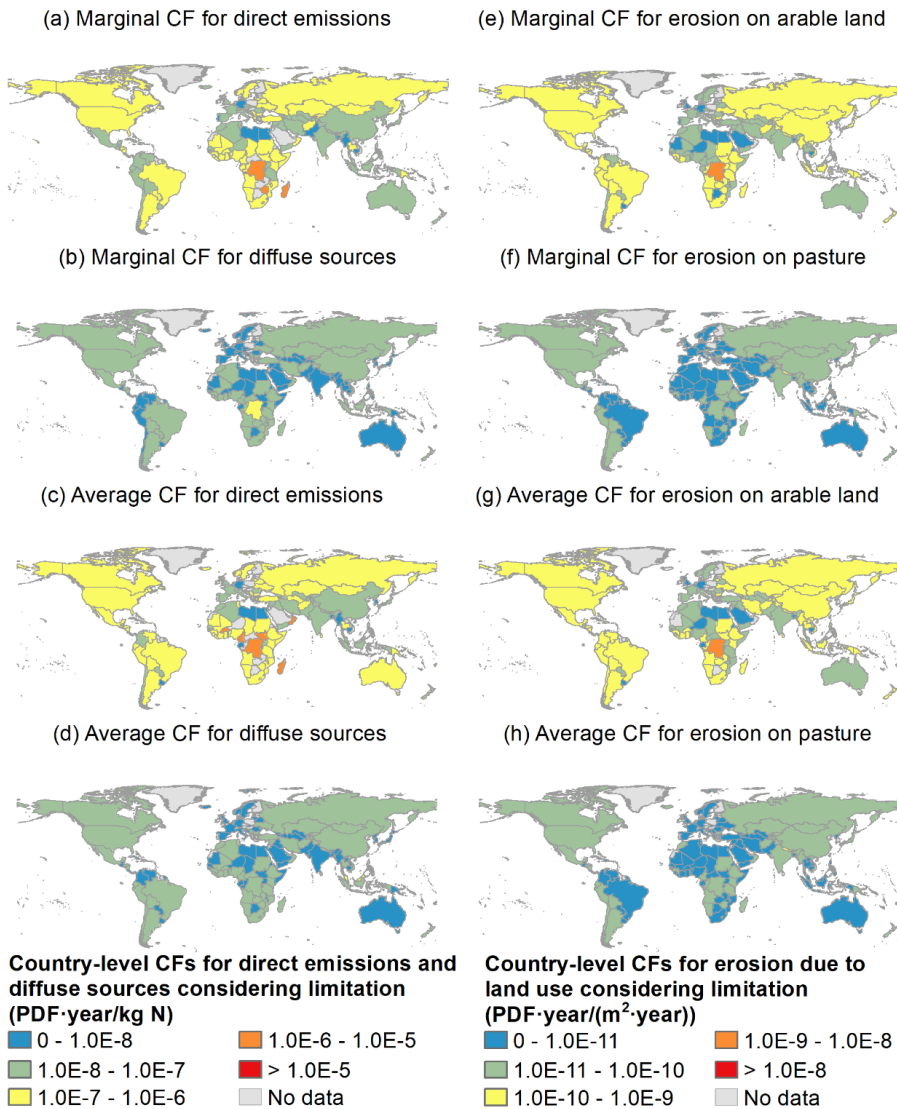


Figure S5.10 Country-level CFs for regional species loss due to N emissions considering N-limited regions only

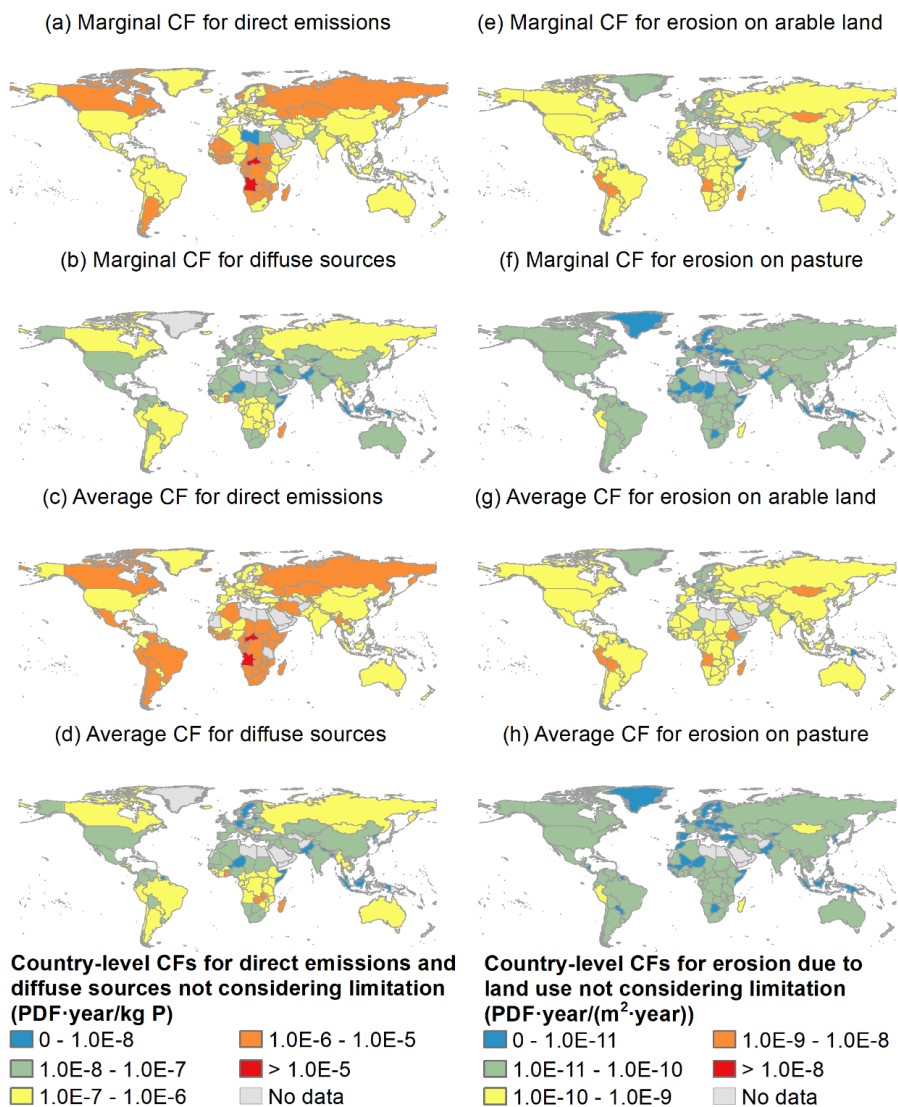


Figure S5.11 Country-level CFs for global species loss due to P emissions not considering the nutrient limitation

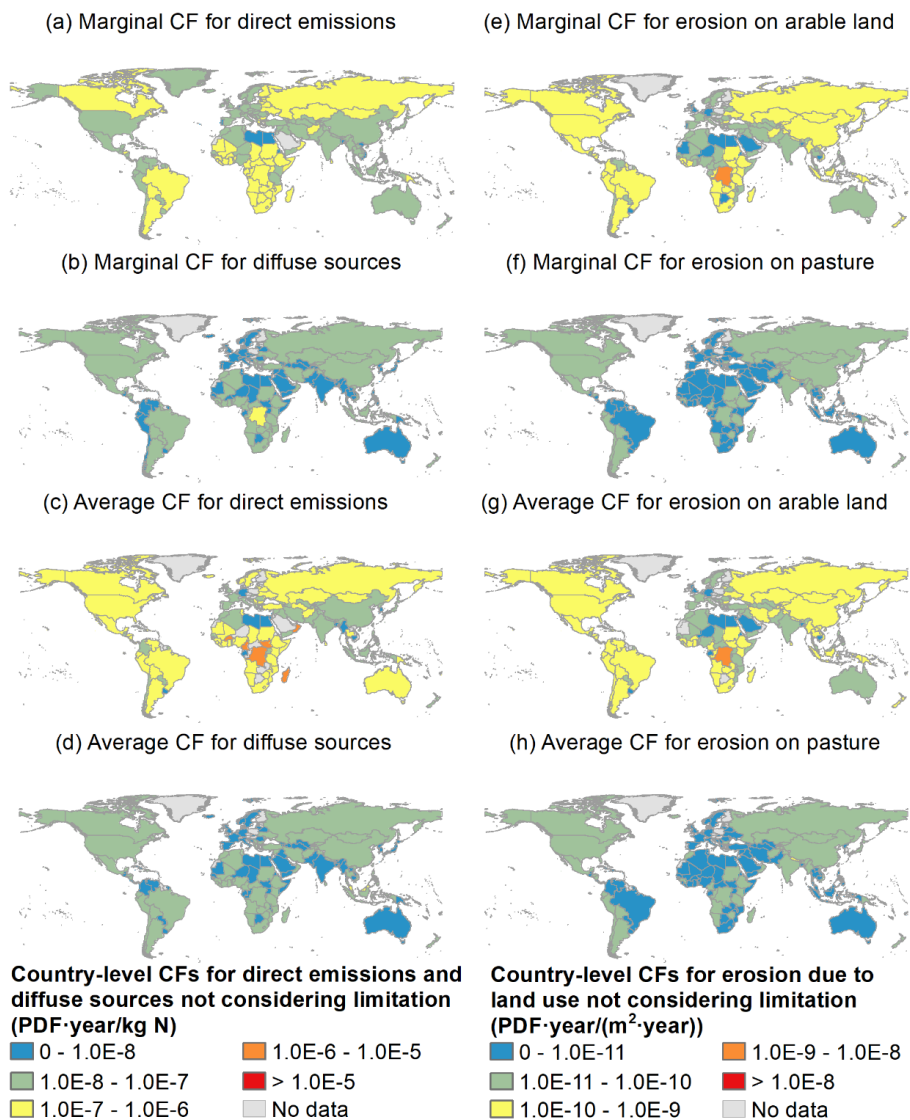


Figure S5.12 Country-level CFs for global species loss due to N emissions not considering the nutrient limitation

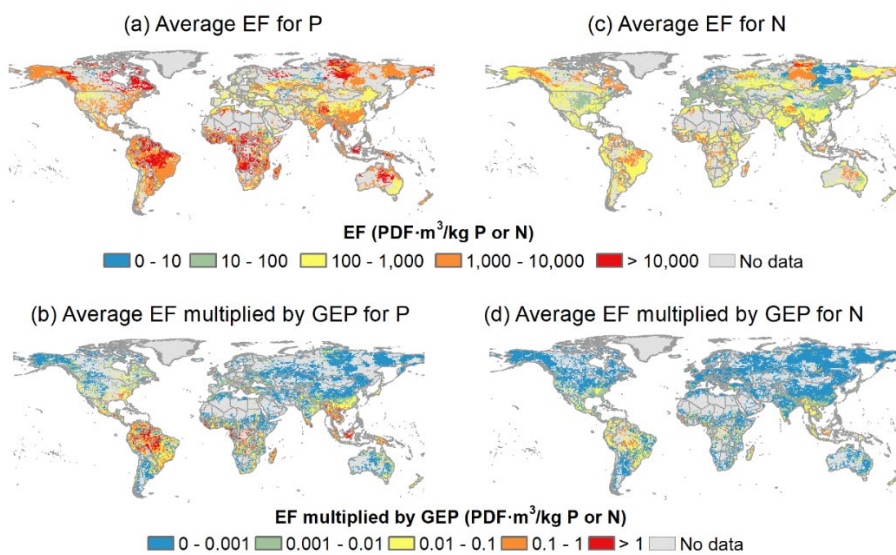


Figure S5.13 EF and EF multiplied by GEP for P and N

Chapter 6

General discussion



6.1 Answers to the research questions

In current eutrophication studies, there exists a notable absence of comprehensive quantification methods to effectively model the loss of biodiversity. It was within this void that my research emerged, weaving a narrative that sought to address two pivotal inquiries: unraveling the extent of influence wielded by phosphorus (P) and nitrogen (N) on biodiversity loss, and discerning the magnitude of impact of these nutrients on fish species. In pursuit of this goal, the narrative of this thesis unfolds as it pioneers the development of comprehensive and regionalized characterization factors (CFs) specifically tailored for the freshwater eutrophication category. This approach is poised to elevate the predictive power and ecoregional precision of life cycle impact assessment (LCIA). Notably, the study meticulously adheres to the guidelines outlined by the Global Life Cycle Impact Assessment Method (GLAM) project, ensuring a methodologically robust and globally applicable framework (Payen et al., 2019; Verones et al., 2019). In detail, by utilizing the Integrated Model to Assess the Global Environment–Global Nutrient Model (IMAGE-GNM, Beusen et al. (2015)), the thesis first established fate factors (FFs) with a spatial resolution of 0.5×0.5 degrees (Chapter 2). It then assessed the performance and role of retention models in IMAGE-GNM to improve nutrient fate predictions (Chapter 3). Thirdly, the research estimated the effects on the species richness at a half-degree resolution based on the relationship between nutrient concentrations and 41-year occurrence records of 13,920 freshwater fish species. This research also estimated robust species sensitivity distributions (SSDs) across global freshwater ecoregions (Chapter 4). Utilizing the aforementioned factors, regionalized CFs were formulated and integrated with global extinction probabilities (GEPs) and nutrient limitation information. Subsequently, global freshwater fish species loss was evaluated based on the CFs and human-generated nutrients, discerned by various emission routes and nutrient types (Chapter 5).

In detail, this thesis achieves the research goal by addressing the four questions mentioned in the first chapter:

Q1: What is the pattern of regionalized nutrient fate, and how do drivers affect the nutrient fate over the global freshwater?

In Chapter 2, we developed a method for regionalized FFs at half-degree resolutions based on the nutrient fate and hydrological parameters modeled by IMAGE-GNM. We took N as an example and analyzed FFs for N over the global freshwater system. Our results reveal that the hydrological conditions can influence the nutrient fate. For instance, low FFs occur in regions characterized by large rivers with high discharge and low residence time, while high FFs occur in water bodies with high residence time, such as lakes and reservoirs. Regarding nutrient removal, high discharge, and low residence time characterize the strong removal by advection, while high residence time and low discharge represent high retention. Advection is the dominant removal process that affects FFs in $\sim 2/3$ of global regions. Retention dominates $< 1/3$ of regions, and water consumption only dominates 1.4% of regions that are water-scarce. These results demonstrate the importance of developing site-specific FFs to assess eutrophication impacts since the geographical and hydrological conditions vary spatially. This chapter, therefore, characterizes FFs for N at high spatial resolution and contributes to the improvement of global eutrophication assessment by introducing soil-freshwater N fate to complement existing P-related fates. The same method was used for calculating FFs for P as a component of CFs in Chapter 5.

Q2: How can retention equations improve model performance?

As mentioned above, retention is one of the most crucial processes affecting the accuracy of nutrient fate modeling, in addition to the hydrological input data (governing advection) and the spatial resolution (van Vliet et al., 2019). The hydrological input data rely on the establishment of gauges and stations, and thus more data with better quality is inaccessible at present. Spatial resolution for a model is always fixed when the model is framed. The retention cannot be measured directly and is modeled by empirical equations. Thus, the choice of empirical equations is crucial for characterizing retention and eventually affects the accuracy of nutrient models. Chapter

3 evaluated the performance of retention equations for global nutrient models and analyzed the influence of driving forces, function form, and equation coefficients. We used methods of one-way Analysis of variance (ANOVA) and post hoc tests as well as multiple criteria, including the mean-Normalized Root Mean Square Error (NRMSE), Pearson's r , and relative bias, to validate IMAGE-GNM based on abundant samples from diverse sources.

Chapter 3 reveals that the specific-runoff-driven equations of Behrendt and Opitz (1999) (q) are the best fit for riverine nutrient retention, and De Klein (2008) performs the best for P retention in lakes. This chapter highlights that 1) the influence of hydraulic drivers in retention models is more important than the function form and coefficients; 2) retention models based on localized coefficients and function forms show better performance globally than those developed at global scales (i.e., the currently used equation of Wollheim et al., 2008, in IMAGE-GNM); 3) the consideration of temperature as a secondary driving force of P retention might increase the accuracy of retention prediction (D'angelo et al., 1991; Jensen and Andersen, 1992; Kim et al., 2003). According to our analysis of the geographical zones, we also find the equation by Behrendt and Opitz (1999) (q) fits well in most regions, while other retention equations perform better than it in some zones. Thus, we suggest applying specific retention equations at the geographical-zone scale rather than the global scale. These conclusions can help to optimize the description of nutrient fate by improving the retention models, and thus further reinforce our understanding of global eutrophication.

Q3: What is the pattern of the regionalized effect on fish species loss across the global freshwater ecosystem?

So far, no existing study developed effect factors (EFs) for N on freshwater species richness (Chapter 4). Chapter 4 regionalized the species sensitivity of freshwater fish against N concentrations at the ecoregion level and provided average and marginal EFs at half-degree resolutions. We used multiple criteria (pseudo R^2 and NRMSE) to evaluate the performance of our SSD equations based on millions of species occurrence

observations recorded over 41 years. The results show good fits of SSDs for all the ecoregions with sufficient data. The results underline the high possibility of species loss in the tropical zone and the vulnerability of cold regions. Similar patterns can be seen for average and marginal EFs, while marginal EFs show slightly more areas with high values ($>100,000 \text{ PDF}\cdot\text{m}^3\cdot\text{kg}^{-1}$) than average EFs. High values for marginal and average EFs can be found in regions with a rapid increase of N concentration currently, e.g., Taimyr, Arabian Interior, Baluchistan, Borneo Highlands, and Sangha. In agreement with other studies (Schulte-Uebbing et al., 2022), the regionalization of species sensitivity at finer resolutions in our study is beneficial for reflecting the spatial details in nutrient effects on species richness beyond the existing studies of a few geographical zones (Cosme and Hauschild, 2017). We applied the same method to calculate EFs for P as a component of CFs in Chapter 5, which complements the analysis of the eutrophication of both nutrients.

Q4: What is the impact of eutrophication on global fish species loss in freshwater ecosystems?

In Chapter 5, we connected FFs from Chapter 2 and EFs from Chapter 4 with GEPs to estimate regionalized CFs for P and N at multiple spatial scales: global, country level, and half-degree grid level. We also provided nutrient limitation information to assess when to implement the best CF. Integrating the CFs considering nutrient limitation with nutrient emissions and land use areas, we assessed the nutrient-induced impacts on global freshwater fish biodiversity. Globally, P causes double the potential species loss compared with N. For the nutrient emissions apart from erosion, high CFs are distributed in densely populated regions that encompass either large lakes or the headwater of rivers, most of which occur in tropical and temperate zones. For erosion, high CFs belong to those areas with intensive agriculture and animal husbandry. Our result estimates an impact of eutrophication on global freshwater fish species richness of 0.138 PDF·year, which agrees with the estimation of 15.6% of species affected by water pollution by Miranda et al. (2022). We also find that the dominant contributor is erosion from arable land, which agrees with Scherer and Pfister (2015). These

agreements reckon that our CFs are reasonable and able to assess the eutrophication impact. Diffuse emissions occupy over 1/4 of the contribution to the impact. These findings confirm that agriculture is the main driver of eutrophication.

6.2 Limitations and future research

Current studies quantify the human impact on biodiversity by either using biodiversity models or LCIA. For aquatic eutrophication, the most recognized biodiversity model, GLOBIO-Aquatic (Janse et al., 2015), models the impacts on mean relative abundance of inland aquatic species using a meta-analysis of studied information. This model considered diverse drivers (eutrophication, erosion/sedimentation, riparian settlements, and others) by combining local/regional case studies. However, considerable variations in observed effects exist among individual cases across geological scales and between drivers. Combining species composition data raises concerns as the interference with drivers is not interpretable and the correlation between a specific driver and local diversity may not apply at a larger regional level. This model cannot directly be used for the impact assessment of goods because they were designed for estimating biodiversity loss in regions as a whole. Consequently, this model should be viewed as complementary to other approaches and indicators (Janse et al., 2015). LCIA becomes crucial because it can explicitly unlock the cause-effect chain of the fate and transport of nutrients and their impact. The previous limitations of LCIA include the difficulty of quantifying site-specific fate and effect of nutrients and the simplified assumptions about nutrient limitations in ecosystems (P limits marine and N limits freshwater). My studies underscore the consideration of both P and N and the regionalization of both fate and effect.

The data availability, the model accuracy, and the implemented methodology lead to various limitations in this thesis. In detail, we discuss below the research limitations of nutrient fate, its effect on biodiversity, and the assessment of the impact of eutrophication.

Existing FF studies, including the one presented in Chapter 2, do not reproduce seasonal information on nutrient fate. Studies such as de Andrade et al. (2021) reckoned that FFs intensely vary spatially but are not highly temporally dependent. Thus, it is more important to regionalize FFs. However, temporal variability on a global scale still requires further study, since nutrient fate relies on hydrological conditions that are sensitive to the seasonal dynamics in climate (Chapter 2).

In the estimation of FFs, limitations in hydrological data restrict the reproduction of the advection and retention process. Due to a lack of data such as water volume, water depth, and damming information, the assumptions in the hydrological model and retention model integrated into IMAGE-GNM introduce uncertainty in the prediction of nutrient fate (Chapter 2). For instance, river damming can lead to a decrease in the hydraulic load, thus causing sediment trapping. This results in a decrease in advection and an increase in nutrient retention (Maavara et al., 2015). In addition, empirical retention equations used in IMAGE-GNM can only characterize the effects of changing hydrological parameters but cannot capture biogeochemical mechanisms for P and N. Apart from biogeochemical mechanisms, the nutrient model has limitations due to the absence of including interactions among nutrient forms, interactions with other elements, and release of P into water bodies from long-term accumulation of anthropogenic P retention in sediments. This ignorance of P release also leads to a larger uncertainty in the representativeness of P than of N in the nutrient model (Chapter 3).

As such, future work in process-based biogeochemical dynamics, especially in the modeling of retention, is needed to better reproduce P and N fate. Such a model would allow us to distinguish the specific forms and to capture the interaction among different nutrient species. For instance, the predictions of nutrient fate and concentrations can be upgraded by using a mechanistic model, IMAGE-DGNM (Vilmin et al., 2020). IMAGE-DGNM can simulate the interactive processes between nutrient species and capture the monthly variability of nutrient fate. The research scope of the current version of IMAGE-DGNM is restricted to specific watersheds, whilst a future version

of global scope can substitute IMAGE-GNM to better support the research on P and N fate and their impact on fish biodiversity (Vilmin et al., 2020) (chapter 2, 3, 4, 5).

In the assessment of EFs, limitations relate to an underlying assumption that fish species loss is caused by P or N increase. However, the occurrence of fish species may be affected by other stressors as well. Despite the major stressor of nutrient enrichment, the decrease in fish occurrence may also be affected by land-use change interactions (Comte et al., 2021), global warming (Barbarossa et al., 2021; Comte et al., 2021), and overuse of water (Pierrat et al., 2022). We thus suggest future studies on EFs to encompass other biodiversity threats concurrently. Such comprehensive consideration will reinforce the understanding of the way nutrient effects and other human pressures interact (chapter 4).

Moreover, the SSDs are limited by the quality of species observations. Uncertainty exists in potential sampling bias for our underlying point occurrence dataset. The issue of lack of observational data in cold regions is particularly prevalent, as pointed out in previous studies (Azevedo et al., 2013; Cosme and Hauschild, 2017). The accessibility to more species occurrence records in the future can reduce such uncertainty for some ecoregions (Chapter 4).

Our CFs on eutrophication impact for N may also include the influence of ecotoxicity (Kroupova et al., 2018), mixing in a different impact category to eutrophication (Chislock et al., 2013; Dodds and Smith, 2016; Payen et al., 2019; Smith et al., 2006). However, we believe this impact is limited because eutrophication is regarded as the predominant impact of N in aquatic ecosystems (Chislock et al., 2013; Dodds and Smith, 2016; Wang et al., 2021), as direct toxicity by certain forms of N at high concentrations, such as ammonia and nitrite, exerts little influence (Jones et al., 2014; Kroupova et al., 2018; Thurston et al., 1981). On the other hand, eutrophication and ecotoxicity are inseparable from N and should be considered comprehensively in their impact on the ecosystem. While previous studies only consider hypoxia (Cosme and Hauschild, 2017), our method covers the comprehensive impact of N. However, disentangling the

eutrophication and ecotoxicity of N is an important work in the future since it matches the standard impact categories (Chapter 5).

Within this thesis, I utilized freshwater fish species richness as a focal point to illustrate the biodiversity challenges influenced by eutrophication. However, relying solely on this metric may be insufficient to fully comprehend the broader impact on freshwater biodiversity. As previously highlighted, freshwater fish hold particular ecological significance, acting as indicators of ecosystem health and contributing to the overall integrity of habitats (Villéger et al., 2017). While species richness is a vital initial step in unraveling the complexities of the biodiversity issue, it represents just one facet of a broader spectrum. Biodiversity encompasses not only a variety of life forms but also involves factors such as cross-taxon congruence and other indicators that contribute to ecosystem health. Future research could delve further into the exploration of more comprehensive indicators associated with biodiversity to gain a more nuanced understanding of its intricacies.

6.3 Implications

This thesis offers practical indicators that can assist economic actors in evaluating the impacts of P and N on the global freshwater ecosystem and incorporate recommendations from GLAM (Payen et al., 2019). The research marks a crucial first step in untangling the intricacies of the biodiversity challenges stemming from human-induced P and N excess. It can serve as a prototype, laying a foundation for future impact assessments of eutrophication in both terrestrial and marine ecosystems as well as other biodiversity indicators. This work also underscores the imperative of aligning

with the United Nations' Sustainable Development Goals (SDGs) 6.3¹ and 15.1² (SDGs, 2015), alongside Kunming-Montreal Global Biodiversity Framework target 7³ (July, 2023), focusing on the conservation of freshwater ecosystems, biodiversity, and the mitigation of excessive nutrient levels. This research contributes to the pursuit of these targets by evaluating the repercussions of curbing nutrient excess as pollutants on freshwater biodiversity in diverse pathways. Consequently, the findings of the thesis offer valuable insights for decision-makers across nations, aiding them in formulating environmental strategies that adhere to international agreements and obligations.

Specifically, the inclusion of fate and effect for N complements the current P-related studies on freshwater environments. The findings highlight the connections between nutrient fate and the physical processes that rely on the hydrological and geographical conditions. This finding emphasizes the importance of regionalization at a fine resolution due to the large spatial variability of hydrological and geographical conditions. With a half-degree resolution, our FFs can be consolidated to any chosen

¹ By 2030, improve water quality by reducing pollution, eliminating dumping and minimizing release of hazardous chemicals and materials, halving the proportion of untreated wastewater and substantially increasing recycling and safe reuse globally.

² By 2020, ensure the conservation, restoration and sustainable use of terrestrial and inland freshwater ecosystems and their services, in particular forests, wetlands, mountains and drylands, in line with obligations under international agreements.

³ Reduce pollution risks and the negative impact of pollution from all sources, by 2030, to levels that are not harmful to biodiversity and ecosystem functions and services, considering cumulative effects, including: reducing excess nutrients lost to the environment by at least half including through more efficient nutrient cycling and use; reducing the overall risk from pesticides and highly hazardous chemicals by at least half including through integrated pest management, based on science, taking into account food security and livelihoods; and also preventing, reducing, and working towards eliminating plastic pollution.

regional scale, taking into account the nutrient emissions or, in the case of erosion, utilizing the land use distribution. This approach enables life cycle assessment (LCA) practitioners to gain insights into the spatial distribution of nutrient fate resulting from production activities across the globe, aligning with their inventory data.

My comprehensive evaluation of retention equations on a global scale can serve as a valuable tool for evaluating the performance of any process in modeling nutrient fate. Employing ANOVA and post hoc tests shows an effective way to reveal the role of diverse components in empirical equations, such as driving forces, function form, and equation coefficients. My findings of the best-fit retention equation can be utilized for elevating the accuracy of FFs by improving the performance of IMAGE-GNM. The geographical assessment of retention equations also facilitates model developers to integrate spatial variability of process functions into global nutrient simulations. Overall, the retention research can potentially contribute to the development of empirical retention equations and the accurate reproduction of nutrient fate in future modeling works.

The selection approach for determining effects provides not only the findings of robust correlations between N content and freshwater fish species richness across 425 ecoregions but also an approach for assessing such relationships for other environmental impacts, as I verified the replicability of the method for P effect in Chapter 5. The regionalization of freshwater-ecoregion-level SSDs underscores the spatial variability of sensitivities of ecosystems to nutrients. It goes beyond previous studies that assessed marine N in five geographical zones and freshwater P in four geographical zones and promotes geographical precision of effect by refining the resolution. My approach also offers a contrasting insight to existing linear EFs that rely on a generic point (Verones et al., 2020), as I calculated the average and marginal EFs that consider current background concentrations on SSDs. These EFs illustrate variations in species richness resulting from both long-term and instantaneous nutrient changes. The EFs can be implemented in LCA research and consequently aid the formulation of sustainable strategies, such as considering the high sensitivity of species

richness in tropical regions and the vulnerability of cold regions.

My research further underscores the benefits of utilizing regionalized indicators with enhanced spatial resolution. With regionalization, I innovate a method to incorporate nutrient limitation into CFs, in contrast to the focus solely on P in previous freshwater studies (Azevedo et al., 2020). My findings therefore recognize that N can contribute ~1/3 to freshwater eutrophication. The insights into nutrient limitation provided by our study offer guidance to LCA practitioners in selecting the most suitable nutrient CF for a specific location.

The global assessment of eutrophication impact conducted in our study not only identifies primary contributors but also sheds light on the severity of human pressures contributing to eutrophication-related biodiversity loss. The consideration of the comprehensive impacts of nutrients on species can be extended to assess eutrophication impact in both terrestrial and marine ecosystems, providing a holistic perspective on the environmental implications of nutrient-related disturbances. Our CFs are harmonized with other indicators considered under GLAM, which might improve the ease of application for LCA practitioners.

References

- Abell, R., Thieme, M.L., Revenga, C., Bryer, M., Kottelat, M., Bogutskaya, N., Coad, B., Mandrak, N., Balderas, S.C., Bussing, W., Stiassny, M.L.J., Skelton, P., Allen, G.R., Unmack, P., Naseka, A., Ng, R., Sindorf, N., Robertson, J., Armijo, E., Higgins, J. V., Heibel, T.J., Wikramanayake, E., Olson, D., López, H.L., Reis, R.E., Lundberg, J.G., Sabaj Pérez, M.H., Petry, P., 2008. Freshwater Ecoregions of the World: A New Map of Biogeographic Units for Freshwater Biodiversity Conservation. *Bioscience* 58, 403–414.
- Adam, J.C., Lettenmaier, D.P., 2008. Application of New Precipitation and Reconstructed Streamflow Products to Streamflow Trend Attribution in Northern Eurasia. *J Clim* 21, 1807–1828.
- Akhtar, N., Syakir Ishak, M.I., Bhawani, S.A., Umar, K., 2021. Various natural and anthropogenic factors responsible for water quality degradation: A review. *Water (Basel)* 13, 2660.
- Alexander, R.B., Elliott, A.H., Shankar, U., McBride, G.B., 2002. Estimating the sources and transport of nutrients in the Waikato River Basin, New Zealand. *Water Resour Res* 38, 4-1-4-23.
- Alexander, R.B., Smith, R.A., Schwarz, G.E., 2004. Estimates of diffuse phosphorus sources in surface waters of the United States using a spatially referenced watershed model. *Water Science and Technology* 49, 1–10.
- Ansari, A.A., Gill, S.S., Khan, F.A., 2011. Eutrophication: threat to aquatic ecosystems. *Eutrophication: causes, consequences and control* 143–170.
- Arheimer, B., Pimentel, R., Isberg, K., Crochemore, L., Andersson, J.C.M., Hasan, A., Pineda, L., 2020. Global catchment modelling using World-Wide HYPE (WWH), open data, and stepwise parameter estimation. *Hydrol Earth Syst Sci* 24, 535–559.
- Arya, S., 2021. Freshwater Biodiversity and Conservation Challenges: A Review. *IJBI* 3.
- Aulenbach, B.T., Buxton, H.T., Battaglin, W.A., Coupe, R.H., 2007. Streamflow and nutrient fluxes of the Mississippi-Atchafalaya River Basin and subbasins for the period of record through 2005. US Geological Survey.
- Azevedo, Ligia B., van Zelm, R., Elshout, P.M.F., Hendriks, A.J., Leuven, R.S.E.W., Struijs, J., de Zwart, D., Huijbregts, M.A.J., 2013. Species richness-phosphorus relationships for lakes and streams worldwide. *Global ecology and biogeography* 22, 1304–1314.
- Azevedo, L B, van Zelm, R., Hendriks, A.J., Bobbink, R., Huijbregts, M.A.J., 2013. Quantitative effects of soil pH on plant species richness: a global assessment. *Environ Pollut* 174, 10–15.

- Azevedo, L.B., Verones, F., Henderson, A.D., van Zelm, R., Jolliet, O., Scherer, L., Huijbregts, M.A.J., 2020. Chapter 8. Freshwater eutrophication. In: LC-IMPACT Version 1.0.
- Barbarossa, V., Bosmans, J.H.C., King, H., Bierkens, M.F.P., Huijbregts, M.A.J., Schipper, A.M., 2021. Threats of global warming to the world's freshwater fishes. *Nat Commun* 12, 1–10.
- Barbarossa, V., Schmitt, R.J.P., Huijbregts, M.A.J., Zarfl, C., King, H., Schipper, A.M., 2020. Impacts of current and future large dams on the geographic range connectivity of freshwater fish worldwide. *Proceedings of the National Academy of Sciences - PNAS* 117, 3648–3655.
- Bare, J., 2011. TRACI 2.0: the tool for the reduction and assessment of chemical and other environmental impacts 2.0. *Clean Technol Environ Policy* 13, 687–696.
- Bare, J., Young, D., Qam, S., Hopton, M., Chief, S., 2012. Tool for the Reduction and Assessment of Chemical and other Environmental Impacts (TRACI). Washington, DC: US Environmental Protection Agency.
- Bare, J.C., 2002. TRACI: The tool for the reduction and assessment of chemical and other environmental impacts. *J Ind Ecol* 6, 49–78.
- Behrendt, H., Opitz, D., 1999. Retention of nutrients in river systems: dependence on specific runoff and hydraulic load. In: *Man and River Systems*. Springer Netherlands, Dordrecht, pp. 111–122.
- Beusen, A.H.W., Bouwman, A.F., Van Beek, L.P.H., Mogollón, J.M., Middelburg, J.J., 2016. Global riverine N and P transport to ocean increased during the 20th century despite increased retention along the aquatic continuum. *Biogeosciences* 13, 2441–2451.
- Beusen, A.H.W., Doelman, J.C., Van Beek, L.P.H., Van Puijenbroek, P.J.T.M., Mogollón, J.M., Van Grinsven, H.J.M., Stehfest, E., Van Vuuren, D.P., Bouwman, A.F., 2022. Exploring river nitrogen and phosphorus loading and export to global coastal waters in the Shared Socio-economic pathways. *Global environmental change* 72, 1.
- Beusen, A.H.W., Van Beek, L.P.H., Bouwman, L., Mogollón, J.M., Middelburg, J.B.M., 2015. Coupling global models for hydrology and nutrient loading to simulate nitrogen and phosphorus retention in surface water—description of IMAGE–GNM and analysis of performance. *Geosci Model Dev* 8, 4045–4067.
- Boettiger, C., Lang, D.T., Wainwright, P.C., 2012. rfishbase: exploring, manipulating and visualizing FishBase data from R. *J Fish Biol* 81, 2030–2039.
- Bouraoui, F., Grizzetti, B., Granlund, K., Rekolainen, S., Bidoglio, G., 2004. Impact of climate change on the water cycle and nutrient losses in a Finnish catchment. *Clim Change* 66, 109–126.
- Bouwman, A.F., Beusen, A.H.W., Billen, G., 2009. Human alteration of the global nitrogen and

- phosphorus soil balances for the period 1970-2050. *Global Biogeochem Cycles* 23.
- Brett, M.T., Benjamin, M.M., 2008. A review and reassessment of lake phosphorus retention and the nutrient loading concept. *Freshw Biol* 53, 194–211.
- Brown, M.B., Forsythe, A.B., 1974. Robust tests for the equality of variances. *J Am Stat Assoc* 69, 364–367.
- Bulle, C., Margni, M., Patouillard, L., Boulay, A.-M., Bourgault, G., De Bruille, V., Cao, V., Hauschild, M., Henderson, A., Humbert, S., 2019. IMPACT World+: a globally regionalized life cycle impact assessment method. *Int J Life Cycle Assess* 24, 1653–1674.
- Chapra, S.C., 1975. Comment on ‘An empirical method of estimating the retention of phosphorus in lakes’ by WB Kirchner and PJ Dillon. *Water Resour Res* 11, 1033–1034.
- Chen, J., He, D., Zhang, N., Cui, S., 2004. Characteristics of and human influences on nitrogen contamination in Yellow River system, China. *Environ Monit Assess* 93, 125–138.
- Chislock, M.F., Doster, E., Zitomer, R.A., Wilson, A.E., 2013. Eutrophication: causes, consequences, and controls in aquatic ecosystems. *Nature Education Knowledge* 4, 10.
- Chorus, I., Welker, M., 2021. Toxic cyanobacteria in water: a guide to their public health consequences, monitoring and management. Taylor & Francis.
- Clark, C.M., Bell, M.D., Boyd, J.W., Compton, J.E., Davidson, E.A., Davis, C., Fenn, M.E., Geiser, L., Jones, L., Blett, T.F., 2017. Nitrogen-induced terrestrial eutrophication: cascading effects and impacts on ecosystem services. *Ecosphere* 8, n/a.
- Comte, L., Olden, J.D., Tedesco, P.A., Ruhi, A., Giam, X., 2021. Climate and land-use changes interact to drive long-term reorganization of riverine fish communities globally. *Proceedings of the National Academy of Sciences - PNAS* 118, 1.
- Corvalan, C., Hales, S., McMichael, A.J., 2005. Ecosystems and human well-being: health synthesis. World Health Organization.
- Cosme, N., Hauschild, M.Z., 2017. Characterization of waterborne nitrogen emissions for marine eutrophication modelling in life cycle impact assessment at the damage level and global scale. *Int J Life Cycle Assess* 22, 1558–1570.
- Cosme, N., Jones, M.C., Cheung, W.W.L., Larsen, H.F., 2017. Spatial differentiation of marine eutrophication damage indicators based on species density. *Ecol Indic* 73, 676–685.
- Cosme, N., Mayorga, E., Hauschild, M.Z., 2018. Spatially explicit fate factors of waterborne nitrogen emissions at the global scale. *Int J Life Cycle Assess* 23, 1286–1296.
- D’angelo, D.J., Webster, J.R., Benfield, E.F., 1991. Mechanisms of stream phosphorus retention: an experimental study. *J North Am Benthol Soc* 10, 225–237.
- de Andrade, M.C., Ugaya, C.M.L., de Almeida Neto, J.A., Rodrigues, L.B., 2021. Regionalized phosphorus fate factors for freshwater eutrophication in Bahia, Brazil: an analysis of

- spatial and temporal variability. *Int J Life Cycle Assess* 1–20.
- De Klein, J.J.M., 2008. From Ditch to Delta, nutrient retention in running waters, PhD thesis.
- de Schryver, A.M., Brakkee, K.W., Goedkoop, M.J., Huijbregts, M.A.J., 2009. Characterization factors for global warming in life cycle assessment based on damages to humans and ecosystems.
- de Visser, S., Scherer, L., Huijbregts, M., Barbarossa, V., 2023. Characterization Factors for the Impact of Climate Change on Freshwater Fish Species. *Ecol Indic*.
- Derrick, B., Ruck, A., Toher, D., White, P., 2018. Tests for equality of variances between two samples which contain both paired observations and independent observations. *Journal of Applied Quantitative Methods* 13, 36–47.
- Díaz, S.M., Settele, J., Brondízio, E., Ngo, H., Guèze, M., Agard, J., Arneth, A., Balvanera, P., Brauman, K., Butchart, S., 2019. The global assessment report on biodiversity and ecosystem services: Summary for policy makers.
- Dodds, W.K., Smith, V.H., 2016. Nitrogen, phosphorus, and eutrophication in streams. *Inland Waters* 6, 155–164.
- Döll, P., Lehner, B., 2002. Validation of a new global 30-min drainage direction map. *J Hydrol (Amst)* 258, 214–231.
- Dorham, M.M., 2014. Effects of eutrophication. *Eutrophication: Causes, Consequences and Control: Volume 2* 29–44.
- Downing, J.A., McCauley, E., 1992. The nitrogen: phosphorus relationship in lakes. *Limnol Oceanogr* 37, 936–945.
- Du, E., Terrer, C., Pellegrini, A.F.A., Ahlström, A., van Lissa, C.J., Zhao, X., Xia, N., Wu, X., Jackson, R.B., *Methodology and statistics for the behavioural and social sciences*, Leerstoel Heijden, 2020. Global patterns of terrestrial nitrogen and phosphorus limitation. *Nat Geosci* 13, 221–226.
- Duan, H., Loiselle, S.A., Zhu, L., Feng, L., Zhang, Y., Ma, R., 2015. Distribution and incidence of algal blooms in Lake Taihu. *Aquat Sci* 77, 9–16.
- Dudgeon, D., Arthington, A.H., Gessner, M.O., Kawabata, Z.-I., Knowler, D.J., Lévêque, C., Naiman, R.J., Prieur-Richard, A.-H., Soto, D., Stiassny, M.L.J., 2006. Freshwater biodiversity: importance, threats, status and conservation challenges. *Biological reviews* 81, 163–182.
- Ekau, W., Auel, H., Poertner, H.-O., Gilbert, D., 2010. Impacts of hypoxia on the structure and processes in pelagic communities (zooplankton, macro-invertebrates and fish). *Biogeosciences* 7, 1669–1699.
- El-Sadek, A., 2011. Spatial and temporal analysis of nitrogen transport and transformation in

- surface water. Arab Gulf Journal of Scientific Research 29, 51–58.
- FAOSTAT database collections, 2008. . Food and Agric. Org. of the U. N.
- Feng, K., Zhang, Z., Cai, W., Liu, W., Xu, M., Yin, H., Wang, A., He, Z., Deng, Y., 2017. Biodiversity and species competition regulate the resilience of microbial biofilm community. *Mol Ecol* 26, 6170–6182.
- Fillos, J., Swanson, W.R., 1975. The release rate of nutrients from river and lake sediments. *J Water Pollut Control Fed* 1032–1042.
- Fishnet2, 2019. Fishnet2 Database.
- Flörke, M., Eisner, S., 2011. The Development of Global Spatially Detailed Estimates of Sectoral Water Requirements, Past, Present and Future, Including Discussion of the Main Uncertainties, Risks and Vulnerabilities of Human Water Demand.
- Francoeur, S.N., Biggs, B.J.F., Smith, R.A., Lowe, R.L., 1999. Nutrient limitation of algal biomass accrual in streams: seasonal patterns and a comparison of methods. *J North Am Benthol Soc* 18, 242–260.
- Gade, A.L., Hauschild, M.Z., Laurent, A., 2021. Globally differentiated effect factors for characterising terrestrial acidification in life cycle impact assessment. *Sci Total Environ* 761, 143280–143280.
- Galloway, J., Dentener, F., Capone, D., Boyer, E., Howarth, R., Seitzinger, S., Asner, G., Cleveland, C., Green, P., Holland, E., Karl, D., Michaels, A., Porter, J., Townsend, A., Vorosmarty, C., 2004. Nitrogen Cycles: Past, Present, and Future. *Biogeochemistry* 70, 153–226.
- GBIF.org, 2019. GBIF occurrence.
- Geographical zone, 2009. *New World Encyclopedia*.
- Goolsby, D.A., Battaglin, W.A., Lawrence, G.B., Artz, R.S., Aulenbach, B.T., Hooper, R.P., Keeney, D.R., Stensland, G.J., 1999. Flux and sources of nutrients in the Mississippi-Atchafalaya River Basin: Topic 3 Report for the Integrated Assessment on Hypoxia in the Gulf of Mexico.
- Grizzetti, B., Passy, P., Billen, G., Bouraoui, F., Garnier, J., Lassaletta, L., 2015. The role of water nitrogen retention in integrated nutrient management: assessment in a large basin using different modelling approaches. *Environmental Research Letters* 10, 65008.
- Grooten, M., Almond, R.E.A., 2018. Living planet report-2018: aiming higher. WWF international.
- Grübler, A., Jefferson, M., McDonald, S., Messner, N., Nakichenovich, H. -H., Rogner, L., Schratzenholzer, 1995. Global Energy Perspectives to 2050 and Beyond. World Energy Council./Int. Inst. for Appl. Syst. Anal.

- Haddeland, I., Skaugen, T., Lettenmaier, D.P., 2006. Anthropogenic impacts on continental surface water fluxes. *Geophys Res Lett* 33.
- Haines-Young, R., Potschin, M., 2010. The links between biodiversity, ecosystem services and human well-being. *Ecosystem Ecology: a new synthesis* 1, 110–139.
- Harrison, I., Abell, R., Darwall, W., Thieme, M.L., Tickner, D., Timboe, I., 2018. The freshwater biodiversity crisis. *Science* (1979) 362, 1369.
- Harrison, J.A., Beusen, A.H.W., Fink, G., Tang, T., Strokal, M., Bouwman, A.F., Metson, G.S., Vilmin, L., 2019. Modeling phosphorus in rivers at the global scale: recent successes, remaining challenges, and near-term opportunities. *Curr Opin Environ Sustain* 36, 68–77.
- Hart, M.R., Quin, B.F., Nguyen, M.L., 2004. Phosphorus runoff from agricultural land and direct fertilizer effects: A review. *J Environ Qual* 33, 1954–1972.
- Hartmann, J., Lauerwald, R., Moosdorf, N., 2019. GLORICH-Global river chemistry database. PANGAEA <https://doi.org/10.1594/PANGAEA.902360>.
- Hauschild, M., 2006. Spatial differentiation in life cycle impact assessment: a decade of method development to increase the environmental realism of LCIA. *Int J Life Cycle Assess* 11, 11–13.
- Hauschild, M., Potting, J., 2005. Spatial differentiation in Life Cycle impact assessment-The EDIP2003 methodology. *Environmental news* 80, 1–195.
- Havugimana, E., Bhople, B.S., Kumar, ANIL, Byiringiro, E., Mugabo, J.P., Kumar, ARUN, 2017. Soil pollution—major sources and types of soil pollutants. *Environmental science and engineering* 11, 53–86.
- Heike, H., Wickham, H., Kafadar, K., 2017. Letter-value plots: Boxplots for large data. *J. Comput. Graph. Stat* 26, 469–477.
- Hejzlar, J., Anthony, S., Arheimer, B., Behrendt, H., Bouraoui, F., Grizzetti, B., Groenendijk, P., Jeuken, M., Johnsson, H., Porto, A. Lo, 2009. Nitrogen and phosphorus retention in surface waters: an inter-comparison of predictions by catchment models of different complexity. *Journal of Environmental Monitoring* 11, 584–593.
- Hellweg, S., Milà i Canals, L., 2014. Emerging approaches, challenges and opportunities in life cycle assessment. *Science* (1979) 344, 1109 LP – 1113.
- Helmes, R.J.K., Huijbregts, M.A.J., Henderson, A.D., Jolliet, O., 2012. Spatially explicit fate factors of phosphorous emissions to freshwater at the global scale. *Int J Life Cycle Assess* 17, 646–654.
- Herschy, R.W., 2012. World Lake Database: International Lake Environment Committee Foundation (ILEC). *Encyclopedia of lakes and reservoirs*. Springer Netherlands, Dordrecht 920–921.

- Holdren, G.C., Armstrong, D.E., 1980. Factors affecting phosphorus release from intact lake sediment cores. *Environ Sci Technol* 14, 79–87.
- Howarth, R.W., Billen, G., Swaney, D., 1997. Regional nitrogen budgets and riverine N and P fluxes for the drainages to the North Atlantic Ocean: natural and human influences. *Oceanographic Literature Review* 5, 448.
- Huijbregts, M.A.J., Steinmann, Z.J.N., Elshout, P.M.F., Stam, G., Verones, F., Vieira, M., Zijp, M., Hollander, A., van Zelm, R., 2017. ReCiPe2016: a harmonised life cycle impact assessment method at midpoint and endpoint level. *Int J Life Cycle Assess* 22, 138–147.
- Hunkeler, D., 2014. LCA Compendium—The Complete World of Life Cycle Assessment (book series) Series editors: Walter Klöpffer and Mary Ann Curran. *Int J Life Cycle Assess* 19, 1779–1781.
- ICMBio, 2019. Portal da Biodiversidade - ICMBio.
- IPCC, (Intergovernmental Panel on Climate Change), 2018. Global warming of 1.5° C: an IPCC special report on the impacts of global warming of 1.5° C above pre-industrial levels and related global greenhouse gas emission pathways, in the context of strengthening the global response to the threat of climate change. Intergovernmental Panel on Climate Change.
- Janse, J.H., Kuiper, J.J., Weijters, M.J., Westerbeek, E.P., Jeuken, M.H.J.L., Bakkenes, M., Alkemade, R., Mooij, W.M., Verhoeven, J.T.A., 2015. GLOBIO-Aquatic, a global model of human impact on the biodiversity of inland aquatic ecosystems. *Environmental Science & Policy* 48, 99–114.
- Jenny, J., Francus, P., Normandeau, A., Lapointe, F., Perga, M., Ojala, A., Schimmelmann, A., Zolitschka, B., 2016. Global spread of hypoxia in freshwater ecosystems during the last three centuries is caused by rising local human pressure. *Glob Chang Biol* 22, 1481–1489.
- Jensen, H.S., Andersen, F.O., 1992. Importance of temperature, nitrate, and pH for phosphate release from aerobic sediments of four shallow, eutrophic lakes. *Limnol Oceanogr* 37, 577–589.
- Jeppesen, E., Kronvang, B., Meerhoff, M., Søndergaard, M., Hansen, K.M., Andersen, H.E., Lauridsen, T.L., Liboriussen, L., Beklioglu, M., Özen, A., 2009. Climate change effects on runoff, catchment phosphorus loading and lake ecological state, and potential adaptations. *J Environ Qual* 38, 1930–1941.
- Joly, C.A., 2023. The Kunming-Montréal Global Biodiversity Framework. *Biota Neotrop.*
- Jones, L., Provins, A., Holland, M., Mills, G., Hayes, F., Emmett, B., Hall, J., Sheppard, L., Smith, R., Sutton, M., Hicks, K., Ashmore, M., Haines-Young, R., Harper-Simmonds, L., 2014. A review and application of the evidence for nitrogen impacts on ecosystem services. *Ecosyst Serv* 7, 76–88.

- Jwaideh, M.A.A., Sutanudjaja, E.H., Dalin, C., 2022. Global impacts of nitrogen and phosphorus fertiliser use for major crops on aquatic biodiversity. *Int J Life Cycle Assess* 27, 1058–1080.
- Kalcic, M.M., Chaubey, I., Frankenberger, J., 2015. Defining Soil and Water Assessment Tool (SWAT) hydrologic response units (HRUs) by field boundaries. *International Journal of Agricultural and Biological Engineering* 8, 69–80.
- Kelly, C.A., Rudd, J.W.M., Hesslein, R.H., Schindler, D.W., Dillon, P.J., Driscoll, C.T., Gherini, S.A., Hecky, R.E., 1987. Prediction of biological acid neutralization in acid-sensitive lakes. *Biogeochemistry* 3, 129–140.
- Kim, L.-H., Choi, E., Stenstrom, M.K., 2003. Sediment characteristics, phosphorus types and phosphorus release rates between river and lake sediments. *Chemosphere* 50, 53–61.
- Kirchner, W.B., Dillon, P.J., 1975. An empirical method of estimating the retention of phosphorus in lakes. *Water Resour Res* 11, 182–183.
- Kroupova, K. H., Valentova, O., Svobodova, Z., Auer, P., Machova, J., 2018. Toxic effects of nitrite on freshwater organisms: a review. *Rev Aquac* 10, 525–542.
- Kramer, D.L., 1987. Dissolved oxygen and fish behavior. *Environ Biol Fishes* 18, 81–92.
- Kroeze, C., Bouwman, L., Seitzinger, S., 2012. Modeling global nutrient export from watersheds. *Curr Opin Environ Sustain* 4, 195–202.
- Kumar, A., 2005. *Biodiversity & Conservation*. APH Publishing.
- Larentis, C., Kotz Kliemann, B.C., Neves, M.P., Delariva, R.L., 2022. Effects of human disturbance on habitat and fish diversity in Neotropical streams. *PLoS One* 17, e0274191–e0274191.
- Lehner, B., Döll, P., 2004. Development and validation of a global database of lakes, reservoirs and wetlands. *J Hydrol (Amst)* 296, 1–22.
- Lehner, B., Liermann, C.R., Revenga, C., Vörösmarty, C., Fekete, B., Crouzet, P., Döll, P., Endejan, M., Frenken, K., Magome, J., 2011. High-resolution mapping of the world's reservoirs and dams for sustainable river-flow management. *Front Ecol Environ* 9, 494–502.
- Lehtiniemi, M., Engstrom-Ost, J., Viitasalo, M., 2005. Turbidity decreases anti-predator behaviour in pike larvae, *Esox lucius*. *Environ Biol Fishes* 73, 1–8.
- Lewis Jr, W.M., Wurtsbaugh, W.A., Paerl, H.W., 2011. Rationale for control of anthropogenic nitrogen and phosphorus to reduce eutrophication of inland waters. *Environ Sci Technol* 45, 10300–10305.
- Liu, S.M., Hong, G.-H., Zhang, J., Ye, X.W., Jiang, X.L., 2009. Nutrient budgets for large Chinese estuaries. *Biogeosciences* 6, 2245–2263.

- Liu, X., Beusen, A.H.W., Van Beek, L.P.H., Mogollón, J.M., Ran, X., Bouwman, A.F., 2018. Exploring spatiotemporal changes of the Yangtze River (Changjiang) nitrogen and phosphorus sources, retention and export to the East China Sea and Yellow Sea. *Water Res* 142, 246–255.
- Maavara, T., Parsons, C.T., Ridenour, C., Stojanovic, S., Dürr, H.H., Powley, H.R., van Cappellen, P., 2015. Global phosphorus retention by river damming. *Proceedings of the National Academy of Sciences* 112, 15603–15608.
- Maotian, L., Qianli, S., Hong, W., 2014. The filter effect of big reservoirs on dissolved silicate flux decrease in the Yangtze River drainage basin. *J Lake Sci* 26, 505–514.
- Marcé, R., Armengol, J., 2009. Modeling nutrient in-stream processes at the watershed scale using Nutrient Spiralling metrics. *Hydrol Earth Syst Sci* 13, 953.
- Mayorga, E., Seitzinger, S.P., Harrison, J.A., Dumont, E., Beusen, A.H.W., Bouwman, A.F., Fekete, B.M., Kroeze, C., van Drecht, G., 2010. Global nutrient export from WaterSheds 2 (NEWS 2): model development and implementation. *Environmental Modelling & Software* 25, 837–853.
- McCrackin, M.L., Harrison, J.A., Compton, J.E., 2013. A comparison of NEWS and SPARROW models to understand sources of nitrogen delivered to US coastal areas. *Biogeochemistry* 114, 281–297.
- McDowell, R.W., Noble, A., Pletnyakov, P., Haggard, B.E., Mosley, L.M., 2020. Global mapping of freshwater nutrient enrichment and periphyton growth potential. *Sci Rep* 10, 3568–3568.
- McDowell, R.W., Sharpley, A.N., 2001. Approximating phosphorus release from soils to surface runoff and subsurface drainage. *J Environ Qual* 30, 508–520.
- Middleton, N., Thomas, D., 1997. *World atlas of desertification.. ed. 2.* Arnold, Hodder Headline, PLC.
- Miranda, R., Miqueleiz, I., Darwall, W., Sayer, C., Dulvy, N.K., Carpenter, K.E., Polidoro, B., Dewhurst-Richman, N., Pollock, C., Hilton-Taylor, C., Freeman, R., Collen, B., Böhm, M., 2022. Monitoring extinction risk and threats of the world's fishes based on the Sampled Red List Index. *Rev Fish Biol Fish* 32, 975–991.
- Mogollón, J.M., Beusen, A.H.W., van Grinsven, H.J.M., Westhoek, H., Bouwman, A.F., 2018a. Future agricultural phosphorus demand according to the shared socioeconomic pathways. *Global environmental change* 50, 149–163.
- Mogollón, J.M., Lassaletta, L., Beusen, A.H.W., Van Grinsven, H.J.M., Westhoek, H., Bouwman, A.F., 2018b. Assessing future reactive nitrogen inputs into global croplands based on the shared socioeconomic pathways. *Environmental Research Letters* 13, 44008.
- Morelli, B., Hawkins, T.R., Niblick, B., Henderson, A.D., Golden, H.E., Compton, J.E., Cooter,

- E.J., Bare, J.C., 2018. Critical review of eutrophication models for life cycle assessment. *Environ Sci Technol* 52, 9562–9578.
- Mori, A.S., Furukawa, T., Sasaki, T., 2013. Response diversity determines the resilience of ecosystems to environmental change. *Biological reviews* 88, 349–364.
- Mori, A.S., Lertzman, K.P., Gustafsson, L., 2017. Biodiversity and ecosystem services in forest ecosystems: a research agenda for applied forest ecology. *Journal of Applied Ecology* 54, 12–27.
- Mulholland, P.J., Helton, A.M., Poole, G.C., Hall, R.O., Hamilton, S.K., Peterson, B.J., Tank, J.L., Ashkenas, L.R., Cooper, L.W., Dahm, C.N., 2008. Stream denitrification across biomes and its response to anthropogenic nitrate loading. *Nature* 452, 202–205.
- Müller, B., Bryant, L.D., Matzinger, A., Wüest, A., 2012. Hypolimnetic oxygen depletion in eutrophic lakes. *Environ Sci Technol* 46, 9964–9971.
- Muralikrishna, I. v, Manickam, V., 2017. Life Cycle Assessment, Environmental Management.
- Nakhaei, N., Boegman, L., Mehdizadeh, M., Loewen, M., 2021. Three-dimensional biogeochemical modeling of eutrophication in Edmonton stormwater ponds. *Ecol Modell* 456, 109684.
- Nathan S Bryan, Hans van Grinsven, 2013. The Role of Nitrate in Human Health. *Advances in agronomy* 119, 153.
- Nedelciu, C.E., Ragnarsdottir, K.V., Schlyter, P., Stjernquist, I., 2020. Global phosphorus supply chain dynamics: Assessing regional impact to 2050. *Glob Food Sec* 26, 100426–100426.
- Norris, G.A., 2002. Impact characterization in the tool for the reduction and assessment of chemical and other environmental impacts: Methods for acidification, eutrophication, and ozone formation. *J Ind Ecol* 6, 79–101.
- Ogidi, O.I., Akpan, U.M., 2022. Aquatic biodiversity loss: Impacts of pollution and anthropogenic activities and strategies for conservation. In: *Biodiversity in Africa: Potentials, Threats and Conservation*. Springer, pp. 421–448.
- Payen, S., Civit, B., Golden, H., Niblick, B., Uwizye, A., Winter, L., Henderson, A., 2019. Acidification and Eutrophication. In: Frischknecht, R., Jolliet, O. (Eds.), *Global Guidance for Life Cycle Impact Assessment Indicators: Volume 2*. Paris.
- Payen, S., Cosme, N., Elliott, A.H., 2021. Freshwater eutrophication: spatially explicit fate factors for nitrogen and phosphorus emissions at the global scale. *Int J Life Cycle Assess* 1–14.
- Payen, S., Ledgard, S.F., 2017. Aquatic eutrophication indicators in LCA: Methodological challenges illustrated using a case study in New Zealand. *J Clean Prod* 168, 1463–1472.
- Pfister, S., Bayer, P., 2014. Monthly water stress: spatially and temporally explicit consumptive

- water footprint of global crop production. *J Clean Prod* 73, 52–62.
- Pierrat, E., Barbarossa, V., Núñez, M., Scherer, L., Link, A., Damiani, M., Verones, F., Dorber, M., 2022. Global water consumption impacts on riverine fish species richness in Life Cycle Assessment. *Sci Total Environ* 854, 158702–158702.
- PLAN, A.B., 2008. *The Atlas of Living Australia*.
- Potting, J., Finnveden, G., 2015. *LCA Compendium—The Complete World of Life Cycle Assessment (book series)* Series editors: Walter Klöpffer and Mary Ann Curran. *Int J Life Cycle Assess* 20, 1338–1341.
- Potting, J., Hauschild, M.Z., 2006. Spatial differentiation in life cycle impact assessment - A decade of method development to increase the environmental realism of LCIA. *Int J Life Cycle Assess* 11, 11–13.
- Prakash, S., Verma, A.K., 2022. Anthropogenic activities and Biodiversity threats. *International Journal of Biological Innovations, IJBI* 4, 94–103.
- Reddy, K.R., Kadlec, R.H., Flaig, E., Gale, P.M., 1999. Phosphorus retention in streams and wetlands: a review. *Crit Rev Environ Sci Technol* 29, 83–146.
- Rosenbaum, R.K., Hauschild, M.Z., Boulay, A.-M., Fantke, P., Laurent, A., Núñez, M., Vieira, M., 2018. Life cycle impact assessment. *Life cycle assessment: theory and practice* 167–270.
- Rosenbaum, R.K., Hauschild, M.Z., Huijbregts (Eds.), M.A., 2015. *Life cycle impact assessment*. Springer.
- Rosenbaum, R.K., Margni, M., Jolliet, O., 2007. A flexible matrix algebra framework for the multimedia multipathway modeling of emission to impacts. *Environ Int* 33, 624–634.
- Roy, P.-O., Azevedo, L.B., Margni, M., van Zelm, R., Deschênes, L., Huijbregts, M.A.J., 2014. Characterization factors for terrestrial acidification at the global scale: A systematic analysis of spatial variability and uncertainty. *Sci Total Environ* 500–501, 270–276.
- Russo, R.C., Thurston, R. v., 1977. The Acute Toxicity of Nitrite to Fishes. *Recent Advances in Fish Toxicology, Environmental Protection Agency, Ecological Research Series EPA 600/3-77-085*, 118-131.
- Saunders, D.L., Kalff, J., 2001. Nitrogen retention in wetlands, lakes and rivers. *Hydrobiologia* 443, 205–212.
- Savage, J.M., 1995. Systematics and the biodiversity crisis. *Bioscience* 45, 673–679.
- Scherer, L., Gürdal, İ., van Bodegom, P.M., 2022. Characterization factors for ocean acidification impacts on marine biodiversity. *J Ind Ecol*.
- Scherer, L., Pfister, S., 2015. Modelling spatially explicit impacts from phosphorus emissions in agriculture. *Int J Life Cycle Assess* 20, 785–795.

- Schindler, David W. Vallentyne, J.R., 2008. Over fertilization of the World's Freshwaters and Estuaries. University of Alberta Press.
- Schindler, D.W., 2006. Recent advances in the understanding and management of eutrophication. *Limnol Oceanogr* 51, 356–363.
- Schipper, A.M., Barbarossa, V., 2022. Global congruence of riverine fish species richness and human presence. *Global ecology and biogeography* 31, 1501–1512.
- Schulte-Uebbing, L.F., Beusen, A.H.W., Bouwman, A.F., de Vries, W., 2022. From planetary to regional boundaries for agricultural nitrogen pollution. *Nature (London)* 610, 507–512.
- SDGs, 2015. Sustainable development goals. Available at this link: <https://www.un.org/sustainabledevelopment/inequality>.
- Seitzinger, S.P., Harrison, J.A., Dumont, E., Beusen, A.H.W., Bouwman, A.F., 2005. Sources and delivery of carbon, nitrogen, and phosphorus to the coastal zone: An overview of Global Nutrient Export from Watersheds (NEWS) models and their application. *Global Biogeochem Cycles* 19.
- Seitzinger, S.P., Styles, R. V, Boyer, E.W., Alexander, R.B., Billen, G., Howarth, R.W., Mayer, B., Van Breemen, N., 2002. Nitrogen retention in rivers: model development and application to watersheds in the northeastern USA. In: *The Nitrogen Cycle at Regional to Global Scales*. Springer, pp. 199–237.
- Seppala, J., Risbey, J., Meilinger, S., Norris, G., Lindfors, G.L., Goedkoop, M., 2001. Best available practice in life cycle assessment of climate change, stratospheric ozone depletion, photo-oxidant formation, acidification, and eutrophication-Backgrounds on general issues.
- Shinohara, R., Tsuchiya, K., Kohzu, A., 2021. Warming of water temperature in spring and nutrient release from sediment in a shallow eutrophic lake. *Journal of Water and Climate Change*.
- Sinada, F., Yousif, S., 2013. Water chemistry and quality of the Blue Nile at Khartoum.
- Smil, 2002. Nitrogen and food production: Proteins for human diets. *Ambio* 31, 126–131.
- Smil, V., 1997. Global population and the nitrogen cycle. *Sci Am* 277, 76–81.
- Smil, V., 1999. Nitrogen in crop production: an account of global flows. *Global Biogeochem Cycles* 13, 647–662.
- Smith, T.J., McKenna, C.M., 2013. A comparison of logistic regression pseudo R² indices. *Multiple Linear Regression Viewpoints* 39, 17–26.
- Smith, V.H., Joye, S.B., Howarth, R.W., 2006. Eutrophication of Freshwater and Marine Ecosystems. *Limnol Oceanogr* 51, 351–355.
- Spieß, A.-N., Neumeyer, N., 2010. An evaluation of R² as an inadequate measure for nonlinear models in pharmacological and biochemical research: a Monte Carlo approach. *BMC*

- Pharmacol 10, 6–6.
- splink, 2019. speciesLink.
- Statham, P.J., 2012. Nutrients in estuaries—an overview and the potential impacts of climate change. *Science of the total environment* 434, 213–227.
- Strokal, M., Kroeze, C., Wang, M., Bai, Z., Ma, L., 2016. The MARINA model (Model to Assess River Inputs of Nutrients to seAs): Model description and results for China. *Science of the Total Environment* 562, 869–888.
- Strömbäck, L., Pers, C., Strömqvist, J., Lindström, G., Gustavsson, J., 2019. A web based analysis and scenario tool for eutrophication of inland waters for Sweden and Europe. *Environmental Modelling & Software* 111, 259–267.
- Sun, C., Shen, Z., Liu, R., Xiong, M., Ma, F., Zhang, O., Li, Y., Chen, L., 2013. Historical trend of nitrogen and phosphorus loads from the upper Yangtze River basin and their responses to the Three Gorges Dam. *Environmental Science and Pollution Research* 20, 8871–8880.
- Sun, C.C., Shen, Z.Y., Xiong, M., Ma, F.B., Li, Y.Y., Chen, L., Liu, R.M., 2013. Trend of dissolved inorganic nitrogen at stations downstream from the Three-Gorges Dam of Yangtze River. *Environmental pollution* 180, 13–18.
- Sutanudjaja, E.H., Van Beek, R., Wanders, N., Wada, Y., Bosmans, J.H.C., Drost, N., Van Der Ent, R.J., De Graaf, I.E.M., Hoch, J.M., De Jong, K., 2018. PCR-GLOBWB 2: a 5 arcmin global hydrological and water resources model. *Geosci Model Dev* 11, 2429–2453.
- Swift, M.J., Izac, A.-M., Van Noordwijk, M., 2004. Biodiversity and ecosystem services in agricultural landscapes—are we asking the right questions? *Agric Ecosyst Environ* 104, 113–134.
- Tao, Y., Wei, M., Ongley, E., Li, Z., Jingsheng, C., 2010. Long-term variations and causal factors in nitrogen and phosphorus transport in the Yellow River, China. *Estuar Coast Shelf Sci* 86, 345–351.
- Tarkalson, D.D., Mikkelsen, R.L., 2004. Runoff phosphorus losses as related to soil test phosphorus and degree of phosphorus saturation on piedmont soils under conventional and no-tillage. *Commun Soil Sci Plant Anal* 35, 2987–3007.
- Tedesco, P.A., Beauchard, O., Bigorne, R., Blanchet, S., Buisson, L., Conti, L., Cornu, J.F., Dias, M.S., Grenouillet, G., Hugueny, B., 2017. Data Descriptor: A global database on freshwater fish species occurrence in drainage basins. *Sci. Data* 4, 1–6.
- Thurston, R. V, Russo, R.C., Vinogradov, G.A., 1981. Ammonia toxicity to fishes. Effect of pH on the toxicity of the unionized ammonia species. *Environ Sci Technol* 15, 837–840.
- Tilman, D., Fargione, J., Wolff, B., D’Antonio, C., Dobson, A., Howarth, R., Schindler, D., Schlesinger, W.H., Simberloff, D., Swackhamer, D., 2001. Forecasting agriculturally

- driven global environmental change. *Science* (1979) 292, 281–284.
- Trabucco, A., & Zomer, R.J., 2019. Global Aridity Index and Potential Evapotranspiration (ET0) Climate Database v2. figshare. Dataset.
- Turner, R.E., Rabalais, N.N., Justic, D., Dortch, Q., 2003. Global patterns of dissolved N, P and Si in large rivers. *Biogeochemistry* 64, 297–317.
- UNEP GEMS/Water Programme, 2007. Water Quality Outlook. Burlington, Canada.
- Van Beek, L.P.H., Wada, Y., Bierkens, M.F.P., 2011. Global monthly water stress: 1. Water balance and water availability. *Water Resour Res* 47.
- van Puijenbroek, P.J.T.M., Beusen, A.H.W., Bouwman, A.F., 2019. Global nitrogen and phosphorus in urban waste water based on the Shared Socio-economic pathways. *J Environ Manage* 231, 446–456.
- van Vliet, M.T.H., Flörke, M., Harrison, J.A., Hofstra, N., Keller, V., Ludwig, F., Spanier, J.E., Stokal, M., Wada, Y., Wen, Y., 2019. Model inter-comparison design for large-scale water quality models. *Curr Opin Environ Sustain* 36, 59–67.
- Venohr, M., Donohue, I., Fogelberg, S., Arheimer, B., Irvine, K., Behrendt, H., 2005. Nitrogen retention in a river system and the effects of river morphology and lakes. *Water Science and Technology* 51, 19–29.
- Verma, A.K., 2016. Biodiversity: Its different levels and values. *International Journal on Environmental Sciences* 7, 143–145.
- Verones, F., Hellweg, S., Antón, A., Azevedo, L.B., Chaudhary, A., Cosme, N., Cucurachi, S., de Baan, L., Dong, Y., Fantke, P., 2020. LC-IMPACT: A regionalized life cycle damage assessment method. *J Ind Ecol*.
- Verones, F., Kuipers, K., Núñez, M., Rosa, F., Scherer, L., Marques, A., Michelsen, O., Barbarossa, V., Jaffe, B., Pfister, S., Dorber, M., 2022. Global extinction probabilities of terrestrial, freshwater, and marine species groups for use in Life Cycle Assessment. *Ecol Indic* 142, 109204.
- Verones, F., Liao, X., de Souza, D.M., Fantke, P., Henderson, A., Posthuma, L., Laurent, A., 2019. Cross-cutting Issues. In: Frischknecht, R., Jolliet, O. (Eds.), *Global Guidance for Life Cycle Impact Assessment Indicators: Volume 2*.
- Villéger, S., Brosse, S., Mouchet, M., Mouillot, D., Vanni, M.J., 2017. Functional ecology of fish: current approaches and future challenges. *Aquat Sci* 79, 783–801.
- Vilmin, L., Mogollón, J.M., Beusen, A.H.W., van Hoek, W.J., Liu, X., Middelburg, J.J., Bouwman, A.F., 2020. Modeling process-based biogeochemical dynamics in surface freshwaters of large watersheds with the IMAGE-DGNM framework. *J Adv Model Earth Syst* e2019MS001796.

- Vollenweider, R.A., 1968. Scientific Fundamentals of the Eutrophication of lakes and flowing waters, with Particular Reference to Nitrogen and Phosphorus as factor in Eutrophication. Paris Rep. Organization for Economic Cooperation and Development (DAS/CSI/68.27) 192.
- Vonlanthen, P., Bittner, D., Hudson, A.G., Young, K.A., Müller, R., Lundsgaard-Hansen, B., Roy, D., di Piazza, S., Largiader, C.R., Seehausen, O., 2012. Eutrophication causes speciation reversal in whitefish adaptive radiations. *Nature* 482, 357–362.
- Wada, Y., Bierkens, M.F.P., 2014. Sustainability of global water use: past reconstruction and future projections. *Environmental Research Letters* 9, 104003.
- Wang, H., García Molinos, J., Heino, J., Zhang, H., Zhang, P., Xu, J., 2021. Eutrophication causes invertebrate biodiversity loss and decreases cross-taxon congruence across anthropogenically-disturbed lakes. *Environ Int* 153, 106494–106494.
- Wernet, G., Bauer, C., Steubing, B., Reinhard, J., Moreno-Ruiz, E., Weidema, B., 2016. The ecoinvent database version 3 (part I): overview and methodology. *Int J Life Cycle Assess* 21, 1218–1230.
- Westin, D.T., 1974. Nitrate and Nitrite Toxicity to Salmonoid Fishes. *The Progressive fish-culturist* 36, 86–89.
- Whitfield, A., Elliott, A., 2002. Fishes as indicators of environmental and ecological changes within estuaries: a review of progress and some suggestions for the future. *J Fish Biol* 61, 229–250.
- Wilson, E.O., 1999. Biodiversity. National Academies Press, Washington.
- Withers, P.J.A., Jarvie, H.P., 2008. Delivery and cycling of phosphorus in rivers: a review. *Science of the total environment* 400, 379–395.
- Wohl, E., Barros, A., Brunzell, N., Chappell, N.A., Coe, M., Giambelluca, T., Goldsmith, S., Harmon, R., Hendrickx, J.M.H., Juvik, J., 2012. The hydrology of the humid tropics. *Nat Clim Chang* 2, 655–662.
- Wollheim, W.M., Vörösmarty, C.J., Bouwman, A.F., Green, P., Harrison, J., Linder, E., Peterson, B.J., Seitzinger, S.P., Syvitski, J.P.M., 2008. Global N removal by freshwater aquatic systems using a spatially distributed, within-basin approach. *Global Biogeochem Cycles* 22.
- Wollheim, W.M., Vörösmarty, C.J., Peterson, B.J., Seitzinger, S.P., Hopkinson, C.S., 2006. Relationship between river size and nutrient removal. *Geophys Res Lett* 33.
- Wood, E.F., Roundy, J.K., Troy, T.J., Van Beek, L.P.H., Bierkens, M.F.P., Blyth, E., de Roo, A., Döll, P., Ek, M., Famiglietti, J., 2011. Hyperresolution global land surface modeling: Meeting a grand challenge for monitoring Earth’s terrestrial water. *Water Resour Res* 47.

- Wurtsbaugh, W.A., Paerl, H.W., Dodds, W.K., 2019. Nutrients, eutrophication and harmful algal blooms along the freshwater to marine continuum. *Wiley Interdisciplinary Reviews: Water* 6, e1373.
- Yan, W., Zhang, S., Wang, J., 2001. Nitrogen biogeochemical cycling in the Changjiang drainage basin and its effect on Changjiang River dissolved inorganic nitrogen. *ACTA GEOGRAPHICA SINICA-CHINESE EDITION*- 56, 507–514.
- Yule, G.U., Kendall, M.G., 1968. *An introduction to the theory of statistics*, Charles Griffin & Co. Ltd, London 66.
- Zhang, X., Zou, T., Lassaletta, L., Mueller, N.D., Tubiello, F.N., Lisk, M.D., Lu, C., Conant, R.T., Dorich, C.D., Gerber, J., Tian, H., Bruulsema, T., Maaz, T.M., Nishina, K., Bodirsky, B.L., Popp, A., Bouwman, L., Beusen, A., Chang, J., Havlík, P., Leclère, D., Canadell, J.G., Jackson, R.B., Heffer, P., Wanner, N., Zhang, W., Davidson, E.A., 2021. Quantification of global and national nitrogen budgets for crop production. *Nat Food* 2, 529–540.
- Zhou, J., Mogollón, J.M., van Bodegom, P.M., Barbarossa, V., Beusen, A.H.W., Scherer, L., 2023. Effects of nitrogen emissions on fish species richness across the world's freshwater ecoregions. *Environ Sci Technol* 57, 8347–8354.
- Zhou, J., Scherer, L., van Bodegom, P.M., Beusen, A.H.W., Mogollón, J.M., 2022a. A Comparison Between Global Nutrient Retention Models for Freshwater Systems. *Frontiers in water* 4:894604.
- Zhou, J., Scherer, L., van Bodegom, P.M., Beusen, A., Mogollón, J.M., *Geochemistry, Bio-, hydro-*, 2022b. Regionalized nitrogen fate in freshwater systems on a global scale. *J Ind Ecol* 26, 907–922.

Summary

Freshwater biodiversity has been threatened by eutrophication due to excessive nutrients in the environment. Releasing the freshwater species from such pressures requires efforts from industry and manufacturers to avoid emissions to vulnerable and high-risk regions. The first step is to know which nutrient influences where and the effects thereof on species loss. These impacts can be assessed by methods of life cycle impact assessment (LCIA). This thesis contributes to such knowledge by improving the LCIA method, for instance, by developing more regionalized and comprehensive indicators as well as adding the consideration of both phosphorus (P) and nitrogen (N) and which of these two nutrients is limiting. To achieve this research goal, this thesis put forward four questions (Q):

Q1: What is the pattern of regionalized nutrient fate, and how do drivers affect the nutrient fate over the global freshwater?

Q2: How can retention equations improve model performance?

Q3: What is the pattern of the regionalized effect on fish species loss across the global freshwater ecosystem?

Q4: What is the impact of eutrophication on global fish species loss in freshwater ecosystems?

To answer the first question, Chapter 2 embedded N into the assessment of the eutrophication impacts on the freshwater system as a complement nutrient to P, which is at the focus of present studies. Based on the Integrated Model to Assess the Global Environment–Global Nutrient Model (IMAGE-GNM), it developed a spatially explicit approach to global fate factors (FFs) for nutrients from direct emissions, diffuse sources, and erosion to freshwater systems at half-degree resolutions. This study underlines the relationship between FFs and hydrological conditions. The results reveal that high FFs mostly exist in retention-dominated regions, while low FFs mainly occur in advection-

dominated regions. The FFs allow life cycle assessment (LCA) practitioners to estimate the fate of nutrients to the downstream locations from the inventory, and its pattern can provide a concept of where the impacts of nutrient emissions are most harmful.

Next to the study about FFs, Chapter 3 goes further into the improvement of the accuracy of simulated nutrient fate. This study evaluated the performance of empirical retention models in IMAGE-GNM by using the mean-Normalized Root Mean Square Error (NRMSE) and Pearson's r in comparison with validation data. We also applied one-way Analysis of variance (ANOVA) and post hoc analyses to check the under- or overestimates of different retention models. We find that the retention models of Behrendt and Opitz considering specific runoff perform the best for predicting riverine retention of P and N, while De Klein's retention model is the best choice for simulating P retention in lakes and reservoirs. The results reveal that empirical equations perform better for N than P globally. The hydraulic-load-driven equations predict lower retention than specific-runoff-driven models. The hydraulic driver in the retention model is more important than function forms and coefficients that affect the simulation of N/P concentrations. The assessment on the global and geographical-zone scale can suggest the best empirical retention equations for nutrient model developers. The analysis of the driving force allows better development of retention models for waterborne eutrophication-related studies. This can further help to improve the accuracy of global nutrient models.

In Chapter 4, we took N as an example to regionalize the quantitative relationships between nutrient concentration and freshwater fish species loss. This study also complements the existing studies on the effect of P in freshwater ecosystems. We calculated the freshwater species sensitivity distributions (SSDs) of hundreds of ecoregions, which goes beyond previous studies that included a few geographical zones only. The SSDs for all the ecoregions with sufficient data display good performance. We provided average and marginal effect factors (EFs). The pattern of EFs reflects the sensitivities of ecosystems to nutrient emissions at a half-degree resolution. The results reveal the high possibility of species loss in the tropical zone and the vulnerability of

cold regions. The SSDs can be utilized for research on evaluating the site-specific species richness loss due to excess nutrients, and EFs can be implemented in characterization factors (CFs) for LCA practitioners.

In Chapter 5, we developed regionalized CFs for freshwater eutrophication at a half-degree resolution and put forward a method to integrate nutrient limitation information with CFs to decide which nutrient has most influence where. The eutrophication impact on global freshwater fish was assessed by coupling the CFs considering nutrient limitation with nutrient emissions and land use information. The estimation of global species loss using our CFs (13.8%) and the conclusion of erosion as the main contributor is in line with the present studies of species loss due to water pollution and erosion. Our work thus can reflect the fish species loss due to freshwater eutrophication and exemplifies how to consider nutrient limitation in eutrophication-related studies. This study provides indicators that allow industry and stakeholders to assess the eutrophication impact on regional and global species richness. The consideration of comprehensive nutrient-species effects and nutrient limitation can be further applied in developing regionalized CFs for eutrophication issues in other ecosystems.

Based on these chapters, this thesis addresses the objective of quantifying the impact of freshwater eutrophication on global fish biodiversity. These studies provide methods to regionalize the nutrient fate, the effect on species richness, and eventually the CFs. The thesis also elaborates on which nutrient affects fish biodiversity where and applies the nutrient limitation in CFs to evaluate the global eutrophication impact.

In future studies, the thesis suggests improving the data availability and global nutrient models, since these are the main reasons that cause uncertainties in such studies of regionalizing eutrophication impact. In particular, an improvement in fish occurrence data can reduce the bias of high uncertainty in cold regions due to the current lack of observations. We also recommend using a process-based model, IMAGE-DGNM, to replace IMAGE-GNM when it is available for a global assessment.

In conclusion, this thesis advances the understanding of 1) the nutrient fate and effect

of N that also plays an important role in freshwater eutrophication, 2) the improvement of accuracy of global nutrient predictions through choosing the best-fit retention models, 3) the relationship between potential species loss and nutrient content at freshwater ecoregion level, 4) the improvement in regionalization of FFs, EFs, and CFs, and 5) the severeness of freshwater fish species richness as affected by eutrophication globally (13.8% global species loss). The thesis, therefore, provides insight into the freshwater eutrophication impact on biodiversity loss. It also proposes methods for future research to assess eutrophication-related impact in terrestrial and marine ecosystems, and can support the stakeholders to mitigate eutrophication-induced biodiversity loss and support decision-makers to formulate the environmental strategies that relate to Sustainable Development Goals 6.3 and 15.1 and Kunming-Montreal Global Biodiversity Framework target 7.

Samenvatting

De zoetwaterbiodiversiteit wordt bedreigd door eutrofiëring als gevolg van een overmaat aan voedingsstoffen in het milieu. Om de zoetwatersoorten van deze druk te bevrijden, moeten de industrie en fabrikanten zich inspannen om emissies naar kwetsbare en risicovolle gebieden te vermijden. De eerste stap is om te weten welke nutriënten waar invloed hebben en wat de effecten daarvan zijn op het voorkomen van soorten. Deze effecten kunnen worden beoordeeld met behulp van levenscyclusanalysemethoden (LevensCyclus Inventarisatie Analyse; LCIA). Dit proefschrift draagt bij aan de kennis van de effecten van nutriënten door de LCIA-methode te verbeteren, bijvoorbeeld door meer regionale en uitgebreide indicatoren te ontwikkelen en door rekening te houden met zowel fosfor (P) als stikstof (N) en welke van deze twee nutriënten beperkend is. Om dit onderzoeksdoel te bereiken, worden in deze dissertatie vier vragen gesteld:

- 1: Wat zijn de regionale patronen van nutriënten op mondiale schaal en hoe beïnvloeden verschillende factoren het voorkomen van voedingsstoffen in het mondiale zoetwater?
- 2: Hoe kunnen retentievergelijkingen de modelprestaties voor het voorspellen van nutriënten verbeteren?
- 3: Wat zijn de regionale patronen in de effecten van nutriënten op het verlies van vissoorten in het mondiale zoetwaterecosysteem?
- 4: Wat is de invloed van eutrofiëring op het wereldwijde verlies van vissoorten in zoetwaterecosystemen?

Om de eerste vraag te beantwoorden, werd in hoofdstuk 2 het transport en voorkomen van N opgenomen in de beoordeling van de impact van eutrofiëring op het zoetwatersysteem, waar de huidige studies zich tot nu toe alleen op P hadden gericht. Op basis van het Integrated Model to Assess the Global Environment-

Global Nutrient Model (IMAGE-GNM) werd een ruimtelijk expliciete benadering ontwikkeld voor mondiale fate factors (FFs) voor nutriënten afkomstig van directe emissies, diffuse bronnen en erosie naar zoetwatersystemen met resoluties van een halve graad. Deze studie onderstreept de relatie tussen FFs en hydrologische omstandigheden. De resultaten laten zien dat hoge FFs vooral voorkomen in regio's die worden gedomineerd door retentie, terwijl lage FFs vooral voorkomen in regio's die worden gedomineerd door advectie. Met behulp van de FFs kunnen levenscyclusanalyses (LCAs) het voorkomen van nutriënten op stroomafwaartse locaties uit de inventarisatie schatten. Ook geven de regionale patronen een idee over waar de effecten van nutriëntenemissies het schadelijkst zijn.

Hoofdstuk 3 gaat verder in op de verbetering van de nauwkeurigheid van gesimuleerd nutriëntengedrag. Deze studie evalueerde de prestaties van empirische retentiemodellen in IMAGE-GNM met behulp van de gemiddelde genormaliseerde Root Mean Square Error (NRMSE) en Pearson's r in vergelijking met validatiegegevens. We pasten ook een variantieanalyse (ANOVA) en post-hocanalyses toe om de onder- of overschattingen van verschillende retentiemodellen te controleren. We ontdekten dat de retentiemodellen van Behrendt en Opitz, die rekening houden met specifieke afvoer, het beste presteren voor het voorspellen van retentie van P en N in rivieren, terwijl het retentiemodel van De Klein de beste keuze is voor het simuleren van P-retentie in meren en reservoirs. De resultaten laten zien dat empirische vergelijkingen mondiaal beter presteren voor N dan voor P. De vergelijkingen die gedreven worden door hydraulische belasting voorspellen een lagere retentie dan modellen gedreven door de specifieke afvoer. De hydraulische sturing in het retentiemodel is belangrijker dan de functievormen en coëfficiënten in het simuleren van N/P-concentraties. We geven een overzicht van de beste empirische retentievergelijkingen op wereld- en geografische zoneschaal, wat gebruikt kan worden door ontwikkelaars van nutriëntenmodellen. De analyse van de sturing van retentie maakt een betere ontwikkeling mogelijk van retentiemodellen voor studies naar eutrofiëring in het

water. Dit kan verder helpen om de nauwkeurigheid van mondiale nutriëntenmodellen te verbeteren.

In hoofdstuk 4 hebben we N als voorbeeld genomen om de kwantitatieve relaties tussen de concentratie van voedingsstoffen en het verlies aan zoetwatervissoorten te regionaliseren. Deze studie is een aanvulling op de bestaande studies naar het effect van P in zoetwaterecosystemen. We berekenden de gevoeligheidsverdelingen (SSDs) van zoetwatersoorten voor honderden ecoregio's, wat verder gaat dan eerdere studies die slechts enkele geografische zones omvatten. De SSDs voor alle ecoregio's met voldoende gegevens laten goede prestaties zien. We hebben de gemiddelde en marginale effectfactoren (EFs) gegeven. Het patroon van de EFs weerspiegelt de gevoeligheid van ecosystemen voor nutriëntenemissies met een resolutie van een halve graad. De resultaten onthullen een grote kans op verlies van soorten in de tropische zone en de kwetsbaarheid van koude gebieden. De SSDs kunnen worden gebruikt voor onderzoek naar de evaluatie van het verlies aan lokale soortenrijkdom als gevolg van een teveel aan voedingsstoffen, en de EFs kunnen worden geïmplementeerd in karakterisatiefactoren (characterisation factors; CFs) voor LCA-practici.

In hoofdstuk 5 ontwikkelden we geregionaliseerde CFs voor zoetwatereutrofiëring met een resolutie van een halve graad en stelden we een methode voor om informatie over nutriëntenlimitaties te integreren met CFs om te bepalen welk nutriënt waar de meeste invloed heeft. De invloed van eutrofiëring op zoetwatervissen wereldwijd werd beoordeeld door de CFs die rekening houden met nutriëntenlimitaties te koppelen aan informatie over nutriëntenemissies en landgebruik. De schatting van het wereldwijde verlies aan soorten met behulp van onze CFs (13,8%) en de conclusie dat erosie de grootste bijdrage levert, komt overeen met eerdere onderzoeken naar het verlies aan soorten door waterverontreiniging en erosie. Ons werk kan dus een beeld geven van het verlies aan vissoorten als gevolg van eutrofiëring van zoet water en is een voorbeeld van hoe nutriëntenbeperking in beschouwing genomen kan worden in studies die

gerelateerd zijn aan eutrofiëring. Deze studie levert indicatoren die de industrie en belanghebbenden in staat stellen om de impact van eutrofiëring op regionale en wereldwijde soortenrijkdom te beoordelen. De beschouwing van de alomvattende effecten van nutriënten en hun limitaties kan verder worden toegepast bij de ontwikkeling van geregionaliseerde CFs voor eutrofiëringsproblemen in andere ecosystemen.

Door de combinatie van deze hoofdstukken beantwoordt dit proefschrift de doelstelling om de invloed van zoetwatereutrofiëring op de mondiale visbiodiversiteit te kwantificeren. Deze studies bieden methoden om het voorkomen van voedingsstoffen, het effect daarvan op de soortenrijkdom en uiteindelijk de CFs te regionaliseren. Het proefschrift gaat ook in op welke nutriënten de biodiversiteit van vissen waar beïnvloeden en neemt informatie over de nutriëntenlimitaties mee in CFs om de wereldwijde invloed van eutrofiëring te evalueren.

Voor toekomstig onderzoek stelt het proefschrift voor om de beschikbaarheid van gegevens en mondiale modellen voor nutriënten te verbeteren, omdat dit de belangrijkste redenen zijn voor onzekerheden in dergelijke studies naar de regionalisering van de invloed van eutrofiëring. In het bijzonder kan een verbetering van de gegevens over het voorkomen van vissen de huidige hoge onzekerheid in koude regio's door het huidige gebrek aan waarnemingen verminderen. We bevelen ook aan om een proces-gebaseerd model, IMAGE-DGNM, te gebruiken om IMAGE-GNM te vervangen wanneer het beschikbaar is voor een wereldwijde beoordeling.

Concluderend kan gesteld worden dat dit proefschrift bijdraagt aan een beter begrip van 1) het voorkomen van nutriënten en het effect van N dat een belangrijke rol speelt bij zoetwatereutrofiëring, 2) de verbetering van de nauwkeurigheid van wereldwijde voorspellingen van nutriënten door het aanreiken van de best passende retentiemodellen, 3) de relatie tussen potentieel soortenverlies en nutriëntengehalte

op eco-regionaal niveau in zoetwater, 4) de verbetering van de regionalisatie van FFs, EFs en CFs, en 5) de ernst van de soortenrijkdom van zoetwatervissen die wereldwijd wordt beïnvloed door eutrofiëring (13,8% soortenrijkdom verlies). Het proefschrift geeft daarom inzicht in de invloed van eutrofiëring in zoet water op het verlies aan biodiversiteit. Het stelt ook methoden voor toekomstig onderzoek om de invloed van eutrofiëring in terrestrische en mariene ecosystemen te beoordelen en kan de belanghebbenden ondersteunen om het door eutrofiëring veroorzaakte biodiversiteitsverlies te beperken en besluitvormers te ondersteunen bij het formuleren van milieustrategieën die betrekking hebben op de Duurzame Ontwikkelingsdoelen (Sustainable Development Goals; SDGs) 6.3 en 15.1 en het Kunming-Montreal Wereldwijde Biodiversiteitsraamwerk (Global Biodiversity Framework; GBF) doel 7.

Acknowledgments

First of all, I want to thank my promotor Peter van Bodegom, my supervisors José Mogollón and Laura Scherer, as well as my external supervisor Arthur Beusen for their support, guidance, and trust during my PhD. It has been a very pleasant journey to work with all of you. I am very thankful for having the chance to learn from you and further develop my research with your help in all aspects. Peter, your concern about my progress in each research and valued guidance on statistics and insight into the knowledge of eutrophication and ecology helped me to keep pace in the four-year route. José, I am deeply grateful for your help in all aspects: learned from you the knowledge in writing papers and developing nutrient models, got your guidance on skills in doing research, and communicating with others. You provided me with chances to continue my research and build networks. With your encouragement, I am not afraid of taking on new adventures. Laura, I highly enjoyed all our long discussions on the life cycle impact assessment research and other different topics. I also learned to pay attention to details and received helps in all aspects from you, including but not limited to research, writing skills, programming, and chances to work with GLAM working group. Arthur, I appreciate your support on models and papers with your abundant knowledge and kind feedback.

Secondly, I would like to thank Valerio Barbarossa. I have greatly enjoyed working with you on the research of fish species. You were so kind to provide support in data, programming, and writing. I want to continue to collaborate with you if there is a chance. I want to express my deep gratitude to the GLAM working group on eutrophication and the GLAM workshop participants from the ecosystem quality task force for valuable discussions about the characterization. The valued insights are from experts including but not limited to Rosalie van Zelm, Alexis Laurent, Stephan Pfister, Andrew Henderson, Koen Kuipers, Francesca Verones, and Martin Dorber. Similarly, I want to thank Arnold Tukker and Martina Vijver, for your

support and valuable discussion in the office and nice talks in the coffee corner.

Thirdly, I want to express my sincere gratitude to the thesis reading committee: Prof. Dr. Jan Willem Erisman, Prof. Dr. Wim de Vries, Dr. Rosalie van Zelm, Prof. Dr. Martina Vijver, and Dr. Valerio Barbarossa for evaluating this thesis.

I sincerely thank the China Scholarship Council (CSC) for their financial support (grant no. 201908430153).

I want to thank my nice colleagues and friends, Joeri Morpurgo and Zili Gu, who are also my paranymphs. I also would like to express my gratitude to my (former) office mates: Joris Timmermans, Nuno De Mesquita César de Sá, Rosaleen March, Maria Myridinas, Pengxuan Xie, Surendra Balraadsing, Mona Delval, Annetrude Boeije.

I am also very appreciative for scientific insights and pleasant talks with teachers and professors in CML: Paul Behrens, Jeroen Guinee, Emilia Hannula, and Oliver Taherzadeh, from whom I learned a lot from their work in food group; Henrik Barmantlo, Thijs Bosker, and Krijn Trimbos, who provide nice discussion in water group; Carlos Felipe Blanco Rocha, Franco Donati, Tomer Fishman, Mingming Hu, René Kleijn, Hai Lin, Alexander van Oudenhoven, Willie Peijnenburg, Roy Remme, Maarten Schrama, Yali Si, Bernhard Steubing, Kat Stewart, Emily Strange, Michiel Veldhuis, Ranran Wang, and Hauke Ward, who have provided scientific insights and joyful talk with me either in IE and EB meetings or in coffee corner.

I also want to thank my teacher, Prof. Dr. Bin Dong, and alumni Dr. Peng Dou and Ir. Yingdi Chen, as well as Dr. Xin Liu, for your support and willingness to present insightful research to CML colleagues. Particularly, I am sincerely thankful for Prof. Dr. Bin Dong's support from my undergraduate period to my PhD. You are my esteemed referee when I apply for PhD candidate in CML.

I got a lot of help and built friendships with many colleagues in CML and outside. I had a pleasant time doing science and getting along with you. My thanks go out

to Kaixuan Pan, Chunbo Zhang, Weilin Huang, Zhongxiao Sun, Xiaoyang Zhong, Chen Tang, Kai Li, Yanan Liang, Shijie Wei, Suiting Ding, Maarten Koese, Dirk-Jan Kok, Tom Nederstigt, Sander van Nielen, Janneke van Oorschoot, Riccardo Mancinelli, Levon Amatuni, Jennifer Anderson, Sam Beorlijst, Catrin Böcher, Stephanie Cap, Qi Chen, Yuchao Song, Zhengyang Chen, Amie Corbin, Antoine Coudard, Emilie Didaskalou, Lan Dupuis, Martijn van Engelenburg, Esther van der Ent, Chenguang Gao, Haye Geukes, Kevin Groen, Rosalie Hagenaars, Carina Harpprecht, Jiahui Wang, Yixin He, Lingli Hou, Jie Hu, Xinpeng Jin, Yi Jin, Meng Li, Baoxiao Liu, Chengyi Liu, Kedi Liu, Yuanyuan Mao, Stewart McDowall, Marc van der Meide, Elizabeth Migoni Alexandre, Brenda Miranda Xicotencatl, Nicolas Navarre, Sofie Rasmussen, Oscar Rueda, Irlan Rum, Mike Slootweg, Natalya Tsoy, Chengjian Xu, Joey Chen, Lingxing Xu, Tales Yamamoto, Xining Yang, Qi Yu, Laura Julia Zantis, Jianhong Zhou, Di Dong, Hu Sheng, and Yujie Zhuang.

Last but not least, I want to express my deep gratitude to my family. I write my words in Chinese so that they can understand what I want to say.

我的爸爸是一个非常温柔且努力的人，我的妈妈是一个坚强又独立的女性。他们是我的榜样，不仅教会了我做人的道理，而且对我关爱有加。在我眼里，他们是这个世界上最伟大的人，也是我最重要的人。我的父母一直支持我每一个选择，包括我远赴荷兰求学深造。在这个世界上，我还有一位重要的人，不仅是我的合作伙伴，也是我十年的伴侣，是我的阳光，水和空气。我最大的愿望就是希望你们能一生平安幸福，健康长寿，能在这个充满了不确定的、美丽又危险的世界里，能更长久地陪伴我。我偶尔脾气不好，突然对你们发脾气，有时候是因为压力大，有时也是莫名其妙一时上头的情绪，感谢你们一直包容我，给我宽容和充满爱的环境。我希望我自己能尽最大的能力对你们好，也让你们感受到爱，同时，也用从你们身上学会的爱和温柔以及我的知识去帮助这个世界上更多不相识的人。

感谢一下余歌的猫咪，小锅巴，你真是太可爱了。和你相处特别治愈，但是你有时候太调皮了。你已经长大了，能不能懂事一点，照顾好余歌？

Curriculum vitae

Jinhui Zhou was born on 16th October 1992 in Changsha, China. She started to study hydrological modeling in 2013 and finished her BSc thesis with the title of *Simulation and evaluation of water resources in Dongshaoxi watershed*. She got a BSc in Engineering in Water Resources and Hydropower at Wuhan University in 2014. She continued the study of hydrological models during her MSc, finished the thesis of *Analysis of extreme rainfall and flood response under climate change in Liujiang river basin*, and got an MSc in Hydrology and Water Resources at Sun Yat-Sen University in June 2016. From 2016 to 2019, she worked as an engineer and researcher in environmental sciences, particularly, nutrient modeling.

In 2019, she started her PhD research on eutrophication's impact on global ecosystems at the Institute of Environmental Sciences (CML), Leiden University. She is supervised by Peter van Bodegom, José Mogollón, Laura Scherer, and Arthur Beusen.

List of publications

Zhou, J., Mogollón, J. M., van Bodegom, P. M., Beusen, A. H. W., & Scherer, L. (2024). Global regionalized characterization factors for phosphorus and nitrogen impacts on freshwater fish biodiversity. *Science of The Total Environment*. 912, 169108. <https://doi.org/10.1016/j.scitotenv.2023.169108>.

Zhou, J., Mogollón, J. M., van Bodegom, P. M., Barbarossa, V., Beusen, A. H. W., & Scherer, L. (2023). Effects of nitrogen emissions on fish species richness across the world's freshwater ecoregions. *Environmental Science & Technology*. <https://doi.org/10.1021/acs.est.2c09333>

Zhou, J., Scherer, L., Bodegom, P. M. van, Beusen, A. H. W., & Mogollón, J. M. (2022). A Comparison Between Global Nutrient Retention Models for Freshwater Systems. *Frontiers in Water*, 4. <https://doi.org/10.3389/frwa.2022.894604>

Zhou, J., Scherer, L., van Bodegom, P. M., Beusen, A. H. W., Mogollón, J.M. (2022). Regionalized nitrogen fate in freshwater systems on a global scale. *Journal of Industrial Ecology*, 26(3), 907–922. <https://doi.org/10.1111/jiec.13227>

Under review/In preparation

Zhou, J., Mogollón, J. M., & van Bodegom, P. M. (2023). Assessing nutrient fate from terrestrial to freshwater systems using a semi-distributed model for the Fuxian Lake Basin, China. [Under review].

Verones, F., Barbarossa, V., Boulay, A.-M., Corella-Puertas, E., Dorber, M., Douziech, M., Golsteijn, L., Hélias, A., Henderson, A., Kuipers, K., Lebrun, M., Link, A., Marques, A., Michelsen, O., Niblick, B., Pierrat, E., Pfister, S., Posthuma, L., Rosa, F., ... **Zhou, J.** (2023). A Global Consensus Life Cycle Impact Assessment Method - GLAM: Ecosystem Quality. [In preparation].

Zhuang, Y., Liu, X., **Zhou, J.**, Sheng, H., Yuan, Z., Zengwei Y. (2023). Connecting phosphorus emissions with freshwater eutrophication potential using improved environmental fate factors based on existing methods. [In preparation].

Presentations

Oral presentation at 11th International Conference on Industrial Ecology (ISIE2023), 2nd-5th July 2023. Special Session: "Biodiversity Loss and Impact Indicators".

Oral presentation at virtual UNEP GLAM expert workshop on ecosystem quality impacts related to marine and freshwater eutrophication, 23rd-26th May 2023. Online. Session: "Freshwater eutrophication impact category".

Oral presentation at Nederlands Aardwetenschappelijk Congres (NAC), 23rd-24th March 2023. Utrecht, the Netherlands. Session: "Human Impacts on the Biosphere".

Oral presentation at the XXI International Nitrogen Workshop (NWorkshop), 24th-28th October 2022. Madrid, Spain. Session: "Agro-Food system".

Oral presentation at Nederlands Aardwetenschappelijk Congres (NAC), 5th-6th September 2022. Utrecht, the Netherlands. Session: "Hydrological Sciences".

Poster presentation at the 8th Global Nitrogen Conference (INI2021), 30th May - 3rd June 2021. Online. Session: "4b. Threats for aquat. Biodiversity"

Propositions

Accompanying the thesis

“Assessing global regionalized impacts of eutrophication on freshwater fish biodiversity”

1. On a global level, advection is the dominant process controlling the fate factors, followed by retention and water consumption (this thesis).
2. Introducing the fate of soil-freshwater nitrogen that complements existing phosphorus-related fates allows for improving global assessments of eutrophication (this thesis).
3. The species sensitivity distributions of freshwater ecoregions highlight strong effects on species richness due to high nitrogen concentrations in the tropical zone and the vulnerability of cold regions (this thesis).
4. The characterization factors for phosphorus and nitrogen impacts on freshwater fish are higher in densely populated regions that encompass either large lakes or the headwater of large rivers (this thesis).
5. Eutrophication is a leading cause of impairment of many freshwater and coastal marine ecosystems in the world (Chislock et al. 2013).
6. Natural sources of nutrients have been declining in the past and will continue to decline due to massive land transformations and increasing anthropogenic sources (agriculture, sewage, aquaculture) (Beusen et al. 2022).
7. There is a need to provide global guidance to practitioners on aquatic eutrophication (GLAM volume 2, 2019).
8. The risk that regional species loss may result in global species extinctions significantly differs per region (Kuipers et al. 2019).
9. Life goes on endlessly generation after generation, old and new; the river moon looks alike year after year, ebbs and flows.

Jinhui Zhou
Leiden, 30 January, 2024